



Entergy Operations, Inc.  
1448 S.R. 333  
Russellville, AR 72802  
Tel 479-858-4710

**Kevin T. Walsh**  
Vice President, Operations  
Arkansas Nuclear One

0CAN090901

September 24, 2009

U. S. Nuclear Regulatory Commission  
Attn: Document Control Desk  
Washington, DC 20555-0001

Subject: Generic Letter 2004-02 Final Supplemental Response  
Request for Additional Information  
Arkansas Nuclear One – Units 1 and 2  
Docket Nos. 50-313 and 50-368  
License Nos. DPR-51 and NPF-6

Dear Sir or Madam:

By letter dated September 15, 2008 (0CAN090801), Entergy Operations, Inc. (Entergy) provided a final supplemental response to Generic Letter (GL) 2004-02, *Potential Impact of Debris Blockage on Emergency Recirculation During Design Basis Accidents at Pressurized-Water Reactors (PWRs)*, dated September 13, 2004 (0CNA090401), for Arkansas Nuclear One (ANO). By letter dated May 21, 2009 (0CNA050905), the NRC issued a request for additional information (RAI) on the final supplemental response due within 90 days. Based on telephone conversations with the NRC Staff on July 16, 2009, August 3, 2009, August 11, 2009, and August 31, 2009, an extension until September 30, 2009, was granted.

Attachments 1 and 2 provide the responses to the RAIs for ANO, Units 1 and 2 (ANO-1 and ANO-2), respectively. Attachment 3 provides the responses to the generic RAIs. Based on the information provided in response to these RAIs and the final supplemental response dated September 15, 2008, Entergy believes that significant and bounding conservatisms exist in the overall holistic approach taken for resolution of GL 2004-02 issues. These conservatisms are summarized in the attached preface to the RAI responses in Attachments 1 and 2 and provide reasonable assurance that sufficient margin exists for the ANO units.

The information contained in Attachment 4 is considered proprietary to Westinghouse Electric Company in its entirety, and therefore, a nonproprietary version is not being provided. Westinghouse requests that the proprietary information be withheld from public disclosure in accordance with 10 CFR 2.390(b)(4). Westinghouse has provided Entergy with authorization to provide the proprietary information. An affidavit by the information owner, Westinghouse, supporting the request for non-disclosure is provided in Attachment 6 as part of the Westinghouse Letter CAW-09-2622. Therefore, Entergy requests that Attachment 4 of this submittal be withheld from public disclosure in accordance with 10 CFR 2.390.

The new commitment contained in this submittal is summarized in Attachment 5. Should you have any questions concerning this submittal, please contact Mr. David Bice at 479.858.5338.

I declare under penalty of perjury that the foregoing is true and correct. Executed on September 24, 2009.

Sincerely,

***Original signed by Kevin T. Walsh***

KTW/nbm

Attachments:

- 1 ANO-1 RAI Responses
- 2 ANO-2 RAI Responses
- 3 Generic RAIs Applicable to both ANO-1 and ANO-2 Concerns with Westinghouse Debris Generation Testing
- 4 Westinghouse ZOI Testing at Wyle Labs – Proprietary
- 5 List of Regulatory Commitments
- 6 Westinghouse Affidavit

cc: Mr. Elmo E. Collins  
Regional Administrator  
U. S. Nuclear Regulatory Commission  
Region IV  
612 E. Lamar Blvd., Suite 400  
Arlington, TX 76011-4125

NRC Senior Resident Inspector  
Arkansas Nuclear One  
P.O. Box 310  
London, AR 72847

U. S. Nuclear Regulatory Commission  
Attn: Mr. Kaly Kalyanam  
MS O-8B1  
One White Flint North  
11555 Rockville Pike  
Rockville, MD 20852

**Attachment 1 to  
0CAN090901  
ANO-1 RAI Responses**

## ANO-1 RAI Responses

In Entergy Operations, Inc. (Entergy's) final supplemental response of September 15, 2008, for Arkansas Nuclear One, Unit 1 (ANO-1), some of the more significant margins and conservatisms used in the strainer head loss calculations and testing were noted in Section 3.f.8. The following summarizes the more significant conservatisms:

### Maximized Debris Generation:

- Calcium-silicate zone-of-influence (ZOI) of 25 pipe break diameters (25D) for lagging fastened with sheet metal screws was based on testing that did not result in failure of the lagging when exposed to the high energy jet with the most vulnerable orientation (i.e., 45° seam angle), nor was the underlying calcium-silicate exposed or released from the lagging.
- Calcium-silicate ZOI of 5.45D for banded lagging was based on testing performed on weaker aluminum lagging compared to the stainless steel lagging installed at ANO.
- A large ZOI of 25D was combined with a credited high degree of destruction (100% fines or small shreds) for high-density fiberglass (HDFG) and Transco Thermal-Wrap fiber insulation covered with stainless steel lagging fastened with sheet metal screws. Such a large ZOI would be expected to result in a much lower degree of insulation destruction to fines.

### Maximized Debris Transport:

- 100% transport of fibers, calcium-silicate, coatings, and latent debris were credited such that all generated debris was assumed to be transported to the strainers.

### Conservative Head Loss Testing:

- Fiber added as fines and very small shreds, separated into multiple containers to avoid agglomeration, slowly poured into a flowing flume to maximize even distribution.
- Near-field settling was not credited and, in fact, was avoided by stirring of the test flume.
- Testing was conducted for an extended time period (330+ hrs) to ensure bounding head loss effects were captured.
- Thin-bed conditions were established in the test with vertical debris distribution throughout the strainer pockets (i.e., including upper pockets) significantly more uniform than would be expected in the plant, based on pouring debris in increments into the top of a flowing flume and stirring of any settled debris materials to resuspend them.

- Testing included an excess of debris material types above those calculated to ensure margin is available to address small changes in analysis, as-found conditions, or installed configurations. The tested quantity exceeded the maximum amount for any debris type for any break (i.e., highest coating particulate from one break combined with highest fiber from a second break and highest calcium-silicate from a third break). The debris loading for strainer head loss testing expressed as a percentage of the amount identified in the debris generation calculation for the limiting break is as follows: total fiber – 141% (lb basis); calcium-silicate – 142%; coatings – 150%; latent particulate – 163%; miscellaneous foreign material – 625% (“tested” as allowance for blockage).

#### Conservative Head Loss Analysis:

- Strainer test head loss measured at room temperature is shown to be acceptable without applying viscosity correction. Strainer testing included flow adjustment checks to verify that jetting or blow-hole conditions would not inhibit the expected head loss reduction associated with reduced viscosity. The viscosity correction may be applied in the future to the head loss results for determining net positive suction head (NPSH) margin or elevated temperature head losses, but the acceptability of the results prior to having applied this correction provides an indication of the significant margin available to address changes in system design or analysis.
- Peak head loss associated with limiting NPSH values are only applicable at elevated sump water temperatures, which occurs relatively early in accident response and not all of the debris would be expected to have eroded and transported to the strainer during this time period; however, the debris loading included 100% of the non-chemical precipitate debris generation totals.
- Bounding flows were used for two-train operation of reactor building spray (RBS) and injection pumps although securing one or both trains of RBS pumps would be expected prior to the formation of chemical effects precipitates at lower sump temperatures.

While not all of the above conservatisms have readily quantifiable impacts to the head loss test results, the aggregate effect provides a very high degree of confidence that evaluated test results are well bounding for any credible or design bases accident that requires sump recirculation. These multiple stacked conservatisms provide defense-in-depth to ensure that the systems and components needed to respond to a loss-of-coolant accident (LOCA) requiring sump recirculation would be able to perform their design function. Since the analysis has not relied upon credible operator actions such as securing one of the two operating trains, or securing RBS pumps at the earliest allowed opportunity, an additional potential course of corrective measures has also been preserved.

Given the very limited amounts of potentially detrimental remaining debris that could be affected by a LOCA, combined with the large surface area strainer installed above the sump pit, the expected outcome for even the incredible occurrence of a design bases double-ended guillotine break of the reactor coolant system (RCS) piping at the most limiting location relative to potentially affected debris sources, is that open screen would remain and thin-bed filtration conditions would not develop. In the unlikely event that such a break occurs and is combined

with the high degree of insulation material destruction credited in the debris generation analysis, combined with full transport of all of this material to the strainer as credited in the strainer testing, and uniform distribution of this material occurs across the strainer surface area similar to that achieved in the strainer test facility, then the strainer head loss and other upstream and downstream effects have been shown to be acceptable as noted in the September 15, 2008, submittal.

Following are the specific responses to the RAIs:

**Debris Generation/ZOI:**

- A1. Provide a more detailed summary of the basis for assuming a 5.45D (D being the pipe diameter) spherical ZOI insulating system involving Thermal-Wrap batting and blanket covered with banded stainless steel jacket. Please address how the differences in materials and structure allow for the same high destructive pressure resistance, both for jacketing over fiberglass blanket/batting versus calcium-silicate and for the blanketing itself relative to the similar materials for which ZOI radii are provided in Table 3-2, "Revised Damage Pressures and Corresponding Volume-Equivalent Spherical ZOI Radii," of the Guidance Report/Safety Evaluation (SE) (Nuclear Energy Institute (NEI) 04-07, "PWR Sump Performance Evaluation" methodology). In addition, please also address uncertainties associated with the original Ontario Power Generation (OPG) testing used to establish the 5.45D ZOI (e.g., scaling of the jet size to the target, determination of damage pressure in the test, and determination of damage threshold).**

Specific ZOI test or analysis data was not found in NEI 04-07 for the piping insulation configuration consisting of Transco Thermal-Wrap insulating pads that are covered with stainless steel lagging and stainless steel banding. The Thermal-Wrap insulating pads are composed of low-density fiberglass insulation encased in a heavy woven fabric blanket. The ZOI of 5.45D credited in NEI 04-07 for banded calcium-silicate pipe insulation, which was based on testing conducted by OPG, was applied as a conservatively bounding ZOI for the Thermal-Wrap pipe insulation installed in ANO-1 based on the following key considerations:

- The OPG test that provided the basis for the 5.45 D ZOI was conducted with 0.016" thickness aluminum external lagging and stainless steel banding straps 0.020" thickness with spacing of 6.5" to 8". During these tests the aluminum lagging was found to be the source of failure.
- The credited ANO-1 insulation was installed per an ANO engineering change package and an ANO insulation specification, which called for 0.010" thickness stainless steel lagging, with stainless steel banding straps 0.020" thickness, and a maximum spacing of 6.5". The ultimate strength of the aluminum lagging material is approximately 26 ksi (for 5005-H16 aluminum), while that of Type 304 stainless steel is approximately 85 ksi at ambient temperature. Therefore, even though the ANO stainless steel lagging is thinner than the aluminum lagging in the OPG test, considerably greater energy would be required to tear the stainless steel lagging.

- The Thermal-Wrap fiberglass insulation has an additional significant barrier to release, even in the event of failure of the stainless steel lagging, due to the fiberglass batting being completely captured in pads of heavy gauge fabric cloth. Even if the Thermal-Wrap fabric were breached, it is likely to capture or retain a portion of the internal fiberglass batting.
- Uncertainties associated with the original OPG testing related to scaling of the jet size to the target, determination of damage pressure in the test, and determination of damage threshold, were addressed in addition to the above conservatisms by crediting 100% destruction of the fiber within the 5.45 D ZOI as transportable fines and very small pieces, which is consistent with the credited 100% fines applied in NEI 04-07 for this ZOI and the calcium-silicate material.
- The OPG testing included conservatisms associated with crediting of a 45° seam angle to enhance failure potential for the metal lagging cover with tests conducted at significantly closer distances not resulting in failure or insulation release with a seam angle away from the jet.

The above considerations provide the basis used by ANO to conclude that it is conservative to apply a 5.45D spherical ZOI for Thermal-Wrap pads used as pipe insulation, when covered with stainless steel lagging and banding on a maximum 6.5" spacing, and combined with a subsequent assumption of 100% release of the underlying fiberglass insulation as 100% transported very small pieces and fines.

**A2. Testing for Transco Thermal-Wrap discussed in Entergy response dated February 28, 2008, indicated that a 7D ZOI was used for that unit's (ANO-2's) analyses. Please explain the differences between these insulation systems which account for the difference in the ZOI radii. If differences between these insulation systems are not the basis for the different ZOIs please provide alternate justification for use of the 5.45D Thermal-Wrap batting ZOI.**

Significant differences exist in the Transco Thermal-Wrap insulation materials used in ANO-1 and ANO-2. The response to RAI A1 describes the ANO-1 Thermal-Wrap insulation, which consists of fiberglass batting encased in a heavy fabric enclosure that is covered with stainless steel lagging and banding straps. The basis for the conservative application of a 5.45D ZOI for this configuration is provided in response to RAI A1. The ANO-2 Thermal-Wrap insulation is not installed on piping but is installed on the top and bottom heads of the pressurizer, and it is not configured with any lagging or metallic covering. Therefore, the ANO-1 Thermal-Wrap pipe insulation that is covered with banding and lagging justifies a smaller ZOI than the ANO-2 Thermal-Wrap blanket pad insulation that is more directly exposed to the jet impingement forces.

**A3. Please provide a more detailed summary of the basis for assuming a 2D spherical ZOI insulating system involving Temp-Mat covered with standard Transco jacketing and fasteners (similar to the surrounding reflective metal insulation (RMI)). In particular, please address how the differences in materials and structure allow for the same high destructive pressure resistance for the blanketing relative to the RMI foils for which ZOI radii are provided in Table 3-2 of the Guidance Report/SE. In this response, please also address uncertainties associated with the scaling of the jet size to the target for the original air jet testing used to establish the 2D ZOI.**

As noted in the final supplemental response dated September 15, 2008, "the interior insulation would not be released unless the outer jacketing was first dislodged." The underlying material of the Transco insulation, be it RMI foils or Temp-Mat blankets filled with fiberglass insulation, is not considered to have a significant effect upon the robustness or ability of the exterior metal lagging and fasteners to withstand high energy jet impingement. The insulation system was installed by Transco and the exterior jacketing and fasteners are consistent, with only the underlying material substituted by Transco in a few locations from RMI foils to Transco Temp-Mat due to interferences limiting the available space for the standard number of foil layers. Locations with lagging covering not consistent with Transco RMI were treated as debris for breaks in that cavity.

The Transco RMI used on the RCS piping includes three locations in the south steam generator (SG) cavity (on the hot leg piping) and three locations in the north SG cavity (one on the hot leg piping and one each on the P-32C and P-32D reactor coolant pump cold leg piping discharges) that contain Transco Temp-Mat blanket insulation instead of RMI foils. The locations are associated with interferences such as restraints, supports, or branch connections, which limit the space for installing the standard number of layers of RMI foils; therefore, Temp-Mat blanket was substituted to minimize thermal losses with a thinner insulation layer.

The north SG cavity did not contain the most limiting quantities of fiber or calcium-silicate insulation (the combination of which was found to produce the most limiting head loss), and therefore, is not the source of the "limiting break." The debris generation calculation does credit the lower hot leg break (designated S1) in the north SG cavity as producing the most detrimental combination of debris from that cavity, but it remains bounded by the limiting break in the south SG cavity. The north SG cavity S1 hot leg break already credited all of the Temp-Mat material in that cavity as debris.

The south SG cavity produces both the largest amount of fiber and calcium-silicate insulation. The three sections of Temp-Mat insulation are located on the hot leg RCS piping, with two locations close to the lower portion of the hot leg (near the reactor vessel nozzle elevation) and one location closer to the upper portion of the hot leg piping (near the upper "candy cane" bend of the hot leg at the top of the SG). The limiting break for ANO-1 was found to be the upper hot leg break (S4), which credits generation of Temp-Mat debris from the upper piece of this insulation but not the lower two. Even though a "2D" ZOI is applied, the distance from the limiting break (S4) to the next sections of Temp-Mat is approximately 7D. Thus, it would require a ZOI of at least 7D in order to involve both the upper and lower sections of Temp-Mat insulation with the limiting break.

The internal fiberglass insulation is credited with 100% destruction to fines and very small pieces that are transported to the sump strainer. For small ZOIs, such as the 2D applied to the Transco RMI, this level of destruction is potentially more realistic. For the larger separation distances (i.e., 7D) associated with the hot leg piping sections of Temp-Mat insulation, such destruction is not considered credible.

The total quantity of Temp-Mat fiber insulation is very limited with only 2.74 ft<sup>3</sup> present in the south SG cavity, where the limiting break is located. Of this total, 0.34 ft<sup>3</sup> is located close to the break and is included in the debris generation totals and 2.4 ft<sup>3</sup> is at a distance greater than 7D away from the break. The limiting break fiber debris total is approximately 21 ft<sup>3</sup> while the strainer head loss test equivalent fiber load was approximately 25.5 ft<sup>3</sup>.

It is of related significance to note the conservatism of the overall treatment of fiber released by the limiting break, which assumes that the fiber from all of the sources has been destroyed into fines and very small pieces with 100% transport such that maximum distribution across the strainer surfaces is achievable. In addition to the Temp-Mat insulation discussed here, the fiber sources include HDFG with a 25D ZOI applied (with actual distances of 42 - 67 feet from the S4 limiting break), Thermal-Wrap unbanded insulation with a 25D ZOI applied, ceramic fiber credited as being present in elbows of calcium-silicate insulation (at 25D and 5.45D depending on unbanded or banded lagging), and cold leg pipe penetration blanket fiber (discussed in RAI A4 response).

The treatment of 100% of the affected fiber insulation being destroyed into fines and small pieces that transport and more evenly distribute over the strainer surface area is considered a very conservative approach that was used in an effort to bound potential uncertainties in other areas of the analysis. This conservatism is of greater impact for ANO-1 given the limited quantity of fiber material, which only supports formation of a thin-bed fiber layer even with 100% transport and optimum distribution. Therefore, crediting the more realistic condition of some fraction of the fiber material being trapped in grating, in piles of RMI and lagging debris, remaining inside dislodged outer blanket covering, or remaining in larger pieces that either do not erode or transport, or if transported, would not evenly distribute over the screen surface to support thin-bed formation, would have provided a disproportionate benefit to ANO-1 by reducing the thickness of the thin-bed fiber layer or potentially resulting in open screen surface area.

#### **Debris Characteristics:**

- A4. Based upon the statement that the debris characteristics assumptions for ANO-1 are consistent with the baseline guidance, the NRC staff expected that all debris sources for which test data did not exist would be assumed to be destroyed into 100% small fines as described in NEI 04-07. However, the fabric blankets installed over the RCS cold leg pipe penetrations were assumed to be destroyed into only 10% fibrous fines. Please provide the technical basis for this assumption. Further, please identify the destroyed form and size distribution of the remaining 90% of this material and provide the underlying technical basis.**

The fabric blankets installed around the cold leg pipe penetrations are not insulation materials but serve as an air flow barrier between the reactor and SG cavities. Crediting that potentially 10% of the weight of these fabric blankets could be destroyed into transportable fiber fines is considered a conservative application for the limiting break versus considering the fabric as a potential foreign material debris source. The basis for this assumption being conservative is as follows:

- The limiting break (S4 – hot leg near top of SG) is a significant distance (i.e., > 42 feet or 14D) from the cold leg pipe penetrations (Babcock and Wilcox (B&W) once-through SG, with limiting hot leg break near top of the SG), which limits the potential for destruction of the blankets into smaller transportable fines. A cold leg break in the vicinity of the penetration, does not result in a more limiting debris release relative to strainer head loss, even if a higher proportion of blanket destruction did occur, due to the reduction in debris from other sources.
- The more credible potential impact to the strainers from the cold leg penetration cover blankets is the transport of small intact sections of the blanket acting as pieces of foreign material. Transport of intact pieces to the strainer would not have a significant impact to strainer head loss due to the strainer surface area and large margin available for foreign material blockage. As noted in the RAI A3 response, there are limited sources of fiber material, such that only thin-bed conditions are possible; therefore, treating a portion of the blanket debris as a source of fiber fines instead of foreign material is conservative relative to potential strainer impact.
- Similar heavy weight, tightly woven fabric materials are used to encase or enclose fiberglass insulation (i.e., Transco Thermal-Wrap). Tests conducted on similar Transco Thermal-Wrap fabric material, at distances closer than those to the limiting break, resulted in the fabric experiencing only a few tears or rips, but not being disintegrated into a credible source of fiber fines.
- While a specific destruction pressure is not established for this type tightly woven fabric material, comparison to K-wool insulation, which is not a tightly woven fabric and has a maximum fabricated density approximately half that of this fabric, would presumably provide a bounding destruction pressure. The value in NEI 04-07 for K-wool of 24 psig destruction pressure and 5.4D ZOI, if applied to the limiting break location, would result in reducing the cold leg fabric fiber contribution to zero.
- The 10% of the combined fabric weight added to the strainer test as fiber was accounted for using a fiberglass fiber fines surrogate which is conservative from a volume and related strainer area coverage perspective compared to using shreds of the coarse fabric threads.

The treatment of 10% of the combined weight of both cold leg penetration fabric covers as fiber fines for strainer testing is concluded to be conservative in context of the above.

**Latent Debris:**

**A5. In the submittal dated September 15, 2008, Entergy indicated that samples had been taken for latent debris in the containment, but the submittal did not provide any details regarding the number, type, and location of samples. Please provide these details. In particular, please identify the extrapolation method used, including the statistical deviation of the results.**

The latent debris sampling and data analysis involved dividing the reactor building into different types of surfaces. The total area of each type of surface in the reactor building was calculated. The surface types included: floor areas, reactor building liner, horizontal ventilation, vertical ventilation, horizontal cable trays, vertical cable trays, walls, horizontal equipment, vertical equipment, horizontal piping, vertical piping, and grating.

A sample was obtained by wiping the sample surface area with a clean Masslin cloth for each type of surface on various elevations at accessible areas. Each sample was bagged, and the sampled surface area was recorded. Fifty samples were taken from the twelve types of areas. The following table summarizes the sampling taken for each surface type.

Surface Type	Surface Area Sampled (ft <sup>2</sup> )		Total Reactor Building Area for Surface Type (ft <sup>2</sup> )
	#Samples	Total	
Floor Areas	4	27.34	19,033
Reactor Building Liner	4	108.94	76,529
Horizontal Ventilation	4	12.46	8,168
Vertical Ventilation	4	38.05	17,235
Horizontal Cable Trays	5	17.76	13,907
Vertical Cable Trays	4	24.02	5,750
Walls	4	61.37	73,692
Horizontal Equipment	4	11.44	3,833
Vertical Equipment	4	30.36	22,886
Horizontal Piping	5	27.02	24,695
Vertical Piping	4	51.24	19,826
Grating	4	1.75	5,347

The samples were weighed and the difference in the before and after cloth sample weight indicated the amount of latent debris present, which was divided by the area sampled to get a surface loading in weight per unit area. Multiple samples of like surfaces were averaged. The data was statistically analyzed and a 90% confidence upper limit was obtained. The total area within the reactor building was multiplied by the 90% upper limit unit surface loading to get the total latent debris on each surface type.

The total latent debris in the reactor building was obtained by adding the surface type totals.

Miscellaneous items, such as various structural steel, pipe, conduit, cable tray, support steel, control rod drive mechanisms, cooling fans, heat exchangers and smaller items such as junction boxes, valve operators, air handlers, seismic restraints, hanging lamps, electrical panels and monitoring devices and others, were not addressed individually in this calculation. The conservatism adopted in the calculation in estimating total areas of major items addressed above is considered to provide enough margin to cover areas of miscellaneous items inside the reactor building. The measurements were taken prior to building clean-up as a conservative measure to obtain a bounding value.

The total latent debris calculated using this approach based on measurements taken during the 1R20 Spring 2007 refueling outage was approximately 123 lbs. This quantity was consistent with the latent debris total measured during the previous outage. The debris testing and analysis included margin for additional particulate and fiber debris beyond this amount. The amount of margin noted in the preface section for ANO-1 under the heading "Conservative Head Loss Testing" lists the margins as percentages, with the latent debris total using a nominal 200 lbs, based on this value having been noted in the NEI 04-07 guidance document and representing a significant margin above measured values at ANO-1. However, use of the nominal latent particulate loading is listed for comparison purposes of available margin. The actual margin allocation could be increased or decreased for latent debris as needed.

#### **Head Loss and Vortexing:**

- A6. The testing conducted by Fauske utilized a debris addition sequence that was potentially non-prototypical and non-conservative. The addition of fibrous debris prior to particulates generally results in lower head losses. The Fauske testing added fibrous debris first. During earlier interactions with the licensee, the NRC staff commented on the debris addition sequence. In its letter dated September 15 2008, the licensee stated that sensitivity testing had been completed on the debris addition sequence. It is possible that the addition of fibrous debris first would not result in non-conservative results, based on the relatively low available fiber at ANO. Please provide the information regarding the sensitivity testing or other analyses showing that the addition of fibrous debris prior to other types of debris is conservative or at least neutral to the ANO test results.**

The test method developed by ANO and employed by Fauske was intended to conservatively maximize strainer head loss response, regardless of whether this biased the test in a prototypic or non-prototypic condition. NEI 04-07, Volume 2, which consists of the NRC's SE of the PWR Sump Performance Evaluation Methodology, states the following in Appendix VIII addressing thin-bed strainer head loss: *"When conducting thin-bed debris tests, it is advantageous to establish as uniform a fibrous debris bed as reasonably possible before significant head loss is achieved. This can be achieved more easily when the particulate is not involved with the fibrous bed formation. When the fibrous debris and particulate debris are introduced at the same time, the debris bed tends toward homogeneity for thicker debris but can lead to lesser head losses for thin-bed formations compared to establishing the fibrous debris bed first at flow velocities*

*sufficient to compact the fiber before the arrival of the particulates. Establishing a fibrous debris bed first and then introducing the particulate can create a more stratified debris bed.” “Although a truly stratified bed is not the anticipated plant accident condition debris bed, it is useful for determining specific debris head-loss properties and generally leads to more severe head losses than the truly mixed debris beds.”*

It is important to note that due to limited total available fiber, only thin-bed conditions are possible for ANO-1. Therefore, while the test was conducted with a test sequence of initial fiber addition, the amount of fiber added remained less than the nominal 1/8" fiber layer for thin-bed effects. Furthermore, given that only thin-bed fiber quantities were possible, significant care was taken during the testing to avoid potential agglomeration of the fiber materials into clumps or mats. The fiber materials were intentionally segregated from the particulate debris materials to avoid potential weighting down of the fiber and biasing the fiber into the lower strainer cartridges. Clumped or agglomerated fibers, could significantly skew even distribution of the fiber, resulting in either open sections of strainer or sections with minimal fiber base. For plants having a significant excess of fiber, this issue would be of less concern for producing non-conservative results. For plants with less than 1/8" available fiber, the less evenly distributed the fiber material, the more likely that debris bed perforations would develop at lower head loss values and the resulting maximum strainer head loss would be reduced. Considerable care was taken to shred the fiber material into fines and very small pieces and it was maintained diluted in numerous containers in an effort to maximize even distribution of fibers over the strainer.

The flume was constructed of clear plastic, allowing observation of the fiber debris as it was poured into the test loop and transported to the strainer. The addition of numerous small batches of fiber (performed over a 40-minute time span) was performed to promote uniform distribution over strainer surfaces. These actions were in response to previous NRC comments regarding observations of strainer tests at other facilities. The February 2, 2007, report addressing the NRC observation of CCI strainer testing notes on page 11 of Attachment 3, "the Staff considered the agglomeration-induced settling of highly concentrated debris as having significant potential to affect the test results in a non-conservative manner." While this test involved settling, which was avoided in the Fauske testing, the concern with agglomeration was noted. An earlier trip report from August 29 – September 1, 2005, testing for General Electric Energy notes on page 3 of Appendix 2, "The important issue with fibrous debris transport is to ensure the fraction of ZOI debris that is destroyed or eroded finely enough that it transports as suspended fiber is conservatively evaluated and represented in the head loss testing." Later on page 4 of Appendix 2 it states, "Since much of the particulate could arrive after the fibrous debris bed is completely or nearly completely formed, a possibility of forming a stratified bed exists. If stratification is an issue, it would apply to the maximum fibrous debris bed rather than thin-beds."

The insulation reduction efforts at ANO-1 significantly reduced the remaining volume of calcium-silicate debris (approximately 1/16" layer if evenly distributed). Testing conducted prior to the final qualification tests had indicated that the debris bed head loss is significantly impacted by the combination of available fiber and calcium-silicate insulation. A deflection point or "knee" was observed in several tests, with head loss remaining near zero prior to reaching this point. Tests with progressively thinner fiber

layers (ultrathin-bed) generally resulted in the need for larger quantities of calcium-silicate insulation to reach this deflection point. This occurrence is assumed to be associated with the capture of sufficient fiber binder fragments from the calcium-silicate insulation in the existing fiber bed until a sufficient fiber layer is formed to establish thin-bed filtration of particulates. Thus, while particulate and calcium-silicate debris could have been added first during the test sequence, without the presence of a thin-bed fiber layer, the material would simply pass through the strainer and continue to recirculate (with the assistance of stirring) until sufficient fiber accumulated on the strainer surface to begin to filter the particulate material. The addition of fiber into a test flume mixture having the particulate and calcium-silicate insulation being circulated and maintained in suspension was believed to be more likely to result in the potential agglomeration of fiber fines and a resulting non-conservative reduction in the uniformity of the fiber bed. Post-testing inspections of debris accumulation on the strainer following a series of earlier tests confirmed that the debris bed was well formed over all of the interior surfaces, which when combined with the careful fiber preparation, segregation, slow addition to a flowing flume, and ability to establish particulate filtering debris beds with very thin fiber layers, provided confidence that the fiber bed was evenly distributed and would provide conservative head loss results.

The fiber layer initially established in the strainer was thin (i.e., < 1/8") and appeared to remain at least partially porous for some period of time based on the murky water condition and the strainer head loss building gradually over several hours of recirculation with repeated stirring of the test loop. The debris bed would achieve brief periods of peak head loss during periods of stirring, followed by gradual declines after stirring was stopped to a lower stable value. The test loop was recirculated and stirred for several hours, left running over night with additional stirring performed of the settled material the following morning. After having run overnight, the test flume was stirred causing the head loss to increase to a peak value, comparable to that seen the previous day, which although not a sustained or stable value was the credited head loss for non-chemical precipitate conditions. The test loop was in operation over 20 hours prior to the initial addition of chemical precipitates and no additional insulation, coating, or particulate debris was added to the test loop after the chemical precipitates were added during the qualification test.

The NRC Staff observations of ANO strainer testing at the Fauske test facilities on August 13-14, 2007, included a demonstration of various aspects of the strainer testing and included the addition of debris at the end of the test that was not intended to replicate strainer qualification testing, but was done to create elevated differential pressures for the benefit of the NRC Staff, allowing those in attendance to witness bore hole or jetting phenomenon without having to wait for an additional test that created higher head loss using "normal" debris addition sequencing. The trip report noted "atypical" debris addition sequence of "fiber, particulate, chemical precipitate, fiber, particulate, chemical precipitate, fiber" with a test observation noting "the addition of calcium-silicate after the chemical precipitate could lead to non-prototypical sequencing effects." The addition of further insulation debris after the introduction of chemical precipitates was not part of the standard test or the qualification tests. This sequencing was performed specifically during the NRC-witnessed test for expediency to generate a higher flume head loss in a short time period to allow the Staff to observe additional test conditions such as bore holes and reduced head loss sensitivity to flow changes when bore holes are present.

In summary, the debris addition sequence used in the strainer head loss testing was designed to maximize strainer head loss for the relatively small volumes of detrimental insulation materials remaining and was performed in accordance with the guidance provided in the NRC's SE of NEI 04-07 for producing the most limiting head loss condition from a thin-bed. While fiber agglomeration and even distribution concerns could potentially have been addressed via the same slow addition of multiple small batches of fiber to the flume after particulate and calcium-silicate insulation had been added, the resulting thin-bed development and associated head loss would not be expected to be different than those achieved with an initial fiber addition. Attention was given to NRC comments from strainer test report observations conducted prior to starting the ANO testing at Fauske, as well as comments provided during the NRC Staff observation of the ANO tests. Numerous lessons learned from the series of tests performed by ANO were also incorporated in an effort to obtain the most conservatively bounding strainer test results. Entergy concurs that many aspects of the strainer tests are non-prototypical, although it remains the site's conclusion based on NRC guidance as well as the performance and observation of over 20 tests that these non-prototypic deviations contribute to a significant conservative impact on the test results relative to actual expected response and that non-conservative biases in the testing do not exist.

- A7. The minimum water level included inventory from the core flood tanks (CFTs). It is not clear that these sources would be available for all breaks. Please provide the minimum strainer submergence that could occur if the CFT volume is not included in the sump inventory. Verify that the vortexing and flashing evaluations bound this condition. Alternately, verify that recirculation is not required for all events where the CFT volume is not fully discharged to the RCS/sump.**

The reactor building minimum water level analysis results provided in Section 3.f.2 of the final supplemental response dated September 15, 2008, are for the most limiting conditions regarding emergency core cooling system (ECCS) pump NPSH and strainer head loss, which are associated with a large break LOCA (LBLOCA). For LBLOCA conditions, the CFT inventory would be released prior to sump recirculation.

It is possible for small break LOCA (SBLOCA) conditions to exist that do not release the CFT inventory, but such conditions would be associated with breaks that allow the RCS pressure to remain elevated such that the high-pressure injection (HPI) pumps would be in service. In this scenario, the low-pressure injection (LPI) pumps provide the suction source to the HPI pumps in "piggy back" operation. This configuration results in significantly lower total flow through the sump strainer and through the LPI pumps. The approximate design flow for each HPI and LPI pump is 500 gpm and 3000 gpm, respectively, with a maximum credited flow of 3547 gpm per LPI pump.

The small break size associated with maintaining RCS pressure such that the HPI pumps are in operation during recirculation would also significantly reduce the debris loading on the sump strainers compared to the ZOI associated with a 36" inside diameter (ID) hot leg pipe break that provides the current limiting condition for debris generation. LOCA break analysis for ANO-1 indicates that breaks as small as 0.06 ft<sup>2</sup> result in CFT inventory release to the RCS within 25 minutes after break opening. This break size is equivalent to a 3.3" diameter pipe compared to the 36" diameter hot leg break (S4) evaluated as the limiting break for strainer head loss. The combination of lower sump flow and lower debris loading would not produce the most limiting head loss conditions.

Ensuring that the sump strainer assembly remains submerged even under less limiting conditions of a SBLOCA is important, and as noted in the Section 3.f.2 of the final supplemental response dated September 15, 2008, the strainer would remain fully submerged even if the CFT inventory is excluded from the sump inventory. The strainer submergence is reduced from a level approximately seven inches above the strainer to submergence of approximately four inches if the CFT inventory is excluded (per simple ratio of CFT inventory to net water inventory and 4.95 ft level providing seven inches of submergence). The vortexing evaluation in Section 3.f.3 of the final supplemental response dated September 15, 2008, notes that both the vortex analysis physical test data and the analytical values determined using the Froude number yield minimum submergence values less than that remaining even if the CFT inventory is not credited. The flashing discussion provided in Section 3.f.14 of the final supplemental response dated September 15, 2008, remains essentially applicable relative to the very small amount of overpressure that would need to be credited to avoid flashing for the head losses associated with LBLOCA debris loading and flow rates even if the CFT inventory were excluded, although as noted above neither the flow rates nor debris loading head losses would be applicable to break conditions that do not result in release of the CFT inventory.

The combination of reduced strainer debris loading, particularly given that existing debris loading only produces thin-bed fiber thickness, and reduced flow loss associated with a SBLOCA would be expected to result in minimal strainer head loss. In the extremely unlikely case that an SBLOCA results in a combination of sufficient debris loading and sump flows such that strainer head loss exceeded the four-inch submergence value associated with the absence of CFT release concurrent with the sump water temperature being near saturated values, then a small amount of overpressure would need to be credited, of magnitude similar to that noted in Section 3.f.14 of the final supplemental response dated September 15, 2008.

- A8. In Entergy's submittal dated September 15, 2008, Table 3.b.4-1 in the debris generation Section 3.b.4-1 appears to underestimate the amount of fibrous debris generated for the different breaks. This information was carried over into the debris amounts included in testing. It was noted that the response the licensee's submittal dated February 28, 2008, had lower debris generation amounts for the individual insulation components. The total fibrous mass listed in the table for each break appears to more closely represent the amounts of fiber reported in the submittal dated February 28, 2008. The volumes of fiber reported in the table clearly represent a higher mass than is reported in the "Total Fiber" row of the table. Based on the submittal dated February 28, 2008, it is likely that testing was conducted with a conservative fiber load, but this assumption and the basis for the inclusion of the higher fibrous volumes in Table 3.b.4-1 is unclear. Please clarify the purpose of Table 3.b.4-1 and verify that the amounts of debris used in testing were scaled from debris amounts that are predicted for the various breaks considered.**

The data in Table 3.b.4-1 of the final supplemental response dated September 15, 2008, was provided with "less than" limits for each debris type that bound the amount determined by the debris generation calculation. The total fibrous mass listed at the bottom of the table was provided as a composite total for all of the individual fiber

sources. The bounding total at the bottom of the table is the limit associated with strainer head loss testing. The method was intended to accommodate future potential minor variations in the specific composition of the fiber total, which would be acceptable provided the total fiber limit was not exceeded. To clarify any confusion this may have caused in regards to the debris data, specific values from the current debris generation calculation are provided in the table below for the same breaks presented in Table 3.b.4-1 of the final supplemental response dated September 15, 2008.

Debris Type	Units	South Break S1	South Break S4	South Break S5	North Break S1	Strainer Test
Transco RMI Foil	ft <sup>2</sup>	11019	4959	1032	11263	0
Calcium-Silicate	ft <sup>3</sup>	6.9	10.2	1.2	4.42	14.5
<b>Fiber Sources</b>						
Transco Temp-Mat	ft <sup>3</sup>	2.4	0.34	0	2	
HDFG	ft <sup>3</sup>	6.0	12.4	12.4	4.3	
Thermal-Wrap Insulation	ft <sup>3</sup>	3.1	0.40	6.3	0	
Cera-Fiber Insulation	ft <sup>3</sup>	0.22	0.31	0	0.12	
Penetration Blanket Fiber <sup>1</sup>	lb	2	2	2	1.5	
Total Fiber w/o latent fiber <sup>2</sup>	lb	66.5	65.3	72.9	45.4	
Total Fiber w/ latent fiber	lb	84.9	83.7	91.3	63.8	115.5

<sup>1</sup> Fabric blankets are installed over the RCS cold leg pipe penetrations into the SG cavities with 10% of the blanket weight credited as becoming fiber fines.

<sup>2</sup> The fiber densities used to determine total fiber mass are 11.8 lb/ft<sup>3</sup> for Temp-Mat, 4.5 lb/ft<sup>3</sup> for HDFG, 2.4 lb/ft<sup>3</sup> for Thermal-Wrap, and 8 lb/ft<sup>3</sup> for Cera-Fiber.

As can be seen from the above values and those noted in Table 3.f.5-1 of the final supplemental response dated September 15, 2008, the tested quantity of debris exceeds the debris generation quantities identified.

- A9. On page 40 of its submittal dated September 15, 2008, the licensee stated that the peak head loss is extrapolated to slightly less than 8 ft at two-train full flow conditions with chemical loading. This extrapolation is based on a comparison of different reduced flow rates that were documented during the test. In particular, the response states that later batches of debris were added at 50% of the scaled two-train flow. Although the flow was later increased by 30%, it is not clear that increasing the flow through a pre-existing debris bed results in equivalent bed compression as forming the debris bed at that increased flow rate. Furthermore, the extrapolation to higher flow rates than were considered in the test program may not be prototypical or conservative due to additional bed compression that can occur at higher flow rates. Please provide the extrapolation methodology in more detail including assumptions made regarding how increased flow velocities affect debris bed formation and compression, and therefore head loss.**

The debris bed was formed at full flow values for the addition of materials other than the later batches of chemical precipitate. The response statement referencing "debris" addition at 50% of the scaled two-train flow should have been worded as chemical precipitate addition. The credited strainer head loss test data is shown in the final supplemental response dated September 15, 2008, Figure 3.o.2.17.i-1 and Table 3.o.2.17.i-1. As can be seen from the debris addition noted in the table, all of the fiber and particulate debris material was added to the test loop at full flow conditions, with the last debris added at time 7577 seconds (2.1 hrs). The test loop was maintained at two-train full equivalent flow through 250369 seconds (69.5 hrs), providing more than ample time for settling and compression of the debris bed. The initial three increments of chemical precipitate addition were also performed during this time period with almost 48 hours of debris bed settling and compression time available at the elevated head loss (approximately 1.5 psid or 3.4-3.5 ft) conditions. The debris bed response to the initial three chemical additions was a rapid climb to a peak head loss of 1.71 psid, followed by a reduction to an approximate head loss of 1.5 psid.

After the flow reduction to an equivalent of approximately one-train flow, the head loss was allowed to stabilize prior to any further chemical additions, with a stable head loss of 0.74 psid or approximately half of the previous two-train head loss value. Two additional increments of chemical precipitate were added at single-train flow equivalent with head loss increasing to approximately 0.85 psid. The flow was increased to two-train flow equivalent and rapidly increased to a peak of 1.89 psid. The flow was reduced to single-train flow with head loss decreasing to a value considerably below the previous stable value prior to the flow changes. The behavior of the debris bed of experiencing momentary peaks with declining and then stabilizing subsequent pressure drop is consistent with previously observed tests where breaches in the debris bed were occurring, such that the debris bed responds initially to increased loading, but the peak values quickly started dropping due to breaches in the thin-bed debris layer with perforations occurring at presumably weaker points in the debris bed allowing jetting or blow-holes to develop. These jetting streams were visually notable in the Fauske strainer test facility. The response of the debris bed head loss to doubling the flow and then lowering it back to the starting flow provides additional evidence to support that the debris bed was not becoming denser or more compact by the added pressure drop but was instead experiencing increased occurrences of debris perforations at the elevated pressure drop. This explains why the head loss settled at a lower instead of higher head loss when the flow was again reduced to single-train equivalent values.

After the head loss stabilized at single-train readings, the head loss did not exceed the previous single-train head loss stable value until after the second chemical precipitate addition. The subsequent responses to additional chemical precipitate additions were limited, with head loss slowly declining versus increasing with time, even after additional amounts of chemical precipitate material were added. The strainer head loss and flow relationship were again checked prior to securing the test. Flow was increased approximately 20%, resulting in a significant increase in head loss. A further flow increase of approximately 10% resulted in an additional increase in peak head loss, but these peak values were quickly followed by declining head losses, and again when flow was reduced back to single-train values, the head loss was lower than the previous values at similar flows. This response again supports that the debris bed was not compacting but was experiencing increased amounts of perforations or jetting through the thin debris bed as the pressure drop increases.

The extrapolated peak head loss was conservatively determined using a greater than 1:1 rate of head loss increase to flow rate increase. This type response was observed near the end of the head loss testing (reference Table 3.o.2.17.i-1 of the September 15, 2008, submittal). This extrapolation is considered to be very conservative given the occurrence of perforations in the debris bed that tend to limit the magnitude of head loss increases. The debris bed would be expected to experience increasing amounts of jetting and perforations as the flow increased and stabilize at a peak head loss at much lower actual values of peak head loss than the conservatively extrapolated change in peak head loss values.

**Debris Source Term:**

**A10. Please identify/describe the specific procedures mentioned in the debris source term for control and maintenance of containment cleanliness.**

The general control of area cleanliness for the site is addressed in procedure 1000.018, *Housekeeping*. The reactor building is designated as housekeeping Level II, with some exceptions associated with Level I requirements around the reactor vessel and fuel transfer areas when the reactor head is removed. The procedure describes Level II housekeeping areas as those where a high order of cleanliness is required and that the purpose is to prevent foreign material from adversely impacting safety-related systems. The reactor building is noted specifically due to the potential for debris to impact operability of the sump. Specific instructions are provided to contain grinding and welding activities to avoid the introduction of grit in the areas; use of mats when dust, debris or particles are generated; periodic cleaning of the work area with loose items controlled and loose trash/debris disposed of properly; consumable items being removed from the work area immediately upon completion of the activity; and cleaning the work area upon completion of work such that surface or airborne abrasive dirt or grit is minimized. The procedure applies to all workers in the affected housekeeping level and also includes the assignment of specific plant areas to work groups for oversight and ownership as well as the use of job-site ownership signs for specific activities, both of which are intended to ensure a level of direct responsibility for maintaining cleanliness.

In addition to the housekeeping procedure, procedure 1015.036, *Containment Building Closeout*, includes specific guidance regarding inspections of the sump screens and areas within the reactor building prior to plant heatup and again prior to reactor building closeout (criticality). The inspections performed per 1015.036 involve multi-discipline teams that address detailed checklist inspections of the sump strainers as well as accessible areas of the reactor building. Instructions are provided to address a wide variety of potential sources of debris or foreign material as well as the storage of materials inside the reactor building.

In addition to these controls, periodic performance of the latent debris surveys will be performed (as previously committed to in Section 3.i.1 of the final supplemental response dated September 15, 2008) to ensure the latent debris quantities remain within tested and analyzed limits. The sump strainer head loss testing and downstream effects analysis included additional margin beyond the measured latent debris value to allow for variations in the periodically measured value without exceeding the tested or analyzed limits. Adjustments to cleanliness practices and/or latent debris sample frequency will be

made in accordance with the remaining margin to ensure conditions remain within analyzed and tested limits as previously committed to in Section 3.i.1 of the final supplemental response dated September 15, 2008.

**Upstream Effects:**

**A11. The discussion of refueling canal drain blockage in the letter dated September 15, 2008, did not provide sufficient technical basis for the staff to conclude that blockage would not occur. Please include additional discussion concerning how the following phenomena could affect the potential for drain blockage: turbulence, sheeting flow, preferentially directed drainage into the canal, and temporarily floating debris (i.e., it was not clear to the NRC staff why all floating debris will be able to pass through the drain). In addition, identify the minimum flow restriction in the drain line versus the sizes and quantities of debris that could be transported through the drain. In light of the discussion above, describe why there is high confidence of no refueling canal drain blockage without an engineered barrier to debris being installed.**

The refueling canal drain is not located on the floor of the deep end but is an open six-inch horizontal flanged pipe stub projecting out of the side wall centered nine inches above the floor of the deep end portion of the canal. The relatively short section of pipe drains the deep end region into the reactor cavity through an unrestricted section of six-inch pipe. The flow out of the reactor cavity is via a blocked open hatch. There are no reducers, grating covers, valves or other items to collect or accumulate debris in the drain outlet flow path from the refueling canal, thus the minimum flow restriction in the drain line is the inside diameter of the pipe, approximately 6". A water level of approximately 3.5' and volume of approximately 1470 ft<sup>3</sup> is credited with hold-up in the refueling canal deep end to support the RBS flow passing through the drain pipe.

A risk-based approach was used to qualify the refueling canal drain capability with respect to blockage rather than attempting to quantify the debris deposited into the refueling canal. Part of the 2,640 gpm total RBS flow rate would distribute to the refueling canal area. Draining of the refueling canal deep end would cause water level to rise above the drain's opening as determined by hydraulic analysis to a predicted steady-state level bounded by the credited hold-up inventory. Small quantities of floating debris, if present, could be drawn into the drain. The floating debris would likely be fines and light debris. That debris would then be deposited into the reactor cavity and the reactor building lower volume, without causing obstruction of the refueling canal drain path.

Insulation debris sizes are generally categorized as fines (dust and insulation particles), small debris pieces (passable through gratings and would sink in hot water), and large pieces (insulations chunks not passable through grating and would sink in hot water). Blowdown debris also consists of qualified and unqualified coatings, component labels and tags, information signs, tape, and latent debris such as dust, dirt, lint, fibers, etc. Debris would become airborne and transferred by the motive force of the high energy line break (HELB) pressure blast creating the potential for it to fall in the refueling canal.

Projectile paths for debris that could be displaced into the refueling canal include the upper openings of each SG cavity and perimeter areas of the reactor building that are either open or feature grating. These paths are the vent paths for the design basis LOCA pressure transient. The most likely path that debris would travel before reaching the refueling canal would be through the SG cavity upper opening for a break within its compartment. Small debris and fines are anticipated to fall into the refueling canal and accumulate on the refueling canal floors. Fines and a portion of small debris are also anticipated to settle out on equipment surfaces and walls throughout the reactor building.

Structural members and system components impacted by large debris would absorb kinetic energy and deflect the debris. Mezzanine gratings within the compartments provide a potential barrier to restrain and filter large debris pieces. Mezzanine gratings within the reactor building perimeter areas provide an additional expected barrier for debris exiting the lower SG compartment. Some debris pieces would likely be further deformed or shredded by impact with gratings. The SG cavity upper elevation is completely covered, other than openings for ladder access, with deck grating having nominal four-inch by one-inch openings. The upper grating is restrained with chains to provide a hinged effect for the anticipated LBLOCA blowdown pressure gradient. Some sections may be welded to the structure and regarded as permanent or fixed gratings. Therefore, debris large enough to block the refueling canal drain is not likely to be deposited into the refueling canal due to the trajectory path required.

The replacement reactor vessel closure head (RVCH) was insulated with Transco RMI. No RVCH RMI insulation (ZOI = 2D) would be expected to be upset due to blowdown forces from a SG cavity break since the RVCH insulation is located outside of the compartments of the assumed break locations. Therefore, the RVCH insulation does not contribute to the blowdown-generated debris that could block the refueling canal drain for the break scenarios that maximize potential strainer head loss.

As noted above, the grating covering at the top of the SG cavities provides an effective barrier to prevent large debris from being ejected from the SG cavities. The ANO-1 debris source term includes a very limited amount of fiber insulation debris, as noted in response to RAI A8. In the unlikely event that a larger section of fiber insulation debris were extruded through the grating openings and landed in the refueling canal, this would occur in the initial phase of the break blowdown, allowing settling in the refueling canal during the period of initial RBS operation while the refueling canal is filling to the drain pipe (center of pipe is located 9" above floor level). As noted in NUREG/CR-6808 Section 5.2.1, "Fiberglass insulation readily absorbs water, particularly hot water, and sinks rapidly (...from 20 to 30 seconds in 120°F water)." Debris consisting of RMI shells and shell fragments, component labels and tags, information signs, and larger RMI foil pieces would become submerged in the accumulated water. Floating debris would likely consist of fines and lighter debris including smaller RMI foil shreds, equipment coatings, and tape. RMI foil thickness is typically two mils, so surface tension may keep some small debris suspended on the water surface. Floating debris in the proximity of the drain could become entrained in the drainage with the increasing water velocity near the drain and would pass through the six-inch drain.

Debris deposited into the refueling canal would have resistance to translate across to the drain. The configuration of the six-inch drain opening being centered nine inches above the canal floor promotes settlement of debris to the canal floor even during drainage. Translational flow of debris in the refueling canal deep end is not anticipated to occur with the flow rates and the drain opening elevated above the floor. Transport of large debris to the canal drain is not expected with the water velocities in the general refueling canal area.

In conclusion, the refueling canal drain is configured to draw water from above the refueling deep end floor. Large and small debris would be expected to rest on the refueling canal floor with the expected drain flow rate. Fines and floating debris would be carried in the drain stream without obstructing or plugging the drain path. Complete blockage of the refueling canal deep end drain by post-LOCA generated debris is not considered a credible outcome.

### **Screen Modification Package:**

**A12. A stainless steel divider plate with square openings of 0.132" is installed between the two halves of the sump. Please provide the technical basis for concluding that blockage would not occur at this plate. Note that if blockage could occur at this plate, then any credit for single-train operation could be with only roughly half the strainer area.**

The stainless steel divider plate inside the sump has a 10 ft<sup>2</sup> area with square openings of 0.132". The strainer is fabricated with perforated plate having 1/16" holes, as noted in Section 3.j.1 of the final supplemental response dated September 15, 2008. Thus, the area of the openings in the internal divider plate is greater than five times larger than the strainer openings. The strainer head loss qualification is based on two-train flow conditions. While it is expected that actions would be taken to secure one of the operating trains after accident conditions have stabilized, this action is not procedurally required, nor credited in the sump analysis. Therefore, conditions that result in flow across the divider plate would be associated with lower total flow through the strainer and an associated reduction in total head loss.

The small surface area divider plate screen could potentially be vulnerable to the accumulation of a fiber bed due to the fiber bypass fraction assigned to the strainer, particularly when significant flow is passing through the divider plate screen such as following a postulated single failure of one train, due to part of the operating train flow passing through the screen. The scenario of greatest interest is the potential for a particulate filtering thin-bed fiber layer to develop on the internal screen from the bypassed fibers and this occurring before most of the debris has transported to the strainer. This scenario is theoretically possible due to the rather large surface area ratio between the strainer and the divider plate screen. A thin-bed fiber layer on the divider plate screen could result in limiting the flow and therefore, the associated debris accumulation on the side of the strainer not having an active suction flow path. This could result in uneven debris distribution across the strainer, directing a disproportionate amount of debris to the portion of the strainer with a flow path not passing through the internal screen. The uneven debris accumulation could subsequently result in the debris loads exceeding those addressed by strainer head loss testing. The potential for this

occurrence is related to the total available fiber, fiber bypass for the main strainer, flow through the divider plate, fiber bypass for the internal divider plate screen, and the fiber bed thickness needed on the divider plate screen to create thin-bed type filtration conditions. These topics are discussed in additional detail below.

The equivalent total fiber volume used in the ANO-1 strainer head loss testing was approximately 25.5 ft<sup>3</sup>. This included additional fiber (approximately 4 ft<sup>3</sup>) beyond the fiber debris load conservatively determined by the debris generation calculation to allow for future changes in analysis or installed insulations. The fiber debris generation analysis used a large conservative ZOI of 25D for HDFG insulation covered by stainless steel lagging secured with sheet metal screws. This large ZOI source accounts for over 50% of the fiber total. All of the fiber was also conservatively assumed to transport to the strainer as fines and very small pieces, with no credit taken for size distribution, fiber erosion, or debris transport reductions. This conservative treatment of the fiber source was applied in spite of the very large ZOI associated with the majority of the fiber generated.

A fiber bypass value of 5% was conservatively applied to the main strainer for downstream effects evaluations even though fiber bypass tests conducted for the CCI strainers found substantially lower fiber bypass values. The fiber bypass tests indicated an average fiber bypass of less than 1.25%.

Maximum flow across the internal divider plate screen occurs when a single train of RBS and LPI pumps are operating. An uneven flow distribution of 60% coming from the side without an in-service suction pipe was assumed, such that 60% of the bypassed fibers from the main strainer would pass across the divider plate screen.

A high fiber bypass is expected for the interior divider plate screen. Fiber strands with properties more conducive to screen capture would be trapped on the exterior strainer perforated plate surface, while fibers passing through these holes would be primarily fragments and isolated strands. These fibers would be expected to have a considerably higher bypass percentage for a clean second screen, even if it had the same size openings. Given that the interior screen does not have the same size openings, but has an opening area greater than five times larger than the exterior screen, the subsequent fiber bypass percentage for the interior screen would be expected to be very high. Sources of test data were not found that evaluated the capture efficiency of very fine fibers (i.e., that would pass through a 1/16" hole) on a wire mesh screen having approximately 1/8" square openings (0.132" square). Most test reports credited that smaller debris could accumulate on screen openings of this size, but such accumulation generally credits a large amount of available fiber or build-up from repeated recirculation of the fiber, with the fiber bed filling in very slowly at first, but more rapidly as the fiber layer becomes established.

Due to the absence of applicable data for the fiber bypass rate for fiber fines that have passed through a small opening and subsequently collect on a much larger opening, a reasonable bounding nominal value of 66% bypass is assigned and is combined with a reduction of the strainer fiber bypass value to 1.25% for discussion of the blockage potential of the internal divider plate. The divider plate screen bypass value of 66% (or 34% accumulation) is supported by NUREG/CR-6885 fiber accumulation data for a 1/8"

screen. Table 5-1 of NUREG/CR-6885 found that for blender processed Nukon fiberglass fiber collected on the screen amounted to less than 25% of the total, which even when conservatively increased to account for “missing” fiber at the end of the test the bypass values were still approximately 63%. Given that these tests were conducted without upstream filtration by a screen having a smaller opening, as is applicable to the ANO-1 divider plate configuration, the use of a 66% bypass value is considered appropriate. The main strainer bypass value is supported by specific test data and is further considered acceptable for this application considering its combination with a bypass value of 66% for the internal divider plate, which is considered significantly low given the 5:1 size ratio for the two screen openings.

A high capture percentage at the sump screen effectively results in only one pass opportunity for accumulation on the interior divider plate screen. For example, a 5% bypass value of transported fibers for their first pass would be reduced to only 0.25% of the fiber total passing through the strainer on its second pass, if capture on the internal divider plate and other surfaces is ignored and no settling in the system or basement occurs. Similarly, for a 1.25% bypass value on the first pass, the reduction would be to 0.0156% of the fiber total passing through the strainer on its second pass. This results in the potential for debris build-up on the interior divider plate screen being reduced to the initial pass of fiber material that bypasses the main strainer.

In order for a fiber bed on the divider plate screen to be capable of thin-bed particulate filtration and the associated build-up of differential pressure, it would be expected to be at least 1/8” in thickness. This is based on the size of the openings being bridged (0.132” square) and the fiber bed being composed of smaller fiber fragments with limited cross-linkage (i.e., that would pass through the 1/16” holes of the outer strainer).

Given the above analysis the resulting potential fiber accumulation on the internal divider plate screen is summarized as follows:

Initial Fiber	% Bypass Main Strainer	% Flow Crossing Divider Plate	% Accumulation on Divider Plate	Fiber on Divider Plate
25.5 ft <sup>3</sup>	1.25%	60%	34%	0.065 ft <sup>3</sup>

Fiber thickness on divider plate screen = (0.065 ft<sup>3</sup> /10 ft<sup>2</sup>) x 12 inches/ft = 0.078” < 0.125”

Therefore, insufficient fiber is available, even including the excess fiber in the strainer test, to develop a layer 1/8” thick given the credible fiber bypass values for the strainer and internal divider plate.

In summary, due to very conservative ZOIs creating the majority of generated fiber, considerably less fiber debris is expected to be generated than the amount credited. Due to the large distances from the limiting break for most of the fiber insulation, much of the fiber that is released would be expected to be in the form of large pieces and significantly less than the 100% value credited in strainer testing would be transported to the strainer as fines and very small pieces. However, even with these conservative fiber debris values combined with the additional fiber debris used in the strainer head loss test and flow through the internal divider plate associated with an active failure, the build-up of a filtering fiber bed on the strainer’s internal divider plate is not a credible outcome.

It is important when considering uncertainties with the preceding analysis to also weigh the potentially beneficial protective function provided by the internal divider plate. The plate, while not providing the same level of filtration protection as the main strainer, does provide an added degree of safety with respect to avoiding a possible common mode failure mechanism associated with a single sump pit providing suction source for both safety-related trains of equipment. Such a condition would be beyond the plant's design bases given the seismic qualification and other analysis to avoid possible threats (i.e., Seismic II/I, HELB dynamic effects, etc.) and detailed cleanliness and closeout inspections that are established to prevent foreign material inclusion or maintenance activities from affecting the strainer function. The presence of the internal divider plate provides an added defense in depth safety factor by greatly diminishing the potential for any of those conditions to adversely affect both trains of safety-related equipment required to function during sump recirculation.

**Structural Analysis:**

**A13. The letter dated November 21, 2007, "Revised Content Guide for GL 2004-02 Supplemental Responses," from NRC to NEI, in Section 3.k, "Sump Structural Analysis," requests a summary of structural qualification design margins for the various components of the sump strainer structural assembly. This summary should include interaction ratios and/or design margins for structural members, welds, concrete anchorages, and connection bolts as applicable. Please provide this information.**

The following additional details are being provided for the structural analysis.

**Design Conditions:**

Minimum sump water temperature during recirculation	60°F = 15.6°C
Maximum sump water temperature during recirculation	255°F = 123.9°C
Maximum containment air temperature	normal 120°F = 48.9°C accident 285°F = 140.6°C
Ambient temperature during installation	80°F = 26.7°C

The following table shows the load combinations to be considered.

Load Combinations:

LC No.	Temp. °C	Temp. °F	Combination	Loading Category	Stress Limit Factor
1	140	284	W	Normal	1
2	49	120	W + DE	Upset	1
3	140	284	W + ME	Faulted	1.5
4	124	255	W + ME + Sloshing	Faulted	1.5
5	15.6-124	60-255	W + W <sub>D</sub> + ME + Δp + Sloshing	Faulted	1.5
6	26.7-30.6	80-87	W + AddL	Normal	1

Where:

- W = Weight of structure
- W<sub>D</sub> = Weight of debris
- Δp = Pressure difference (0.0176 MPa)
- DE = Design Earthquake
- ME = Maximum Earthquake
- Sloshing = Sloshing Load
- AddL = Additional load during outage caused by radiation shielding blankets

Load combinations 1 to 3 and 6 are calculated with an empty pool. The other load combinations consider a filled pool and therefore the specific loads would be considered (e.g. sloshing, buoyancy). A temperature of 284°F for load combination 1 is a conservative assumption.

Allowable Stresses:

Allowable stresses are in accordance with the applicable code, "AISC; Manual of Steel Construction" for hot rolled parts and the "AISI; North American Specification for the Design of Cold-Formed Steel Structural Members" for cold formed parts.

Thermal Expansion:

To compensate the different thermal expansion of steel and concrete, sliding joints are provided between the sub floor framework and the supports. At the north and west wall the sliding parallel to the wall is allowed and restricted normal to the wall. At the east and south wall the sliding is allowed parallel and normal to the wall. Therefore, there are no significant temperature stresses if the strainers are exposed to air or are fully submerged. The temperature difference between bottom of strainer (submerged in hot sump water) and top of strainer (exposed to cooler containment spray) also does not cause significant temperature stresses because the strainers are free to move in vertical direction. For these reasons the specified temperatures are used only for evaluating the material properties.

A separate structural analysis for trash racks was not necessary, since this function is incorporated into the strainer design. The front face of the CCI strainer module design serves as a barrier for large debris pieces from reaching the strainer perforated plate surfaces which are recessed in pockets in each module. The vertical height of the strainers also serves to limit large debris from reaching the front of most of the modules since larger debris pieces, if transported, would be expected to remain on or near the floor.

The following load combinations represent the worst case loading for each component.

Coversheets:

Maximum coversheet displacement 5.1 mm (0.201")

Stress limit applies in case under consideration (load combination 5):

- Yield strength at 70°F  $F_y = 206.8 \text{ MPa} = 30 \text{ ksi}$
- Allowable stress value (membrane and bending)  $(0.9 \cdot F_y) = 186.1 \text{ MPa} = 27 \text{ ksi}$
- Allowable stress value (membrane)  $(0.66 \cdot 0.9 \cdot F_y) = 122.8 \text{ MPa} = 17.8 \text{ ksi}$
- Membrane stress (excluding local stress concentrations)  $100 \text{ MPa} = 14.5 \text{ ksi} < 17.8 \text{ ksi}$
- Membrane plus bending stress (excluding discontinuities and local stress concentrations)  $70 \text{ MPa} = 10.2 \text{ ksi} < 27 \text{ ksi}$

In this case, the worst case localized stress was selected for the membrane stress. Other than the some localized stress located at corners and bolt holes, the general membrane stress for the coversheet is zero or insignificant. Therefore, the membrane plus bending stress is generally equal to the bending stress throughout the coversheet.

Uplift at circumference:

The maximum uplift due to the pressure load at the circumference is 0.08 mm (0.003"). With the additional vertical loads (earthquake and weight contribute about 50% to the vertical loading) considered by linear interpolation the gap rises to about 0.16 mm (0.006"). This is a fifth of the allowed linear gap of 1/32" (0.79mm).

Framework:

The maximum framework displacement is 2.2 mm (0.087"). The maximum deflection of the mass point of the valve operator is 1.86 mm (0.073").

The stress limit applies in the case under consideration (load combination 5) (because buckling stress limit is the same as for bending no further evaluation is made):

- Yield strength at 70°F  $F_y = 206.8 \text{ MPa} = 30 \text{ ksi}$
- Allowable stress value (membrane and bending)  $(0.9 \cdot F_y) = 186.1 \text{ MPa} = 27 \text{ ksi}$
- Allowable stress value (membrane)  $(0.66 \cdot 0.9 \cdot F_y) = 122.8 \text{ MPa} = 17.8 \text{ ksi}$
- Membrane stress (excluding local stress concentrations)  $82 \text{ MPa} = 11.9 \text{ ksi} < 17.8 \text{ ksi}$
- Membrane plus bending stress (excluding discontinuities and local stress concentrations)  $120 \text{ MPa} = 17.4 \text{ ksi} < 27 \text{ ksi}$

Columns:

The columns are checked for compression. The maximum loads on the columns are:

- East Column                    63.3 kN = 14.2 kips
- West Column                    45.3 kN = 10.2 kips
- Stress limit                     $F_a = 13.76$  ksi
- Compression stress     $f_a = 5.929$  ksi <  $F_a$  13.76 ksi

Support Brackets:

The most loaded supports of each type are analyzed

The stress limit applies in the case under consideration (load combination 5):

- Yield strength at 70°F  $F_y = 206.8$  MPa = 30 ksi
- Allowable stress value (membrane and bending)  $(0.9 \cdot F_y) = 186.1$  MPa = 27 ksi
- Allowable stress value (membrane)  $(0.66 \cdot 0.9 \cdot F_y) = 122.8$  MPa = 17.8 ksi
- Allowable stress value for stiffener (buckling)  $(0.9 \cdot F_y) = 186.1$  MPa = 27 ksi
- Allowable stress value for fillet weld  $(0.3 \cdot F_u) = 144.8$  MPa = 21 ksi

Support	Membrane Stress <sup>1</sup> (ksi)	Allowable Membrane Stress (ksi)	Membrane + Bending <sup>2</sup> (ksi)	Allowable Membrane + Bending (ksi)	Buckling Stress – Stiffener <sup>3</sup> (ksi)	Allowable Buckling-Stiffeners (ksi)	Fillet Weld Stress <sup>4</sup> (ksi)	Allowable Fillet Weld Stress (ksi)
1.1	15.4	17.8	21.8	27	5.4	27	10.9	21
2.1	10.4	17.8	24.7	27	10.4	27	13.6	21
3.1	14.6	17.8	17.1	27	8.7	27	13.6	21
4.3	13.1	17.8	17.6	27	7.3	27	8.2	21
5.2	10.4	17.8	22.9	27	5.4	27	8.2	21

<sup>1</sup> Membrane stress excluding local stress concentrations

<sup>2</sup> Membrane plus bending stress excluding discontinuities and local stress concentrations

<sup>3</sup> Buckling stress on stiffeners excluding local stress concentrations

<sup>4</sup> Stress on fillet welds excluding local stress concentrations

Anchor Bolts:

Because no increases of the allowable forces apply, anchor bolt loads are stated only for load combination 5(W + WD + Δp + ME + Sloshing). The force direction is according to the coordinate system of the supports.

- $F_x$ : horizontal force parallel to sump wall
- $F_y$ : vertical force (positive ⇒ bolt force acts downwards); negative ⇒ bolt force acts upwards)

- $F_z$ : horizontal force perpendicular to sump wall (positive  $\Rightarrow$  compression force; negative  $\Rightarrow$  tension force)
- $f_v$ : shear load
- $f_t$ : tension load

The load is assumed to act in the most limiting direction; therefore, the calculated anchor bolt loads are conservative. Furthermore, the simulated position of the anchor bolt is at the middle of the allowed installation space and the reduction factors are conservatively calculated for the minimum distances and spacing. If the anchor bolts are installed at higher positions the tension forces are reduced.

Anchor Bolt Loads (forces in N)

Support	Weight + Pressure + ME + Sloshing					Comb
	F <sub>x</sub>	F <sub>y</sub>	F <sub>z</sub>	f <sub>v</sub>	f <sub>t</sub>	
1.1	-2905	-489	-6290	3512	6552	27.5%
1.1	2862	-173	-6517	3414	6789	28.6%
1.1*	-243	12154	-1768	13072	1842	93.8%
2.1	-5258	-365	-7041	6276	7334	40.8%
2.1	-251	8460	-10396	9102	10829	77.4%
2.1	5400	-1648	-8933	6751	9305	55.7%
2.1*	153	8676	856	9331	0	47.7%
2.2	-2016	3869	-4821	4803	5022	23.2%
2.2	-1163	4999	-8583	5550	8940	48.7%
2.2	2437	7187	-8512	8255	8866	58.9%
2.2*	751	8606	956	9297	0	47.5%
2.3	-436	6336	-9549	6833	9947	60.7%
2.3	234	1637	-9727	1782	10132	47.5%
2.3	273	7996	-6197	8604	6455	45.5%
2.3*	-131	8652	963	9305	0	47.5%
3.1	620	7367	-9592	7956	9992	65.7%
3.1	-149	-1407	-11175	1768	11641	59.4%
3.1	-491	5236	-13923	5660	14503	95.1%
3.2	-124	1998	-13359	2153	13916	80.1%
3.2	212	-567	-9622	752	10023	45.4%
3.2	-91	6455	-6367	6942	6632	39.3%
3.3	-1361	11716	-10272	12701	10700	95.8%
3.3	875	3674	-9993	4086	10409	54.8%
3.3	597	2612	-9139	2897	9520	45.2%
4.1	-1125	3156	-3046	3649	3173	12.3%
4.1	-657	5659	-4596	6135	4788	26.7%
4.1	1715	7873	-5484	8708	5713	42.0%
4.2	-1408	5506	-4191	6153	4366	24.9%
4.2	-78	6136	-4786	6599	4985	29.4%
4.2	1533	6406	-4743	7126	4941	31.3%
4.3	-1826	6983	-5362	7817	5585	37.3%
4.3	-50	7433	-6018	7993	6269	41.7%
4.3	1865	7817	-5647	8694	5883	42.8%
5.1	-920	6555	-5231	7133	5449	33.8%
5.1	-38	10754	-8975	11563	9349	79.1%
5.1	220	8087	-7623	8700	7941	54.8%
5.1	565	3432	-3145	3751	3276	13.0%
5.2	-747	6321	-4563	6855	4753	29.3%
5.2	-13	10089	-9411	10849	9803	78.5%
5.2	103	9614	-9294	10338	9681	74.9%
5.2	706	6138	-4395	6654	4578	27.7%

\* These bolts are installed at minimum embedment depth and the lower limits are applied

Analysis of Connection Angles:

The connecting bolts are lubricated and tightened to 70% of tensile strength.

For load combination 1, the stress limits applied are:

- Yield strength at 284°F  $F_y = 157.1 \text{ MPa} = 22.8 \text{ ksi}$ .
- Allowable stress value (membrane and bending)  $(0.75 \cdot F_y) = 117.8 \text{ MPa} = 17.1 \text{ ksi}$
- Allowable stress value (membrane)  $(0.66 \cdot 0.75 \cdot F_y) = 77.8 \text{ MPa} = 11.3 \text{ ksi}$
- Allowable stress value for partial groove weld  $(0.3 \cdot F_u) = 128.2 \text{ MPa} = 18.6 \text{ ksi}$

Type 1: Angle 1:

- Membrane stress (excluding local stress concentrations)  $17 \text{ MPa} = 2.5 \text{ ksi} < 11.3 \text{ ksi}$
- Membrane plus bending stress (excluding discontinuities and local stress concentrations)  $24 \text{ MPa} = 3.5 \text{ ksi} < 17.1 \text{ ksi}$

Connecting bolts allowables for load combination 1 are:

Allowables			Calculation Area		
	[MPa]	[ksi]		[mm <sup>2</sup> ]	[in <sup>2</sup> ]
Tension ( $F_t$ )	247.2	35.8	$A_t$	157	0.243
Shear ( $F_v$ )	73.7	10.7			

Type 2: Angle 39:

- Membrane stress (excluding local stress concentrations)  $19 \text{ MPa} = 2.8 \text{ ksi} < 11.3 \text{ ksi}$
- Membrane plus bending stress (excluding discontinuities and local stress concentrations)  $28 \text{ MPa} = 4.1 \text{ ksi} < 17.1 \text{ ksi}$
- Stress on partial groove welds (excluding local stress concentrations)  $< 13 \text{ MPa} = 1.9 \text{ ksi} < 18.6 \text{ ksi}$

Type 3: Angle 43:

- Membrane stress (excluding local stress concentrations)  $25 \text{ MPa} = 3.6 \text{ ksi} < 11.3 \text{ ksi}$
- Membrane plus bending stress (excluding discontinuities and local stress concentrations)  $43 \text{ MPa} = 6.2 \text{ ksi} < 17.1 \text{ ksi}$
- Stress on partial groove welds (excluding local stress concentrations)  $< 13 \text{ MPa} = 1.9 \text{ ksi} < 18.6 \text{ ksi}$

For load combination 5, the following stress limits applied are:

- Yield strength at 70°F  $F_y = 206.8 \text{ MPa} = 30 \text{ ksi}$
- Allowable stress value (membrane and bending)  $(0.9 \cdot F_y) = 186.1 \text{ MPa} = 27 \text{ ksi}$
- Allowable stress value (membrane)  $(0.66 \cdot 0.9 \cdot F_y) = 122.8 \text{ MPa} = 17.8 \text{ ksi}$
- Allowable stress value for partial groove weld  $(0.3 \cdot F_u) = 144.8 \text{ MPa} = 21 \text{ ksi}$

Type 1: Angle 13:

- Membrane stress (excluding local stress concentrations) 85 MPa = 12.3 ksi < 17.8 ksi
- Membrane plus bending stress (excluding discontinuities and local stress concentrations) 176 MPa = 25.5 ksi < 27 ksi

Allowables for load combination 5 are:

Allowables			Calculation Area		
	[MPa]	[ksi]		[mm <sup>2</sup> ]	[in <sup>2</sup> ]
Tension (F <sub>t</sub> )	375.2	54.4	A <sub>t</sub>	157	0.243
Shear (F <sub>v</sub> )	102.2	14.8			

Type 2: Angle 39:

- Membrane stress (excluding local stress concentrations) 74 MPa = 10.7 ksi < 17.8 ksi
- Membrane plus bending stress (excluding discontinuities and local stress concentrations) 86 MPa = 12.5 ksi < 27 ksi
- Stress on partial groove welds (excluding local stress concentrations) <41 MPa = 5.9 ksi < 21 ksi

Type 3: Angle 31:

- Membrane stress (excluding local stress concentrations) 84 MPa = 12.2 ksi < 17.8 ksi
- Membrane plus bending stress (excluding discontinuities and local stress concentrations) 150 MPa = 21.8 ksi < 27 ksi
- Stress on partial groove welds (excluding local stress concentrations) <82 MPa = 11.9 ksi < 21 ksi

Analysis of Strainer Box:

The maximum displacement is 7.2 mm (0.283"). Even with the relatively large deflection of the cover, no gap can occur at the circumference because the cover plates are bolted together with the bent flanges of the sidewalls.

Stress limits applied for the case under consideration (load combination 5):

- Yield strength at 70°F F<sub>y</sub> = 206.8 MPa = 30 ksi
- Allowable stress value (membrane and bending) (0.9\*F<sub>y</sub>) = 186.1 MPa = 27 ksi
- Allowable stress value (membrane) (0.66\*0.9\*F<sub>y</sub>) = 122.8 MPa = 17.8 ksi
- Allowable stress value for stiffener (buckling) (0.9\*F<sub>y</sub>) = 186.1 MPa = 27 ksi
- Membrane stress (excluding local stress concentrations) 110 MPa = 16 ksi < 17.8 ksi

- Membrane plus bending stress (excluding discontinuities and local stress concentrations) 110 MPa = 16 ksi < 27 ksi
- Buckling stress on stiffeners (excluding local stress concentrations) 110 MPa = 16 ksi < 27 ksi

Similar results in this case are due to insignificant bending stresses in the strainer box.

#### Analysis of Strainer:

Maximum displacement is 3.0 mm (0.118”).

Stress limits applied for case under consideration (load combination 5):

- Yield strength at 70°F  $F_y = 206.8 \text{ MPa} = 30 \text{ ksi}$
- Allowable stress value (membrane and bending)  $(0.9 \cdot F_y) = 186.1 \text{ MPa} = 27 \text{ ksi}$
- Allowable stress value (membrane)  $(0.66 \cdot 0.9 \cdot F_y) = 122.8 \text{ MPa} = 17.8 \text{ ksi}$
- Membrane stress (excluding local stress concentrations) 50 MPa = 7.3 ksi < 17.8 ksi
- Membrane plus bending stress (excluding discontinuities and local stress concentrations) 180 MPa = 26.2 ksi < 27 ksi

#### Analysis of Cartridges:

The maximum displacement is 1.19 mm (0.047”).

The stress limits applied for the case under consideration (load combination 5):

- Yield strength at 284°F  $F_y = 206.8 \text{ MPa} = 30 \text{ ksi}$ .
- Allowable stress value (membrane and bending)  $(0.9 \cdot F_y) = 186.1 \text{ MPa} = 27 \text{ ksi}$
- Allowable stress value (membrane)  $(0.66 \cdot 0.9 \cdot F_y) = 122.9 \text{ MPa} = 17.8 \text{ ksi}$

#### Unperforated sheets:

- Membrane stress (excluding local stress concentrations) 49 MPa = 7.11 ksi < 17.8 ksi
- Membrane plus bending stress (excluding discontinuities and local stress concentrations) 80 MPa = 11.6 ksi < 27 ksi

#### Perforated sheets:

- The calculated stresses are multiplied by the factor  $P/h=2.778$  to account for the perforation.
- Membrane stress (excluding local stress concentrations) 38 MPa = 5.51 ksi < 17.8 ksi
- Membrane plus bending stress (excluding discontinuities and local stress concentrations) 105 MPa = 15.2 ksi < 27 ksi

**A14. The Revised Content Guide for GL 2004-02 requests a summary of the evaluations performed for dynamic effects such as pipe whip and jet impingement associated with HELBs. The submittal which was provided merely states that, "...there are no credible jet impact hazards..." and "(t)here are no credible pipe whip effects..." Please provide a summary of these evaluations citing the reasons for the conclusion (e.g., protective barriers, the absence of high-energy sources, separation distance, administrative operational restrictions, etc.).**

The evaluation of potential dynamic effects such as pipe whip and jet impingement associated with HELBs was performed using standard criteria for such reviews. The evaluation includes both drawing reviews and field walkdown inspections. Some of the key inputs, assumptions, and analysis points are noted below:

Inputs:

- Break locations greater than ten pipe diameters from a target pipe or conduit are excluded from consideration for jet impingement damage. The selection of ten pipe diameters is based on NUREG/CR-2913 which demonstrates that the pressure on a target asymptotically approaches zero at a distance of ten pipe diameters from the break. This criterion is used in this calculation for target piping/conduit. Since the strainer may be somewhat less robust than pipe or conduit, an additional distance margin (80%) is utilized in this analysis ( $L/D > 18$ ). (L) is the vertical distance from the break to the maximum water level, and (D) is the nominal pipe diameter. The actual L/D is determined and, where applicable, shown to be greater than 18 pipe diameters.
- Dynamic effects of large breaks in the reactor coolant main loop piping are eliminated from consideration based on B&W Owners Group Reports BAW-1847, Revision 1, and BAW-1889P.
- The west secondary shield wall is 4'-0" thick and a significant portion of the strainer assembly is located below an opening in this wall.
- Entergy has committed to the single failure requirements of 10 CFR 50 Appendix K for ANO-1. Only active failures were considered in the evaluation of the final acceptance criteria for ANO-1.
- Active failures did not include check valve failures.
- Category 1 SBLOCAs ( $0.002 - 0.005 \text{ ft}^2$ ) do not result in sufficient RCS inventory loss to result in recirculation mode prior to orderly shutdown.

Pipe Break Assumptions:

- Non-mechanistic breaks (whose locations are arbitrarily selected without regard to any stress criteria) are assumed to occur at any location in piping systems operating at 300 psig or greater.

- Breaks in  $\frac{3}{4}$ " diameter or smaller lines are considered not to cause damage to other larger piping or system as is the generally accepted design practice.
- Piping is evaluated up to the first check valve from the RCS. Since ANO-1 only considers active failures that do not include check valves, the check valves are assumed to function and prevent an unisolable LOCA.
- Only line breaks postulated to create an unisolable primary system leak requiring operation in the recirculation mode are evaluated.
- ANO-1 SAR Section 16.3.9 addresses leak-before-break (LBB) with respect to the main RCS hot and cold legs and the dynamic effects from a LOCA. Based on the SE for NEI 04-07 and the LBB analysis for ANO-1, the LBLOCA from the cold legs is excluded from consideration of dynamic loads on the sump strainer.

Analysis:

Piping subject to HELBs were identified by first reviewing the RCS piping and instrumentation diagrams for piping connected to the RCS piping. For these lines, the closest isolation valve to the RCS piping was identified. Next, the piping isometric and piping area drawings were reviewed to determine the location of the piping relative to the strainer location. Pipe breaks were assumed to occur at any point in the unisolable portions of the RCS connected piping which may result in jet impingement or pipe whip on the strainers.

Mainsteam, feedwater, and SG blowdown piping were not considered since breaks in these lines do not require the plant to enter the recirculation mode of operation and thus do not require operation of the reactor building sump strainer. Similarly, piping connected to the RCS downstream of the identified isolation valve was not considered since it does not result in an unisolable break and does not require the plant to enter the recirculation mode.

The horizontal or vertical distance (L) from the break to the strainer envelope is divided by the nominal pipe diameter (D). This resultant L/D is used to evaluate the potential for damage due to jet impingement and pipe whip. An L/D of greater than 18 is established by engineering judgment to be sufficient to preclude damage to the strainer modules. Based on this conservative L/D value, many HELB locations are demonstrated not to require further consideration.

The HELB locations may be eliminated as potential impacts for any of the following reasons:

- The HELB locations are sufficiently distant (in three dimensions) from the strainer modules or conduit or piping entering the sump.
- The strainer modules or piping is shielded from the HELB by a wall, floor, or other structure.
- The HELB does not result in the plant entering recirculation mode and thus the strainer is not required to safely shut down the plant.

- Based on LBB, HELBs in the reactor coolant main loop piping are eliminated from consideration; however, a critical crack is assumed in the cold leg piping.

Pipe whip is evaluated on a case-by-case basis. Unisolable sections of the line are determined not to pose a pipe whip hazard to the strainers for any of the following reasons:

- The length of ruptured pipe is insufficient to reach the strainers.
- The geometry of the pipe routing precludes a pipe reaction that causes a pipe whip hazard to the strainers.
- The pipe break is small enough such that it does not result in the plant entering recirculation mode and thus the strainer is not required to safely shut down the plant.

In summary, the above inspection and analysis criteria was applied with the location of the ANO-1 sump strainer assemblies to conclude that there are no potential HELB sources that create pipe whip, jet impact, or missile hazards for the containment sump strainers. The HELB lines evaluated were addressed as not posing a threat due to distance from the strainers, a break not requiring sump recirculation, shielding, or excluded by LBB or similar criteria.

#### **Downstream Effects/In-Vessel:**

**A15. The NRC staff does not consider in-vessel downstream effects to be fully addressed at ANO-1 as well as at other PWRs. ANO-1's submittal refers to draft WCAP-16793-NP, "Evaluation of Long-Term Cooling Considering Particulate, Fibrous, and Chemical Debris in the Recirculating Fluid." The NRC staff has not issued a final SE for WCAP-16793-NP. The licensee may demonstrate that in-vessel downstream effects issues are resolved for ANO-1 by showing that the licensee's plant conditions are bounded by the final WCAP-16793-NP and the corresponding final NRC staff SE, and by addressing the conditions and limitations in the final SE. The licensee may also resolve this item by demonstrating without reference to WCAP-16793 or the NRC staff SE that in-vessel downstream effects have been addressed at ANO-1. Please report how it has addressed the in-vessel downstream effects issue within 90 days of issuance of the final NRC staff SE on WCAP-16793.**

The following preliminary review relative to the WCAP-16793, Revision 1 acceptance criteria is provided for comparison purposes only, since this document is not yet approved by the NRC, and additional changes to the acceptance criteria may be forthcoming.

The following table provides an ANO-1 comparison to the fuel analysis report. The more restrictive TRAPPER "fine mesh" debris limits for AREVA fuel are used as a limiting case.

Debris Type	Debris load per fuel assembly (lb)	Maximum debris load per qualification testing (lb)	% of allowable
Fiber	$\leq 0.24$	0.0326	13.6
Particulate	$\leq 29$	4.5	15.5
Chemical	$\leq 13$	4.35	33.5
Calcium-silicate	$\leq 6$	1.19	19.8
Microporous insul.	$\leq 1.2$	0	0

As can be seen from the above comparisons, the ANO-1 maximum debris load per analysis and testing remains significantly below the allowable values in the preliminary revision to WCAP-16793. While the final SE approved acceptance criteria for fuel blockage may change, given the ANO-1 margins to the current acceptance criteria the ANO-1 fuel analysis is anticipated to remain satisfactory. A formal response to this RAI will be provided pending issuance of the NRC's SE.

**Attachment 2 to  
OCAN090901  
ANO-2 RAI Responses**

## ANO-2 RAI Responses

In Entergy Operations, Inc. (Entergy's) final supplemental response of September 15, 2008, for Arkansas Nuclear One, Unit 2 (ANO-2), some of the more significant margins and conservatisms used in the strainer head loss calculations and testing were noted in Section 3.f.8. The following summarizes or clarifies the more significant conservatisms:

### Maximized Debris Generation:

- Calcium-silicate zone-of-influence (ZOI) of 25 pipe break diameters (25D) for lagging fastened with sheet metal screws was based on testing that did not result in failure of the lagging when exposed to the high energy jet with the most vulnerable orientation (i.e., 45° seam angle), nor was the underlying calcium-silicate exposed or released from the lagging.
- Calcium-silicate ZOI of 5.45D for banded lagging was based on testing performed on weaker aluminum lagging compared to the stainless steel lagging installed at ANO.

### Maximized Debris Transport:

- 100% transport of fibers, coatings, calcium-silicate fines and latent debris was credited to the strainers.
- Calcium-silicate fines transport tests conducted for ANO indicate that significantly less than 100% of the fines would transport to the strainer at velocities applicable to the ANO-2 basement during recirculation. As clarified in response to request for additional information (RAI) B6, no transport reduction was applied to calcium-silicate insulation fines as a conservatism to address possible uncertainties related to application of laboratory determined calcium-silicate erosion values to a post-loss-of-coolant accident (LOCA) environment.

### Conservative Head Loss Testing:

- Fiber added as all fines and very small shreds, separated into multiple containers to avoid agglomeration, slowly poured into a flowing flume to maximize even distribution.
- Near-field settling was not credited, avoided by stirring of the test flume.
- Testing was conducted for an extended time period (122+ hrs) to ensure bounding head loss effects were captured.
- Thin-bed conditions were established in the test with vertical debris distribution throughout the strainer pockets (i.e., including upper pockets) significantly more uniform than would be expected in the plant, based on pouring debris in increments into the top of a flowing flume and stirring of any settled debris materials to resuspend them.

- Testing included an excess of all debris material types above those calculated to ensure margin is available to address small changes in analysis, as-found conditions, or installed configurations. The final debris loading for strainer head loss testing expressed as a percentage of the amount identified in the debris generation calculation for the limiting break is as follows: total fiber – 261%; calcium-silicate – 218% of erosion total or 114% of debris generation total; coatings – 114%; latent particulate – 319%; miscellaneous foreign material – 760% (“tested” as allowance for blockage); chemical precipitates – 393%.
- Strainer testing was also conducted for another break, which produced higher fiber but lower calcium-silicate debris to ensure the most limiting debris mixture was used for credited strainer head loss.

#### Conservative Head Loss Analysis:

- Strainer test head losses measured at room temperature were acceptable without applying viscosity corrections. Strainer testing included flow adjustment checks to verify that jetting or blow-hole conditions would not inhibit the expected head loss reduction associated with reduced viscosity. Viscosity corrections may be applied in the future to the head loss results for determining net positive suction head (NPSH) margin or elevated temperature head losses, but the acceptability of the results prior to having applied this correction provides an indication of the significant margin available to address changes in system design or analysis.
- Peak head loss values were used versus more representative steady-state values.
- Head loss limits associated with NPSH requirements are only applicable at elevated sump water temperatures, which occurs relatively early in accident response and not all of the debris would be expected to have eroded and transported to the strainer during this time period; however, the debris loading included 100% of the fiber and particulate debris and a bounding quantity of calcium-silicate debris.
- Bounding flows were used for two-train operation of containment spray system (CSS) and injection pumps although securing one or both trains of CSS pumps would be expected prior to the formation of chemical effects precipitates at lower sump temperatures.

While not all of the above conservatisms have readily quantifiable impacts to the head loss test results, the aggregate effect provides a very high degree of confidence that evaluated test results are well bounding for any credible or design bases accident that requires sump recirculation. The multiple stacked conservatisms provide defense-in-depth to ensure that the systems and components needed to respond to a LOCA requiring sump recirculation would be able to perform their design function. Further, margin has been incorporated into the testing and analysis to allow for changes that may result from future identified debris sources or changes in the installed debris types without invalidating the strainer head loss test results or downstream effects analysis. Since the analysis has not relied upon credible operator actions such as securing one of the two operating trains, or securing CSS pumps at the earliest allowed opportunity, an additional potential course of corrective measures has been preserved.

Given the limited amounts of potentially detrimental remaining debris that could be affected by a LOCA, combined with the large surface area strainer installed, the expected outcome for even the incredible occurrence of a design bases double-ended guillotine break of the reactor coolant system (RCS) piping at the most limiting location relative to potentially affected debris sources, is that open screen would remain and thin-bed filtration conditions would not develop. In the unlikely event that such a break occurs and is combined with the high degree of insulation material destruction credited in the debris generation analysis, combined with high levels of transport of this material to the strainer as credited in the strainer testing, and uniform distribution of this material occurs across the strainer surface area similar to that achieved in the strainer test facility, then, the strainer head loss and other upstream and downstream effects have been shown to be acceptable as noted in the September 15, 2008, submittal.

Following are the specific responses to the RAIs:

**Debris Generation/ZOI:**

- B1. Please explain what it means to position the target with its center 90° from the jet (Table 3.b.3-1 in your letter dated February 28, 2008), specifically, whether this statement refers to a seam orientation of 90°. Provide the basis for this position being the most limiting position, since previous information indicates a seam orientation of 45° is the most limiting. This previous experience appears to be consistent with the statement on page 5 of the letter dated February 28, 2008, which indicates that Test #1 (with a 12D equivalent ZOI and 45° seam orientation) resulted in target material being dislodged from the pipe. Presumably no target material was dislodged in the test with a 7D equivalent ZOI. However, the only test conducted at an equivalent ZOI of 7D is one at a 90° seam orientation. Clarify the results for the tests discussed above and justify that the seam orientation for the 7D test was conservative.**

The jet impingement testing conducted by Westinghouse at the Wyle Labs test facility and documented in report WCAP-16836-NP included the testing of Transco Thermal-Wrap blankets or pads. The Thermal-Wrap blankets or pads tested were 2' by 4 ft by 4 in thick. The interior consists of low-density fiberglass batting that is encased in a thick, tightly woven fabric. These style blankets or pads are installed in ANO-2 on the pressurizer top and bottom heads, as well as around the interior of the lower pressurizer support base. The installation consisted of segments of the Thermal-Wrap pads that are not covered with metal lagging or otherwise enclosed in metal shielding. The pad was placed in a metal frame test stand to restrain them during the jet impingement test. The test stand included a solid back with the front and side cage framing to allow venting/escape of the impingement test fluids. The initial test oriented the bottom seam of the test pad in front of nozzle with the pad oriented at a 45° angle. The test resulted in the test pad being ejected out of the test stand and landing approximately 60 feet behind the test stand. The test pad outer blanket was not torn or destroyed and no insulation escaped. While this response is likely to be similar to the response that may be expected to occur in the plant, the test sample was not exposed to the jet impingement for the entire duration of the test, as was intended, thus adjustments were made to better restrain the test pads in the stand.

The test stand was modified to include solid metal side plates having oval shaped vent openings. This design was viewed as reducing the risk of blanket extrusion out of the test stand. Also, the stand orientation was shifted from a 45° angle to perpendicular (i.e., 90° angle) to the test nozzle. The 45° angle is important for tests performed with insulation that includes lagging, since earlier tests had shown that this seam angle for piping insulation was the most favorable (or conservative) for initiating damage by allowing the jet to catch the edge of the seam and tear the lagging away, exposing the underlying insulation. In the case of the Thermal-Wrap blanket pads the orientation of the jet relative to the blanket seam was not viewed as affecting the likelihood of failure of the seam, since there were not applicable failure mechanisms such as with a banded metal lagging lap joint on circular pipe. The 45° angle was also believed to have been partially responsible for the pad being ejected from the test stand. Therefore, unlike the jet impingement tests involving metal lagging that had a much higher potential for failure if the edge of the metal lap joint was oriented to allow it to be caught by the high energy jet, the Thermal-Wrap blanket seam orientation with respect to the test nozzle is not believed to affect the outcome of the tests, since there is no similar lip or other weak point that is more prone to failure based on orientation.

**B2. Considering that the ANO-2 debris generation analysis diverged from the approved guidance in NEI 04-07, please provide details on the testing conducted that justified the ZOI reductions for Transco Thermal-Wrap. Section C of this Enclosure includes a list of questions that the NRC staff has developed based on concerns with Westinghouse testing conducted at Wyle Labs. It is noted that ANO referenced WCAP-16836-NP, which was not specifically reviewed by the NRC staff. However, the NRC staff believes that the questions that were developed during the NRC staff review of the similar WCAPs apply generically to the testing credited by ANO.**

See responses to RAIs B22 through B50 in Attachment 3 and the discussion in Attachment 4 related to Westinghouse ZOI testing documented in WCAP-16836-NP.

As noted in the response to RAI B3a, the Transco Thermal-Wrap testing conducted at Wyle Labs by Westinghouse includes tests at equivalent ZOI distances of 7D and 12D. The response to RAI B3a provides additional detail regarding the test results and installed insulation for these two ZOI distances. Due to the distances of the installed Thermal-Wrap insulation in the ANO-2 containment from the potential break locations, the fiber debris totals for the analyzed breaks are not changed by the application of a 7D or 12D ZOI for the Thermal-Wrap material.

The ANO-2 design analysis for debris generation uses a 7D ZOI for Transco Thermal-Wrap. Due to the on-going resolution of NRC questions related to the ZOIs for materials tested by Westinghouse at Wyle Labs, information regarding the acceptability of strainer head loss is provided for an alternate case associated with a 17D ZOI for Thermal-Wrap. Transco's Thermal-Wrap is similar in construction to Nukon blanket insulation, with low-density fiberglass insulation batting encased in a heavy fiberglass cloth outer covering; therefore, the 17D ZOI noted in NEI 04-07 for this material is considered a conservative bounding ZOI value for Thermal-Wrap as well.

The strainer head loss tests conducted by Fauske for ANO included a variety of different debris loads. In anticipation of potential future changes to the installed or analyzed debris generation values, these tests included excess quantities of debris materials beyond that currently identified in the debris generation analysis (and erosion/transport analysis, where applicable). Different combinations of excess materials were included in various tests in accordance with the principal type of debris present for the break or set of breaks being evaluated by the test. The bounding head loss test for ANO-2 as described in the September 15, 2008, submittal and in these RAI responses included considerable calcium-silicate margin with lower excess fiber margin. This test serves as the “design” strainer head loss test for ANO-2 and compared to other strainer qualification tests, produced the highest strainer head loss results for two-train maximum flows with and without chemical effects precipitates, and a comparable but slightly lower head loss for the low-pressure safety injection (LPSI) pump failure to trip maximum flow condition.

In order to support a Thermal-Wrap ZOI larger than 7D or 12D, an alternate strainer head loss test could be credited for ANO-2. This test includes thin-bed fiber loading that bounds an ANO-2 limiting break with a 17D ZOI for Thermal-Wrap. The test includes a bounding quantity of all debris sources including calcium-silicate, but has considerably less margin for calcium-silicate insulation than the credited test. The head loss values for this test are also lower than those currently credited, other than for the LPSI flow condition. The strainer head loss values for the credited test are noted in response to RAI B14. A comparison between the credited test and the alternate higher fiber and lower calcium-silicate test results are provided below:

	Equiv. Head Loss @ Max Design Flow Credited Test (7D)	Equiv. Head Loss @ Max Design Flow Alt. Test (17D)	Allowable Head Loss	Maximum Design Flow
LPSI Flow	0.58 ft	0.62 ft	0.984 ft	12,735 gpm
2-Train Flow w/o chemicals	0.87 ft	0.34 ft	1.8 ft	7035 gpm
2-Train Flow w/ chemical effects debris load	3.4 ft	2.54 ft	5.9 ft	7035 gpm

NOTE: Additional calcium-silicate and fiber debris was added in the credited test between the LPSI and the two-train flow reading, resulting in the higher head loss value at lower flow, and additional calcium-silicate was added again after the two-train flow reading prior to adding chemical precipitates. The alternate test was conducted with a single debris loading versus an increasing debris load and was conducted at two bounding flow conditions, with equivalent head loss readings at the lower design maximum flow determined by linear extrapolation.

The currently credited strainer head loss test, with debris loading based on a Thermal-Wrap ZOI of 7D, provides ANO-2 with greater available margin for calcium-silicate debris but notably higher associated head loss results for the two-train flow condition with and without chemical precipitate materials and slightly lower associated head loss for the LPSI pump failure to trip condition. Both the currently credited strainer test and the alternate strainer test provide acceptable strainer head loss results. The currently credited case provides bounding debris loads for all debris sources with a Thermal-Wrap ZOI of 7D (results bound 12D ZOI as noted in RAI response B3a), while the alternate case provides bounding debris loads for all debris sources with a Thermal-Wrap ZOI of 17D.

Although an alternate test case is available to address possible changes to the ZOI applicable to Thermal-Wrap insulation blankets, this test case is not currently credited in the ANO-2 analysis documents and was not used as the basis for the September 15, 2008, submittal or related RAI responses in this submittal. The above alternate analysis and test results are provided for information purposes. Per the responses to the RAIs in this submittal, the Wyle Labs jet impingement tests were conservatively performed in a manner consistent with previous NRC or industry sponsored tests and these tests provide an appropriately bounding ZOI for the tested material. However, if the results of the on-going reviews of the 7D tests result in the need to significantly change the credited ZOI for Thermal-Wrap insulation, then in addition to the changes to the onsite ANO design documents, multiple sections of the September 15, 2008, submittal as well as the associated RAI responses in this submittal would need to be revised to reflect crediting the alternate test case.

With regards to related analysis such as downstream effects that could be affected by a change in fiber loading by an increase in the Thermal-Wrap ZOI, the analysis already includes sufficient fiber to bound the amount resulting from a 17D Thermal-Wrap ZOI.

**B3a. Page 5 of your letter dated September 15, 2008 (*should be February 28, 2008*), states that Transco Thermal-Wrap located at a distance of 7D would be expected to become dislodged, but not sustain damage due to jet impingement, such that fibrous debris would be generated. This statement appears to be based on observations that a blanket during Test #1 was dislodged, which apparently occurred at a 12D scaled ZOI. In light of the fact that Transco Thermal-Wrap was dislodged at an equivalent ZOI of 12D, what is the basis for defining a spherical ZOI of 7D for the plant condition?**

As noted in the response to RAI B1, Transco Thermal-Wrap insulating pads were tested at the Wyle Labs test facility by Westinghouse for ANO. The tests address the insulation installed at ANO-2 on the top and bottom heads of the pressurizer as well around the interior of the bottom skirt or base support just below the lower head.

The Transco Thermal-Wrap blanket tests were intended to sufficiently restrain the test blanket in order to determine the robustness of the cover material when subjected to a high energy jet and were not intended to show that the blankets would be ejected away from their installed location. The test stand cage restraint used in the initial 12D ZOI test, while somewhat less restrictive than the modified cage used for the subsequent tests, was still considered to be more restrictive than the installed configuration of the blankets

in the ANO containment. The initial test resulted in the blanket being ejected out of the stand away from the source of the equivalent 12D ZOI break. Therefore, similar response of being ejected away from the break was concluded to be the most credible result of steam jet interaction at 7D or 12D ZOI distances. However, additional testing was conducted to determine if the blankets could withstand the high energy jet forces at those distances if restrained.

The Transco Thermal-Wrap blanket that was dislodged at an equivalent ZOI of 12D was not damaged after having been ejected approximately 60 feet from the test stand. The blanket cover was intact and there was no loss of the internal fiberglass insulating material. Thus, if a blanket were similarly dislodged such that it was not exposed to sustained high energy jet impingement, then it would be expected to also retain its internal fiberglass insulation in similar fashion. The Thermal-Wrap blanket tests included two additional tests following the test in which the blanket was extruded out of its stand. The second test was also at a 12D ZOI with a modified test stand to eliminate the potential for the blanket to be ejected out of the stand. Following the successful completion of the 12D ZOI test, a third test was conducted at a ZOI of 7D.

The results of the second test, conducted at an equivalent ZOI of 12D, demonstrated that even if restrained, the blanket material of the Transco Thermal-Wrap insulation would not be damaged. Thus, the fibrous internal material would not be a debris source. The reconfigured test stand, used in the second and third tests, restricted the test blanket from being ejected during the test. The tested configuration was to evaluate the blanket materials ability to withstand the forces of jet impingement rather than to represent the more loosely constrained as-built configuration.

While an additional test at a 7D ZOI was conducted, as described below, which provided supporting evidence for a reduction in the credited ZOI to 7D, the Thermal-Wrap fiber contribution to break debris loads is not affected by the reduction in ZOI from 12D to 7D. This is due to the installed locations of the ANO-2 Thermal-Wrap and changes made to the modeled break locations which maximized combinations of calcium-silicate and Thermal-Wrap fiber debris. Explanations of this are provided following the below description of the 7D ZOI test.

The third test involving the Transco Thermal-Wrap insulating blanket placed the test stand 80.4" from the jet nozzle (7D equivalent ZOI). The third test resulted in a small amount of internal fibrous insulating material being released from the blanket, although this was determined to be due to interaction with the test stand. Observations of the test article immediately after the test was secured and of the video record of the test determined that the jet forced the blanket into the pressure relief holes cut into the test stand. As the blanket was forced into the pressure relief holes in the stand, the insulation material in the blanket became compacted and acted as a plug. Post-test pictures document the blanket having compacted to approximately 1/3 its normal height and extruding out the upper vent openings of the stand. Fluid entering the blanket due to the jet force was restricted from exiting the blanket through the compacted insulation material. The combination of additional fluid retention in the blanket, the flashing of liquid within the blanket resulting in increased stress in the blanket cover material, and the interaction of the blanket material with the test stand collectively over-stressed the blanket material until the seam on the right side was torn open. The torn seam provided

an outlet path for the steam and vapor trapped in the blanket and allowed extrusion of a small amount of the insulating material through the seam, while the rest of the insulating material remained intact inside the blanket. The seam failure occurred as the test was being terminated after approximately 25-30 seconds of jet impingement while the discharge tank isolation valve was closing.

It was observed that the blanket did not fail due to direct jet impingement, but rather due to the interaction of the blanket with the test stand. Other than the small amount of insulation material blown out at the ruptured seam, the majority of the insulation material remained enclosed within the blanket. The lower left side of the blanket was also found torn in three places. These tears were not located along the seams or in an area subject to direct jet impingement, but were also located at an area where the blanket was extruded through slots in the test stand provided for pressure relief. These tears were evaluated to have been caused by interaction with the test stand frame. No insulation had separated from the blanket at these small tears.

The Transco Thermal-Wrap blanket was tested in a configuration that was not representative of the installation configuration at ANO-2 since the intent of the testing was to restrain the blanket to allow evaluation of the cover material performance under jet impingement. The observed damage to the blanket and seam were not at locations of jet impingement, but at locations where unintended interactions of the test blanket and test stand were occurring due to shifting of the blanket/pad within the stand. This damage mechanism resulted in a small amount of fiber release from the test blanket at a 7D ZOI, but was determined not to be representative of expected response in the plant. Thus, based on the absence of damage to the Thermal-Wrap outer cover fabric or seams in areas exposed to the jet impingement in any of the three tests, the cause of the limited damage observed in the 7D test being attributable to localized interaction issues with the test stand device, and the more likely expected response of the pads being dislodged intact from their location on the pressurizer heads, the test results were concluded to bound a ZOI of 7D.

These tests were performed to address the specific application of the Transco Thermal-Wrap pads installed on the pressurizer at ANO-2. Since the materials being evaluated are installed at only two discrete locations (i.e., top and bottom of the pressurizer), further explanation is provided regarding the significance of the credited ZOI and its application to ANO-2.

The pressurizer is located within the south steam generator (SG) cavity in ANO-2 but includes a shield wall at the bottom of the pressurizer and a concrete floor slab, which includes an annulus opening for the pressurizer surge line. The Thermal-Wrap insulation on the lower pressurizer head and mounting skirt is shielded from direct jet impingement from breaks other than breaks of the surge line itself (evaluated as break "S4" in the debris generation calculation). The insulation on the top of the pressurizer head could be affected by a hot leg break, although it is at a distance of greater than 12D at its closest point. The Thermal-Wrap insulation destructive test ZOI of 12D was based on the closest proximity of a hot or cold leg RCS pipe to the Thermal-Wrap insulation on top of the pressurizer being greater than a 12D ZOI distance. A second ZOI test distance of 7D was selected in order to bound the distance away from the bottom of the pressurizer where a surge line break would need to be considered and still potentially release the

Thermal-Wrap insulation on the bottom head and skirt. The two principal breaks of interest at the time of the ZOI testing were a hot leg break that released a significant amount of calcium-silicate insulation and potentially fiber from the pressurizer head (if a ZOI >12D was applicable), and a surge line break that released a larger amount of fiber insulation (larger volume of Thermal-Wrap on the bottom head/skirt area) but a smaller amount of calcium-silicate insulation.

However, after the Thermal-Wrap ZOI tests were conducted in Summer 2007, additional insulation removal was performed during the 2R19 outage (Spring 2008) that significantly reduced the amount of insulation (particularly calcium-silicate insulation) potentially affected by all breaks. Following these modifications, the pressurizer surge line break (S4) location was conservatively relocated further from the pressurizer and below the floor slab in order to maximize both the amount of calcium-silicate (located further from the pressurizer) and Thermal-Wrap fiber insulation at the bottom of the pressurizer and skirt area. Due to the surge line pipe orientation turning underneath and away from the pressurizer floor slab past this break location, significant shielding or shadowing of the Thermal-Wrap would occur.

Thus, while a 7D ZOI has been established from the Wyle Labs tests, the credited break locations have already maximized the potential combination of fiber from Thermal-Wrap insulation and calcium-silicate insulation, unless a ZOI of > 12D were credited. The 12D ZOI tests included two different tests, with one resulting in the test pad being ejected from the stand and the second test with the pad being retained in the test stand. None of the internal fiberglass insulation was released from the blanket in either test.

**B3b. Please describe to what extent the ZOI testing was prototypically scaled to model the size distribution of the debris resulting from the insulation destruction testing.**

The resulting insulation debris credited as being produced from the ZOI Thermal-Wrap tests conducted for ANO was treated as having been destroyed to 100% fines and very small pieces that would all transport to the strainers. This addresses the potential change in size distribution associated with an increase in the credited destruction pressure for this material from the 60% small fines and 40% larger piece distribution accepted in NEI 04-07 for Nukon insulation with a credited destruction pressure equivalent to a 17D ZOI.

See the response to RAI B4 for discussion of the calcium-silicate size distribution.

**B3c. Please provide a basis for concluding that the behavior observed in Test #1, where insulation was dislodged without releasing fibrous debris, is repeatable.**

The basis for the lack of release of fiber insulation from the Transco Thermal-Wrap blankets was that in each of the three tests, the outer fabric or seams were not ripped or torn as a result of impingement from the high energy fluid from the test jet, including the initial test in which the tested blanket was ejected from the test stand. The conclusion that internal fibrous debris would not be released is based upon the robustness of the fabric blanket cover layer used in the Transco Thermal-Wrap insulation. Further discussion of the test results and the application of the test to ANO-2 is provided in response to RAI B3a.

**Debris Characteristics:**

- B4. The NRC staff SE on NEI 04-07 recommended that calcium-silicate debris be assumed as 100% small fines. The assumption made in the supplemental responses appears to be that 40% of calcium-silicate debris is fines and 60% is large pieces. Please provide a technical basis for the assumed debris size distribution for calcium-silicate. In addition, please provide a comparison between the assumed calcium-silicate debris size distribution and the sizes of the calcium-silicate pieces used in the erosion testing program that shows that the tested size distribution is prototypical or conservative.**

The size distribution of calcium-silicate insulation as applied to ANO-2 was derived from the NRC supported Ontario Power Generation (OPG) testing as documented in NUREG/CR-6808. NEI 04-07, Volume 1, Section 3.4.3.3.3 notes this information source stating that "Test 5 indicated that the size categories adopted by this guideline would be 50% for small fines and 50% for large calcium-silicate pieces. Given the uncertainties in the subsequent erosion by the post-DBA water, this guideline assumes that 100% of calcium-silicate in a ZOI is destroyed as small fines." The size distribution for Test 5 as presented in Table 3-6 of NUREG/CR-6808 indicates that of an initial weight of 2109 g, the following post-test weights were noted: 1112 g remained on the target (or pipe) representing 52.7%; 238 g of debris pieces were greater than three inches, representing 11.3%; 247 g of debris pieces were one inch to 3 inch size, representing 11.7%; 31 g were less than one inch, representing 1.5%; and 481 g were classified as dust, representing 22.8%. Thus, the referenced test data indicates that of the initial mass only 47% was released from the target pipe and of that quantity approximately 50% was fines and less than one-inch sized pieces, but this represented only 24.3% of the total calcium-silicate insulation weight.

The NRC's Safety Evaluation (SE) for NEI 04-07, documented in Volume 2 of that document, notes in the SE of Section 3.4.3.3 that "Materials for which the debris generation is not known well enough to conservatively estimate debris size distributions; therefore, maximum destruction is assumed." While no specific reference of this category to calcium-silicate was made it presumably was intended to address materials that are classified with 100% destruction to fines. Appendix II of the SE in Section II.3.3.2 notes that the OPG tests addressed a limited range of damage pressures (approximately 24 to 65 psi) with Table II-9 providing the results of calcium-silicate debris size distribution integration over the ZOI with an equivalent ZOI of 5.4D having a fraction of small fines at 42% and an equivalent ZOI of 6.4D having a small fines fraction of 34%.

NUREG/CR-6808 includes two sets of test data regarding destructive steam jet testing of calcium-silicate insulation as described in Sections 3.2.2.3 and 3.2.2.5. Data Tables 3-4, 3-5, and 3-6 provide the results from these tests. From Table 3-5 it is noted that of tests with a single layer of aluminum cladding that four out of seven tests with seam orientations other than 45° did not result in the release of any insulation, with one of the three that did release material noted only as "small amount" and not included in the debris totals of Table 3-6. The five tests conducted with a 45° seam angle all resulted in the release of some insulation. The seven test results reported in Table 3-6 were only those that resulted in appreciable release of calcium-silicate insulation. The use of 40% small fines provides a conservatively bounding value relative to applicability to ANO based on the following:

- Entergy has applied a ZOI of 25D for calcium-silicate installed with stainless steel jacketing secured with sheet metal screws instead of the customary banding. This very large ZOI is equivalent to a destruction pressure of < 3.5 psi.
- Entergy has applied a ZOI of 5.45D from NEI 04-07 derived from the OPG tests with weaker aluminum lagging compared to the stainless steel lagging used at ANO.
- The “Studsvik” tests, described in Section 3.2.2.3 of NUREG-6808, were performed with the jet positioned between two and ten break diameters from the sample. The tests were conducted with boiling-water reactor (BWR) equivalent steam conditions of 1160 psia and 535°F. The stagnation pressure at the erosion limit (or maximum distance from the break where significant erosion was observed) was 24 psia or approximately 9.3 psig, which is equivalent to a ZOI distance of approximately 12D. The tests resulted in small pieces to fines ranging from 23% to 45%.
- The OPG tests described in Section 3.2.2.5 were performed with water/steam jets supplied from a 1450 psia source at 324°F. The targets consisted of calcium-silicate insulation covered with aluminum lagging and stainless steel banding. Tests were conducted with the jet between five and 20 break diameters (not ZOI) from the pipe. The test data indicates that the amount of dust or fines combined with pieces under one inch ranges from 15% - 31%. Even at the 5D tests 53% of the calcium-silicate remained intact on the pipe and only 36% was liberated as dust up through three-inch pieces. At 20D, 78% of the calcium-silicate remained on the piping and only 18% was dust through three-inch pieces.
- OPG tests with seam orientations other than 45° resulted in the lack of insulation release from the majority of tests and included relatively close test distances of five to seven break diameters from the test nozzle.
- Standard insulating practice for lagging seam orientation on horizontal pipe is not random, but is to point the seam opening downward. This orientation is used to avoid the potential for fluids dripping on the lagging from catching on an upward turned seam angle and wetting the underlying insulation. Since approximately half of the ANO-2 ZOI affected calcium-silicate insulation is in horizontal pipe below the limiting break location, a favorable 45° seam angle relative to the break jet would not exist. Therefore, much of the calcium-silicate insulation credited as debris would most likely neither be released nor exposed.

In comparison, the 25D ZOI used for unbanded insulation (i.e., lagging secured with sheet metal screws) results in the majority of the unbanded calcium-silicate insulated pipe in the affected SG cavity being included in the break total for larger pipe breaks. The destructive test performed for ANO at 25D ZOI equivalent distance for pressurized water reactor (PWR) pressure/temperature conditions did not result in failure of the insulation lagging and did not liberate any of the internal insulation and is therefore considered a conservative ZOI. The “Studsvik” test indicated that significant erosion of calcium-silicate samples from the break jet did not occur beyond a destruction pressure of 24 psia or approximately 9.3 psig, which is equivalent to a ZOI of approximately 12D. At increased distances decreased amounts of material would be liberated as fines or small pieces. The ANO-2 calcium-silicate insulation ZOIs include 5.45D banded calcium-silicate, which produces only 10% of calcium-silicate debris generated), and 25D

for calcium-silicate covered with sheet metal screwed lagging, which produces over 2/3 of calcium-silicate debris generated. The approximately 20% of the calcium-silicate insulation debris remaining is not generated directly by the break, but is located outside the SG cavities and is associated with unlagged calcium-silicate, primarily mastic cement, that were conservatively treated as debris due to potential exposure to spray or submergence. This 20% of the total calcium-silicate insulation would not have any initial fines associated with the break, since its only source of release is through erosion from CSS or immersion. Thus, based on the above comparison of industry test data results and ANO-2 conditions, crediting the composite ZOI generated calcium-silicate debris as initially consisting of 40% fines and 60% large pieces is considered a conservative distribution.

**Latent Debris:**

**B5. Your letter dated September 15, 2008, indicated that you had taken samples for latent debris in your containment, but the submittal did not provide any details regarding the number, type, and location of samples. Please provide these details; in particular, identify the extrapolation method used, including the statistical deviation of the results.**

The latent debris sampling involved dividing the containment surfaces into different types and calculating their area. The surface types included: floor areas, containment liner, horizontal ventilation, vertical ventilation, horizontal cable trays, vertical cable trays, walls, horizontal equipment, vertical equipment, horizontal piping, and vertical piping.

A sample was obtained by wiping the sample surface area with a clean Masslin cloth for each type of surface on various elevations at accessible areas. Each sample was bagged and the sampled surface area was recorded. Forty-two samples were taken from the eleven types of areas. The following table summarizes the sampling taken for each surface type.

Surface Type	Surface Area Sampled (ft <sup>2</sup> )		Total Containment Area for Surface Type (ft <sup>2</sup> )
	#Samples	Total	
Floor Areas	4	52.5	33,186
Containment Liner	4	80.39	75,983
Horizontal Ventilation	4	36.75	10,576
Vertical Ventilation	4	78.71	15,834
Horizontal Cable Trays	4	22.83	23,731
Vertical Cable Trays	3	98.75	6,690
Walls	4	89.51	62,676
Horizontal Equipment	3	21.31	5,709
Vertical Equipment	4	94.8	25,568
Horizontal Piping	4	45.84	25,598
Vertical Piping	4	59.13	6,362

The samples were weighed and the difference in the before and after cloth sample weight indicated the amount of latent debris present, which was divided by the area sampled to get a surface loading in weight per unit area. Multiple samples of like surfaces were averaged. The data was statistically analyzed and a 90% confidence upper limit was obtained. The total area within containment was multiplied by the 90% upper limit unit surface loading to get the total latent debris on each surface type. The total latent debris in containment was obtained by adding all of the surface type totals.

Miscellaneous items, such as various structural steel, pipe, conduit, cable tray, support steel, control rod drive mechanisms, cooling fans, heat exchangers and smaller items such as junction boxes, valve operators, air handlers, seismic restraints, electrical panels, monitoring devices and others, are not addressed individually in this calculation. The conservatism adopted in the calculation in estimating total areas of major items addressed above is considered to provide enough margin to cover areas of miscellaneous items inside the containment. The measurements were taken during the refueling outage prior to building clean-up as a conservative measure to obtain a bounding value.

The total latent debris calculated using this approach was approximately 47 lbs. The debris testing and analysis included margin for significant additional particulate and fiber debris beyond this amount. The amount of margin noted in the introductory section for the ANO-2 RAI responses under the heading "Conservative Head Loss Testing" lists the margins as percentages, with the latent debris comparison percentage based on a nominal 150 lbs. This value represents a significant margin above the measured value for ANO-2 as well as that measured for ANO-1. However, use of the nominal latent particulate loading is listed for comparison purposes of available margin. The actual margin allocation of the excess fiber and particulate included in the strainer head loss test could be increased or decreased for latent debris, coatings, or insulation, as needed due to future changes in analysis and/or plant conditions.

#### **Debris Transport:**

- B6. It is not apparent that the calcium-silicate transport testing for ANO-2 was conducted in a manner that is prototypical or conservative with respect to the plant conditions during a design basis event. Based on Reference 2, it appears that this calcium-silicate transport testing will not be credited in the analyses demonstrating strainer adequacy for ANO-2. Please confirm the basis for this statement.**

The final supplemental response dated September 15, 2008, Section 3.e.5, wording is revised by this response with regards to the crediting of calcium-silicate fines transport. The analysis of calcium-silicate erosion and transport testing performed by Fauske concludes that these test results support a significant reduction in the total amount of calcium-silicate reaching the sump strainer as fines due to a combination of both limited erosion and limited transport of this material. The results of the reductions associated with both erosion and transport were presented in the final supplemental response dated September 15, 2008, Table 3.e.5-1. The credited erosion rate for calcium-silicate has been updated as noted in response to RAI B7, and the transport testing is conservatively not credited.

In regards to calcium-silicate erosion and transport analysis, the final supplemental response dated September 15, 2008, states, "While these numbers were arrived at using relatively conservative treatment of the test data, it is recognized that considerable uncertainty exists when extrapolating laboratory test conditions to a post-LOCA environment." To address this uncertainty, the results of the calcium-silicate fines transport testing are not credited for reduction of the amount of fines arriving at the strainer, such that all fines created are credited with 100% transport to the strainer. This does not consider the transport analysis to be invalid, but avoids the added uncertainties associated with crediting a specific threshold for transport reduction of fines and provides significant conservatism to address any remaining uncertainty with the amount of credited calcium-silicate fines created from both the initial breaks and erosion of larger pieces. Neglecting the transport reduction results in a very substantial increase (multiple of approximately 17x) in the amount of calcium-silicate fines assumed present in the initial 72-hour period and more than doubles the final calcium-silicate to be addressed for the final head loss value.

In summary, not crediting the transport test results and assuming 100% transport of the calcium-silicate fines to the sump strainer is believed to result in a conservative margin that bounds the recognized uncertainties in the application of laboratory test results for calcium-silicate erosion to the dynamic interaction conditions of a post-LOCA containment environment. While uncertainties exist in the establishment of numeric limits for erosion of calcium-silicate insulation debris based upon the results of laboratory tests, the underlying conclusions from the series of tests conducted are believed to remain valid. Specifically, the conclusions from the tests are, 1) calcium-silicate insulation affected by a LOCA is not 100% reduced to fines, and 2) fines that are generated are not 100% transported to the sump strainer. These conclusions were reached for the ANO-2 materials and conditions related to the applied ZOIs, installed insulation configurations, ANO-2 flow velocities, and the ANO-2 strainer type and location. Further discussion of the Fauske testing of calcium-silicate erosion tests, transport tests, and dissolution tests are provided in response to RAI B7.

- B7. In the NRC staff's audit report for Salem Nuclear Generating Station, Units 1 and 2, dated August 12, 2008, several technical issues were identified with respect to erosion testing that had been performed at the contractor's facilities. These technical issues included (1) non-conservatism associated with the modeling of turbulence in the test flume, (2) the use of regularly shaped debris pieces as opposed to irregular pieces that would be more prone to erosion, and (3) anomalies in the test data, wherein a significant number of long-term tests had lower cumulative eroded mass values than short-term tests. Please address whether and to what extent these issues affected the erosion testing for ANO-2 conducted at the Fauske facilities.**

The credited 30-day erosion total for calcium-silicate large pieces is being revised from the values listed in Section 3.e.5 of the final supplemental response dated September 15, 2008, to 30% based on the following considerations:

- The volume of calcium-silicate debris generated is conservatively large based on the use of a 25D ZOI for this material covered with sheet metal screw fastened lagging versus stainless steel lagging.
- Banded calcium-silicate insulation, with a ZOI of 5.45D, represents only approximately 10-20% of the total calcium-silicate generated by the limiting breaks of interest.
- Approximately half of the calcium-silicate insulation debris generated by the limiting break *S6 Cold Leg* and one-third of that generated by the break *S1 Hot Leg* with the next highest calcium-silicate insulation debris total is from horizontal pipes located below the breaks. Standard insulation practices results in a downward facing lagging seam angle, which is not likely to result in release of insulation debris.
- Calcium-silicate fines transport testing conducted for ANO indicates that substantially less than 100% of the fines generated would be expected to transport to the strainer. ANO did not credit the transport reduction and did not credit near-field settling in strainer head loss testing, providing a significant source of compensating conservatism to address possible uncertainties with the calcium-silicate erosion test results.

The erosion rate is applied for two time periods: the initial three days and the 30-day time period as shown in the table below. These time periods address the early elevated temperature period when NPSH margins are at a minimum, and the 30-day time period when debris loading is at a maximum, but strainer structural design limits govern the maximum allowable head loss.

Erosion and Transport Values for ZOI Generated Calcium-Silicate Fines:

	Initial Fines	+ Large Piece Erosion	Fines	% Fines Transported	Net
3-day	40%	13.9% of 60%	49%	100%	49%
30-day	40%	30% of 60%	58%	100%	58%

Erosion and Transport Values for non-ZOI Generated Calcium-Silicate Fines:

	Initial Fines	Erosion	Fines	Transported %	Net
3-day	0%	13.9%	13.9%	100%	13.9%
30-day	0%	30%	30%	100%	30%

Details of both the erosion and transport testing, which included dissolution testing, conducted at Fauske for ANO are included in this response. The response to RAI B6 provides updates to the final supplemental response dated September 15, 2008, Section 3.e.5 regarding the conservative exclusion of the calcium-silicate fines transport

test results to address potential test uncertainty issues with application of the erosion test data. Calcium-silicate erosion testing was performed by Fauske for ANO, and the following brief description of the test is provided:

- Tested at flow velocity of 0.7 feet per second (fps).
- Test performed with 12 total samples, six each of one-inch and two-inch cubes of calcium-silicate insulation.
- Exposure times of 17, 45, 66, 90, 112, and 135 hours were included.

The following addresses erosion testing results and conclusions. The table below presents the eroded sample mass for each of the 12 samples. The mean and standard deviations for each of the six samples of each sample size are determined to be 7.2% ±1.2% for the nominally two-inch pieces and 11.5% ±1.4% for the nominally one-inch pieces. The eroded mass for each sample size is seen to be approximately constant with little correlation to exposure interval. This interpretation would suggest that only a low percentage (< 14%) of the initial debris mass would be eroded by a continuous water stream even for a longer exposure interval. Furthermore, if the eroded mass is not a function of exposure interval, then an erosion rate calculated for longer and longer exposure intervals would become smaller and smaller.

Sample #	Sample Size	Initial Mass (g)	Final Sample Mass (g)	Eroded Mass (g)	Eroded Mass (%)	Erosion Time (hrs)
1	2" x 2"	31.0746	29.4770	1.5976	5.1412	17.22
2	2" x 2"	29.5848	27.5593	2.0255	6.8464	45.23
3	2" x 2"	29.1102	26.7656	2.3446	8.0542	66.50
4	2" x 2"	30.1820	27.8156	2.3664	7.8404	90.52
5	2" x 2"	33.6802	30.8740	2.8062	8.3319	112.83
6	2" x 2"	34.4052	32.0130	2.3922	6.9530	134.88
1	1" x 1"	2.9209	2.6103	0.3106	10.6337	17.22
2	1" x 1"	3.6729	3.2273	0.4456	12.1321	45.23
3	1" x 1"	3.6726	3.3027	0.3699	10.0719	66.50
4	1" x 1"	3.3100	2.9360	0.3740	11.2991	90.52
5	1" x 1"	3.8459	3.3102	0.5357	13.9291	112.83
6	1" x 1"	3.4007	3.0217	0.3790	11.1448	134.88

The following provides erosion testing observations:

- The largest percentage mass lost was 13.9% for a one-inch cube and 8.3% for a two-inch cube.

- The “eroded” mass for each sample size is approximately constant with little correlation to exposure interval.
- A decreasing erosion rate (determined by extrapolating measured erosion out for 30 days) is seen with increasing exposure duration, consistent with the above observation.

The following critique has been applied to the test results by ANO:

- Testing was conducted at room temperature. Dissolution of calcium-silicate at elevated temperatures was reported in NUREG 6772, contributing to the guidance in NEI 04-07 calling for the assumption of 100% reduction of displaced calcium-silicate into fines. Testing conducted at Fauske facilities with calcium-silicate insulation used at ANO and conditions similar to those documented in NUREG 6772 (i.e., tests conducted at 20°C and 80°C) did not indicate a temperature dependency for dissolution of calcium-silicate in water. A weight change less than 5% occurred for ambient temperature and elevated temperature tests. These tests indicate that for material consistent with that installed at ANO-2, increased calcium-silicate dissolution at elevated temperatures would not be expected to occur; therefore, the test results are considered applicable over the range of post-LOCA sump temperatures.
- The tests showed a higher percentage mass loss for the smaller one-inch cube sample compared to the two-inch sample. This appears to be based on the surface area to mass ratio, with most of the “erosion” being related to disturbed material at the sides of the blocks from the cutting/preparation phase and the initial wash-off of these disturbed edges during the test being the likely cause of the majority of the observed mass reduction, since the results did not show a time exposure dependency. Erosion of large pieces would include pieces presumably both larger and smaller than one-inch blocks and irregularly shaped pieces may have a higher surface area to mass ratio than the square blocks tested. NUREG 6808 Table 3-6 provides information regarding the size distribution of calcium-silicate insulation debris generated by simulated breaks at varying distances. This data shows that at all of the distances tested, the mass fraction of released debris as pieces less than one inch is small (<31% of mass of pieces released). Thus, the use of the higher erosion values associated with the one-inch test cubes being applied to all calcium-silicate pieces should be conservatively bounding with regards to actual values that include variations in the sizes and the surface area to mass ratio of debris pieces.
- The test was conducted with fully immersed pieces, representative of larger pieces that have fallen to the basement (flooded), but may not be representative of pieces that have become exposed to CSS droplet impingement erosion due to dislodged lagging or pieces lodged in or landing on grating surfaces. It is noted above that NUREG 6808 test results show a substantial majority of the displaced calcium-silicate remains as pieces larger than one inch, which would not readily pass through grating having rectangular openings approximately 1” x 3<sup>3</sup>/<sub>4</sub>”. While there are no grating levels that cover the entire SG cavity at any elevation other

than at the top level of the D-ring, there are numerous platforms throughout the SG cavity that cover portions of the interior. Insulation dislodged from piping in the lower sections of the SG cavities (where most of the calcium-silicate insulation is located) would fall directly into the basement, but those dislodged from the middle and upper portions of the cavity (above the hot leg or cold leg break elevations) would have a higher likelihood of being captured on grating and subjected to potentially different erosion rates due to CSS droplet impingement. The conservatively bounding velocity used in the erosion testing, combined with the conservative use of a maximum erosion rate of 30% or approximately 215% of the highest measured percentage mass loss is considered to sufficiently bound the potential uncertainty associated with application of the erosion test results to calcium-silicate insulation exposed to containment CSS instead of the water velocity in the containment basement.

- The test velocity of 0.7 fps may not bound all velocities in the basement, such as in the affected SG cavity where injection water spilling from the break is flowing from the cavity. The computational fluid dynamics (CFD) modeling of the containment basement indicates that velocities outside the SG cavity are much lower than 0.7 fps, with the lowest maximum velocity in the flow path to the sump outside of the SG cavity being below 0.2 fps. Calcium-silicate pieces that initially fall to the basement floor following the break could be carried out of the cavity by wavefront action as water spills onto the floor and flows outward during the initial fill-up period. Additional pieces may continue to fall into the basement, including in the SG cavities due to washdown from CSS or after erosion of pieces trapped on grating such that they fall through. Pieces remaining in or falling into the high velocity regions would be expected to be transported to a lower velocity region due to velocities exceeding the tumbling or transport velocity. NUREG-6772 documents testing performed on calcium-silicate insulation pieces (Section 3.3.1) noting an incipient tumbling velocity of 0.25 fps and a bulk tumbling velocity of 0.35 fps. Since the flow paths from all postulated breaks must exit the SG cavity and enter the basement area where much lower flow velocities exist, most calcium-silicate insulation debris would not be expected to experience sustained velocity of even 0.35 fps, if unimpeded flow paths were present for the debris to exit the SG cavity. The floor region in the affected SG cavity would likely remain congested due to the significant amount of reflective metal insulation (RMI) debris, metal lagging, and other dislodged materials that either do not experience “tumbling” velocities or become hung or constrained on other obstacles on the floor. This congestion could have both positive and negative effects relative to trapping large calcium-silicate insulation pieces since some pieces could be exposed to higher erosion causing velocities while others are shielded from erosion or transport due to the debris congestion. While considerable uncertainties exist, the assumption that all large calcium-silicate insulation pieces would be continuously exposed to an average erosion velocity of 0.7 fps is considered to be significantly conservative.

In summary, as noted in the final supplemental response dated September 15, 2008, Section 3.e.5, the “three-day” calcium-silicate erosion amount that is applicable for the amount of fines during the period of high temperature sump operation when NPSH is the most limiting parameter for strainer head loss was based on the 13.9% measured mass reduction from the 112.83-hour test sample, that had been exposed to erosion for

4.7 days. The 30-day erosion total of 30% represents a significant increase over the largest measured loss even though the “eroded” mass was approximately constant with little correlation to exposure time. The credited erosion represents approximately 215% of the largest measured mass loss or 260% of the mean mass loss for the smaller pieces.

Review of applicability of NRC Staff’s audit report of Fauske erosion testing of Nukon and Kaowool fibrous materials for the Salem station with respect to the three principal technical issues noted in this RAI are viewed as being appropriately addressed via similar conservative treatment of the test results as was credited with the Salem test audit as follows:

- Non-conservatism associated with the modeling of turbulence in the test flume: The Fauske erosion testing conducted for ANO included similar use of turbulence suppressor and flow straightener as was done with the Salem test. The ANO test was performed with a bounding high velocity condition and included significant conservatisms in treatment of the test data as noted above and in the application discussion below.
- The use of regularly shaped debris pieces as opposed to irregular pieces that would be more prone to erosion: The Fauske erosion testing for calcium-silicate used cut cube shaped pieces of both one-inch and two-inch squares to evaluate differences, if any, associated with size and surface area to mass ratio. ANO used the higher erosion results from the smaller one-inch test cubes and the conservatism of using this size debris is noted in the above discussion.
- Anomalies in the test data, wherein a significant number of long-term tests had lower cumulative eroded mass values than short-term tests: The data results from the twelve samples tested by Fauske for ANO are provided in the above table. The variations in the test results from six different erosion exposure intervals are not considered anomalies but support the conclusion that the eroded mass of each sample size is approximately constant with little correlation to exposure interval. The mean and standard deviations for each of the six samples of each sample size were  $7.2\% \pm 1.2\%$  for the nominally two-inch pieces and  $11.5\% \pm 1.4\%$  for the nominally one-inch pieces. In spite of the absence of a correlation of exposure time to eroded mass, a significant increase above the relatively stable measured erosion values was applied for the 30-day final mass loss.

#### Transport Testing:

Transport testing for calcium-silicate fines was performed by Fauske for ANO, and the following brief description of the test is provided:

- Tested at flow velocities of 0.15 and 0.25 fps
- Tests performed with one-inch thick layer of pulverized calcium-silicate fines
- Exposure times of 24 and 72 hours included

- Transport tests were conducted to quantify the observed propensity of calcium-silicate fines to settle in test flume during the strainer head loss tests, during which prolonged stirring was required to keep them in suspension.
- Credited all fines washed out of tray as transported, even though the fines may only have “transported” to the floor downstream of the sample tray and may not indicate that the material would be carried up into the strainer

The table below presents the transport test results for the five tests. The first test was influenced by localized higher velocities near the corners of the flume partition, which was addressed in subsequent test by moving the sample back from the corner of the partition. The significantly higher transport rate experienced in the first test due to localized higher velocities shows that a strong dependency exists on flow velocities in the containment basement, with higher velocities resulting in a rapid increase in the transportability of calcium-silicate fines. The transported mass for the subsequent three tests conducted at 0.25 fps is seen to be approximately constant with little correlation to exposure interval. This interpretation would suggest that only a low percentage (< 6%) of the calcium-silicate fines exposed to a flow velocity <0.25 fps would be expected to transport to the sump strainer even for a longer exposure interval. Furthermore, if the transported mass at a bounding flow velocity outside the SG cavity is not a function of exposure interval, then a transport rate calculated for longer and longer exposure intervals would become smaller and smaller.

Test #	Mean Water Velocity (ft/s)	Exposure Duration (days)	Initial Dry Mass (g)	Post-Exposure Dry Mass (g)	Transported Mass (g)	Percent Transported (%)
CST01	0.25	1	907.2	778.2	129.0	14.2 <sup>(1)</sup>
CST02	0.25	3	907.2	862.7	44.5	4.9
CST03	0.25	3	907.2	854.7	52.5	5.8
CST04	0.25	1	907.2	857.7	49.5	5.5
CST05	0.15	1	907.2	883.4	23.8	2.6

(1) Non-prototypic localized flow acceleration occurred during this test.

Transport testing observations are provided as follows:

- The largest percentage mass lost from the samples with 0.25 fps velocity was 5.8% over a three-day period when localized flow acceleration was removed.
- The mass lost with the 0.15 fps flow velocity was 2.6% over one day.
- The “transported” mass at 0.25 fps was approximately constant between the one-day and three-day test, indicating a limited dependency on exposure duration.

- The extrapolated 30-day transported fraction based on the maximum percentage mass reduction (CST03) from the test is 45%. This transported fraction used extrapolation of the “rate” from the three-day results out to 30 days, if the “rate” is considered applicable (i.e., relatively constant sample mass between one-day and three-day tests are ignored).
- Transport did not replicate movement of fines into a strainer cartridge located above the floor, only movement out of the sample tray, including transport to the floor next to the tray.

The following critique has been applied to the test results by ANO:

- Testing was conducted at room temperature. Dissolution of calcium-silicate at elevated temperatures was reported in NUREG 6772. While the transport testing was conducted with 100% fines, to ensure possible high temperature dissolution would not impact the transport test results, dissolution testing was also conducted. Testing conducted at Fauske facilities with calcium-silicate insulation used at ANO and conditions similar to those documented in NUREG 6772 did not identify a temperature dependence for dissolution of calcium-silicate in water. A weight change less than 5% occurred for ambient temperature and elevated temperature tests. These tests indicate that increased calcium-silicate dissolution at elevated temperatures would not be expected to occur; therefore, the transport test results are not affected.
- The test in general shows that significant amounts of calcium-silicate fines would not readily transport when exposed to the low velocities outside of the SG cavities in the flow path to the sump. Establishing a mass transport percentage based on tests conducted on a one-inch thick layer of material is only bounding for a calcium-silicate fines debris layer of one inch or more in thickness (i.e., the same or smaller surface area to mass ratio). If the actual debris layer were half the test thickness, a transport “rate” on a mass basis should be approximately double that in the test, given the same surface area and flow velocity. With only 48.2 ft<sup>3</sup> of calcium-silicate insulation affected by the limiting break, the maximum surface area covered by a one-inch layer would be approximately 578 ft<sup>2</sup>, if all of the calcium-silicate were turned into fines, which based on erosion testing is not being assumed. This area represents only a small percentage of the basement surface area. Peak velocities in the basement outside the break cavity in the flow paths to the sump screens are below even the 0.15 fps value, per CFD analysis, with velocities in most of the floor areas a great deal below this amount. While a perfectly distributed layer of the available calcium-silicate debris would be considerably less than one inch thick, the vast majority of this layer would be exposed to velocity much lower than the minimum tested value and settling with little or no transport of fines would be applicable for most of the basement.
- Conversely, the more calcium-silicate that is assumed to be exposed to the small area outside the SG cavity with a flow velocity closer to the minimum test velocity would result in thicker layers than the test value of one inch. These two competing variables are concluded to be offsetting, particularly based on use of the higher 0.25 fps velocity results.

- The test results appear to indicate the absence of time dependency for the transport fraction, since the one-day percent transported of 5.5% at 0.25 fps was in between the two three-day results of 4.9% and 5.8%. The lack of increase with time indicates that significant conservatism results from using a 30-day rate based on ten intervals of the three-day test results. While the test did not show a correlation between increased time exposure and increased transport percentage, the application of this 30-day rate increased the 5.8% non-time dependent maximum value to 45%.
- The first test results (CST01) show that the presence of turbulence or localized acceleration (caused in the initial test setup by a sharp cornered flow constriction in the test flume adjacent to the test sample) has a strong influence on the transport results. The potential for localized turbulent conditions in the containment basement flow stream may exist due to debris congestion from RMI pieces, metal lagging, other dislodged materials, permanently installed materials and from flows entering the basement. Due to higher velocities in the affected SG cavity it is assumed all of the calcium-silicate fines would transport out of cavity and enter the basement area where much lower flow velocities exist. Thus, the area of interest is the flow path outside of the SG cavity to the sump strainer. The containment basement annulus region outside the SG cavities has less turbulent action from falling water entering the flow stream to the strainer since the break flow is in the SG cavity and CSS water enters the basement flow path in a smaller number of discrete locations due to solid floors on upper containment elevations. The calcium-silicate fines would be expected to settle in these regions due to the low velocities with limited transport occurring to the strainer. Other debris materials are also likely to be transported out of the affected SG cavity and settle on the floor of the basement due to the significant velocity reduction occurring upon exiting the cavity. This “debris trail” would also be expected to follow the principal flow paths to the sump strainers, which includes the region noted as having the bounding velocity (outside the SG cavity). This congestion could have both positive and negative effects relative to debris transport with localized velocities higher in some areas and lower in others, although the overall impact would be expected to result in a lower average velocity in a debris congested region at the floor with the flow profile spreading over a wider region of the basement. While considerable uncertainties exist, the assumption that all calcium-silicate fines would be continuously exposed to an average transport velocity of 0.25 fps is considered to be significantly conservative relative to the flow path to the sump strainer outside the SG cavity.

In summary, as noted in the final supplemental response dated September 15, 2008, Section 3.e.5, the “three-day” calcium-silicate transport amount was based on the 5.8% measured value from the highest 72-hour test sample. The 30-day transport total of 45% was determined using:

$$\text{Fraction Transported} = 1 - (1 - \text{three day rate})^{10}$$

This is with the three-day transport rate taken from the highest percentage transport value of 5.8%. This extrapolated erosion rate is further considered significantly conservative in light of the absence of a correlation of erosion to exposure interval from the test data.

However, as noted in the response to RAI B6, the fines transport test results were not used to establish a time-dependent calcium-silicate fines at the strainer. The only reduction in calcium-silicate at the strainer is associated with the transport of pieces and their erosion rate to fines.

- B8. Based on the discussion in your letter dated September 15, 2008, it appeared that only one computational fluid dynamics (CFD) analysis was performed for ANO-2. It is not apparent that sufficient basis is provided for considering this single simulation to be the bounding case in the supplemental response. In particular, the NRC staff noted that, under steady-state conditions during the recirculation phase of a LOCA, the total flow rate out of the D-rings should not be dependent on the direction of the flow from the break (as stated in the supplemental response), but simply the total flow rate from the break. Please provide adequate basis to demonstrate that the debris transport conditions for the single CFD simulation performed for ANO-2 represents the limiting condition.**

As a clarification, the total flow out of the D-ring is not dependent on the direction of flow from the break, only the total flow rate from the break combined with CSS water entering the D-ring compartment. The CFD model discussed in the final supplemental response dated September 15, 2008, provides an appropriately bounding case for analysis purposes to evaluate two-train emergency core cooling system (ECCS) sump recirculation flows. The modeling performed for ANO-2 included multiple LOCA scenarios for different break locations and pipe sizes. The ANO-2 CFD modeling was ultimately used for flow velocity input to debris transport and erosion testing associated with calcium-silicate insulation. Transport reductions were only applied to calcium-silicate pieces, but were conservatively not credited to fines in order to address possible uncertainties with debris generation and calcium-silicate erosion tests. All other debris materials were credited with 100% transport to the strainer. The ANO-2 CFD model was used to evaluate conditions outside of the SG cavities to determine the lowest maximum velocity present in the flow path to the sump strainer. The strainer tests did not credit near-field settling and thus were not reliant upon CFD model results. Since the ANO-2 sump strainer is located outside of the SG cavities and only one exit path exists for flow to the basement region, the total water flow out of the compartment is not affected by the specific break location, orientation, or size (relative to a LBLOCA) in the SG cavity. The CFD simulation noted in the response represents a sufficiently limiting condition for the application of its results based on flow values used in the model.

**B9a. Your letter dated September 15, 2008, states that the single failure of a LPSI pump to trip at the switchover to recirculation can be addressed in 30 minutes, and the flow from a LPSI pump does not appear to be considered in the debris transport calculation. In support of these assumptions, please provide the basis for the determination that the single failure of a LPSI pump to trip at switchover can be addressed in 30 minutes.**

The initial response time was based on estimates of time needed to detect and address the condition of a LPSI pump failure to stop following sump recirculation. Emergency Operating Procedure (EOP) guidance includes instructions following sump recirculation to verify the LPSI pumps have stopped. This procedure guidance and available control room indications provide for early detection that a LPSI pump has failed to stop as designed in response to sump recirculation. Expected initial response would be an attempt to secure the pump using the pump hand switch in the control room. Only a very limited subset of potential single failure mechanisms would result in the pump continuing to operate at this point. Indication that the pump continued to operate after this initial attempt to manually stop it would be readily available and would prompt the initiation of manual operator action outside of the control room (i.e., in the electrical switchgear room). Following further review with operations personnel of a possible scenario of operator action required in the emergency switchgear room, the original 30-minute estimate is considered to remain realistically bounding.

While the 30-minute response time is considered sufficient to address a LPSI pump failure to trip following sump recirculation, the exact response time does not impact the analysis and testing performed for GL 2004-02 resolution. Strainer head loss testing included flows that bound those with a LPSI pump operating in addition to two trains of high-pressure safety injection (HPSI) and CSS pumps. The debris loading with the elevated LPSI pump flow included >100% of the total 30-day fiber, latent debris, and coating particulates determined by the debris generation calculation as well as calcium-silicate debris that exceeded the initial fines and the three-day erosion total for this material. The velocity outside the SG cavities in the flow path to the strainer remains below the bulk tumbling velocity for calcium-silicate even with the elevated LPSI pump flows, leaving the calcium-silicate pieces subject to erosion but unable to transport to the strainers and be carried up off the floor into the strainer pockets.

Thus, the exact time period during the start of sump recirculation necessary to respond to a single failure of a LPSI pump failure to stop is not critical since significant excess material was included in the strainer head loss testing with the elevated LPSI flows present as noted in response to RAI B9b.

**B9b. Given that, at the increased flow rate with a LPSI pump running, one containment pool turnover could occur on the order of 30 minutes, please provide the basis for not accounting for the increased flow from the single failure of a LPSI pump to trip in the debris transport calculation.**

As noted in the response to RAI B9a, the strainer debris loading was only reduced for calcium-silicate pieces. Velocities outside of the SG cavities in the flow path to the sump strainer remain below the bulk tumbling velocity (0.35 fps per NUREG/CR-6772) for this material even with LPSI pump flows. While calcium-silicate fines transport was

evaluated via laboratory testing, no reductions were applied to fines transport. The strainer debris load when flows bounded those associated with a possible single failure of a LPSI pump exceeded 100% of the fiber debris, 100% of the latent debris, 100% of the coating debris, 100% of the miscellaneous foreign material debris, and a quantity of calcium-silicate insulation debris that exceeded the combined initial fines and three-day erosion quantity for this material.

The impact of a LPSI pump failure to trip at the start of sump recirculation is that higher velocities would exist in the basement. The amount of CSS flow is not affected. The flow spilling from the break and into the water in the basement would be increased by the added LPSI flow causing higher flow velocities in the affected SG cavity as well as in the flow paths to the sump outside of the SG cavity. These higher flows could potentially result in higher erosion rates of calcium-silicate insulation pieces as well as higher amounts of transport of the calcium-silicate pieces, depending on the amount of conservatism already included with these terms.

As noted in the response to RAI B4, the calcium-silicate debris source term is composed of 80% ZOI generated debris and 20% unlagged material outside of the SG cavities potentially subject to erosion from CSS or immersion. The initial amount of fines is therefore 32% of the total (based on 40% fines from ZOI generated calcium-silicate debris as discussed in the RAI B4 response, and 80% of the total calcium-silicate debris being ZOI generated). Thus, all of the initially generated fines from the break (i.e., 32% of total calcium-silicate debris) have already been credited with 100% transport to the strainer at time zero. An additional amount of calcium-silicate was present in the test performed with the LPSI pump flows, which significantly exceeded the three-day erosion total for calcium-silicate pieces, providing margin to address future modifications or analysis changes.

The erosion testing was conducted at a velocity of 0.7 fps, which significantly bounds the bulk tumbling velocity reported in NUREG-6772 (0.35 fps) such that pieces would be expected to transport to lower velocity regions unless in a congested flow path. The CFD modeled velocities outside the SG cavities in the flow paths to the sump were considerably below the incipient tumbling velocity for calcium-silicate pieces for the two-train flow conditions. The erosion test velocity remains bounding by a significant margin of flow velocities outside the SG cavities with two-train flows combined with a LPSI pump single failure to stop. Thus, the bounding velocities used in the erosion testing and the conservative debris loading present in the credited head loss test conducted with the elevated LPSI pump single failure flows adequately bound the affects of the elevated LPSI flows even if they were to exist for an extended period.

**B9c. Also, please state whether conditions exist for which EOPs would either direct or allow plant operators to operate a LPSI pump in recirculation mode under design basis conditions (e.g., during hot leg recirculation). If such conditions exist, please justify the assumption in the debris transport calculation that a LPSI pump would not be operated under design-basis post-LOCA conditions.**

The EOPs have instructions that operators confirm both LPSI pumps have stopped following sump recirculation. The EOPs do not include direction or allowance for restart of the LPSI pumps while in recirculation mode.

**B10. Debris transport results for Thermal-Wrap insulation, while provided in your letter dated February 28, 2008, (Table 3.e.6-2), are not provided in the corresponding table in your letter dated September 15, 2008 (Table 3.e.6-1). Based on the information in your letter dated September 15, 2008, it was not clear to the NRC staff whether, for example, this insulation was removed from the plant, whether the limiting analyzed break was changed, or whether changes to the analysis resulted in its removal from the debris source term. Please provide a basis for the observed discrepancy, identify the final transport results assumed for Thermal-Wrap debris, and confirm the characteristic size distribution assumed for this debris.**

Thermal-Wrap insulation was not included in Table 3.e.6.1 of the September 15, 2008, final supplemental response due to it not being generated by the limiting break, S6, for strainer head loss. This insulation type remains installed on the top and bottom of the pressurizer with the lower pressurizer Thermal-Wrap insulation released by an evaluated break of the pressurizer surge line (break S4). Testing conducted for the higher fiber, lower calcium-silicate debris combination associated with the surge line break did not produce head loss results that were as limiting as the cold leg break, S6. Analysis for the pressurizer surge line break included conservative assumptions of 100% release of the Thermal-Wrap insulation installed on the lower pressurizer head and skirt as fines and very small pieces combined with 100% transport of this material to the sump strainer, thus a transport fraction of 1.0 was used at ANO-2 for Thermal-Wrap insulation with a size distribution of 100% fines and very small pieces.

Modifications performed during the 2R19 (spring 2008) refueling outage included the complete removal of insulation from some pipes, changes to the insulation types on other lines, and the addition of banding to numerous pipes with existing calcium-silicate insulation. These insulation modifications resulted in significant reductions in the volume of calcium-silicate insulation released from various analyzed breaks, which had been found in previous testing to be a critical constituent in elevated strainer head loss when combined with fiber debris. The limiting break for peak head loss conditions prior to the 2R19 insulation modifications when the February preliminary submittal was made, was still being determined between the S4 pressurizer surge line break that releases the Thermal-Wrap insulation on the bottom head and skirt of the pressurizer creating a higher fiber but lower calcium-silicate release, and either a hot leg or cold leg break that released less fiber but much more calcium-silicate.

Following the 2R19 insulation modifications, the A-cold leg break was determined via testing to be the most limiting break. It released the largest amount of calcium-silicate insulation of the analyzed breaks which, even with a low fiber content, still resulted in the largest head loss condition. The downstream effects analysis included fiber debris loads that bounded those associated with the surge line break which was conservatively combined with other breaks that produce the largest particulate debris load, such that a bounding downstream evaluation addresses any break scenario, regardless of which break may be more limiting for strainer head loss.

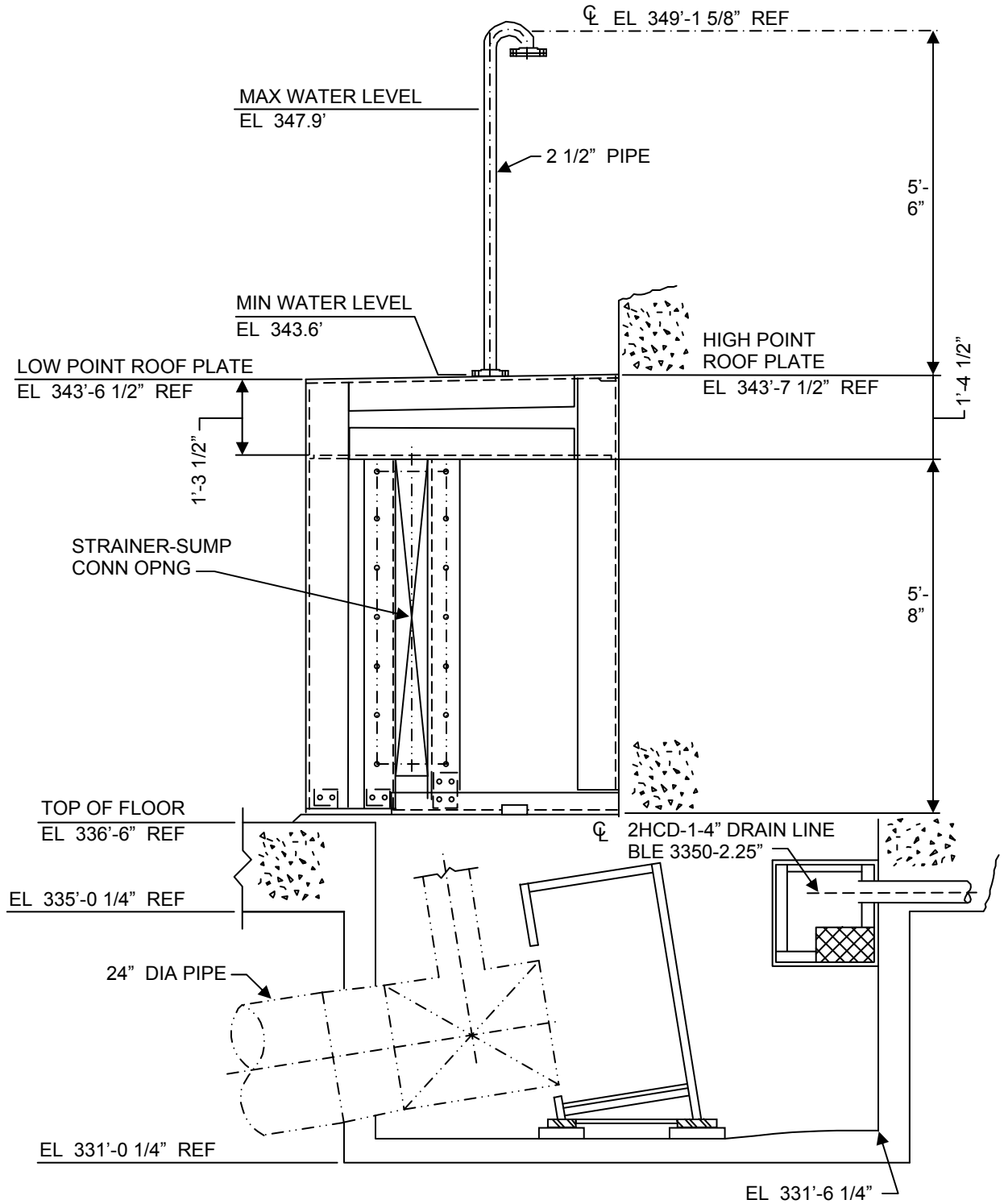
**Head Loss and Vortexing:**

**B11. Please provide additional information on the potential interactions between the emergency sump and the floor drains that empty into the sump. Could the floor drains provide a source of air into the sump? Can the floor drains provide a source of water to bypass the strainer allowing debris into the sump? Are the floor drains always below the minimum water level and covered by the minimum height of water postulated during recirculation? Please provide a diagram showing the relative elevations of the strainer, the strainer vent, the maximum and minimum water levels, the sump and vortex suppression structures, the floor drains, and the ECCS suction pipe(s) that exit(s) the sump.**

The ANO-2 strainer includes a vented central plenum above the sump pit, such that the strainer internal pressure stays in equilibrium with the external containment pressure. The strainer plenum vents are above the maximum containment flood level. Increases in strainer head loss would accordingly result in a change in water level, not internal pressure, as noted in final supplement response dated September 15, 2008, Sections 3.f.11 and 3.f.14. The sump contains two internal box strainers used to strain inputs from equipment and floor drains that enter the sump below floor level. These box strainers are designed with stainless steel mesh to prevent particles greater than 1/16" from entering the sump through the floor drains, which is consistent with the strainer hole size. Because the sump strainer is vented, these floor drains do not present a concern for the introduction of air into the sump strainer, since any air initially in the drain lines would vent during containment flooding phase and the lines would remain filled to the water level present inside the strainer assemblies. Other floor drains that enter the sump pit below the strainer plenum, which are not filtered are isolated from the sump via locked closed isolation valves. Thus, the floor drains do not provide an unfiltered source of water that could bypass the sump strainer. The floor drains that flow into the sump through the box strainers do not need to be covered by the minimum water level during recirculation, since as noted above, this does not create the potential for air entrainment into the sump due to the vented configuration.

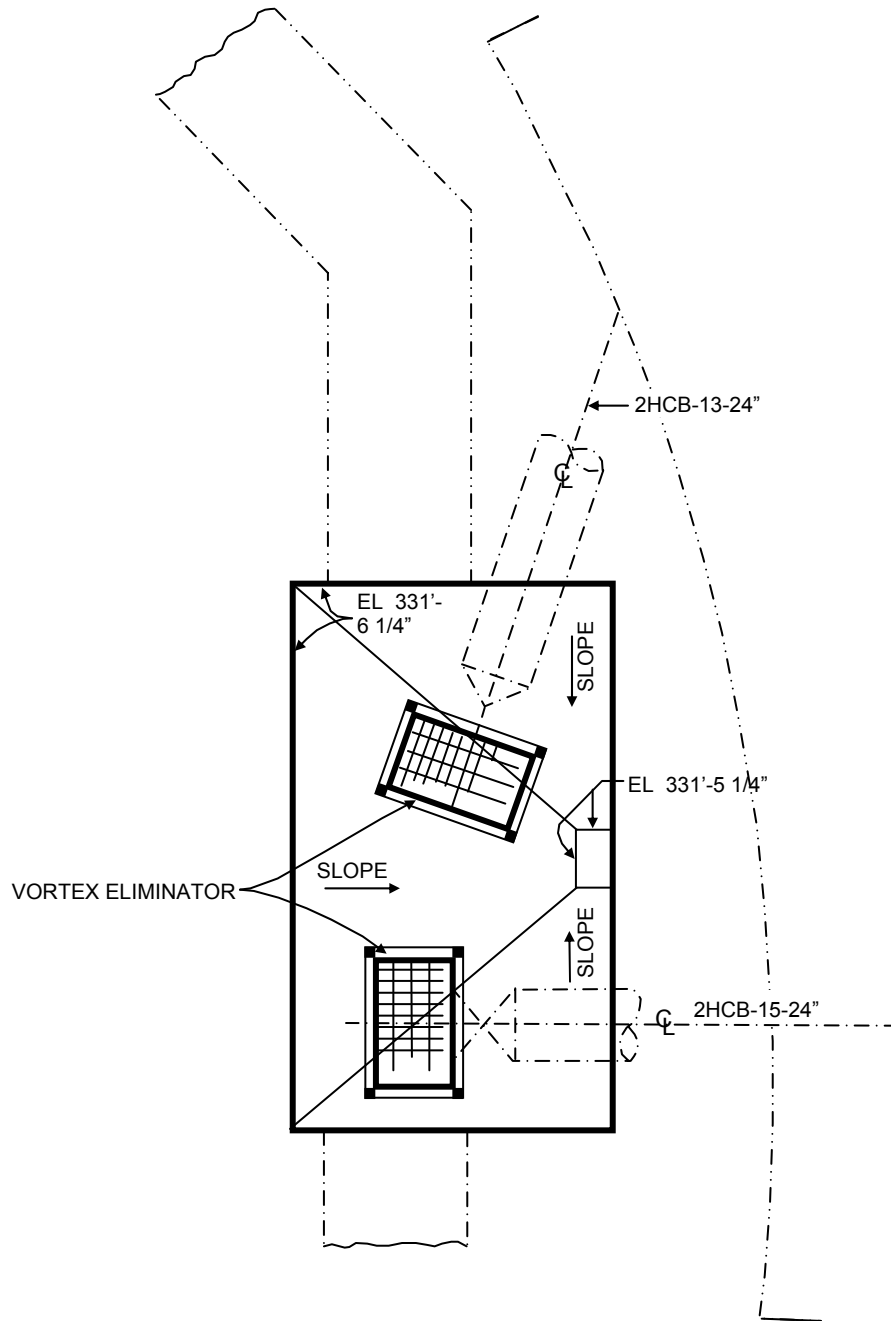
The following diagrams provide views of the relative layout and selected elevations of the strainer plenum, vent, maximum and minimum water levels, vortex suppression structures, entry location for the screened floor drains that empty directly into the sump, and the ECCS suction pipes exiting the sump.

Sump Pit and Strainer Plenum Assembly Composite Elevation View (not to scale)



**SUMP PLENUM AND PIT VIEW**  
ELEVATION LOOKING WEST

Plan View of Sump Pit with ECCS Suction Piping



PLAN @ ELEV. 331'-6 1/4"

**B12. Please provide the methodology used for calculation of clean strainer head loss.**

Clean strainer head loss was calculated in two separate aspects. One involved head loss across the strainer cartridges themselves and the second evaluated the internal head loss within both the strainer assembly “duct work” and the collection plenum assembly located above the sump pit into which the two branches of strainer assemblies connect. The head loss through the clean strainer cartridges was performed analytically and was validated through strainer tests conducted at both CCI test facilities and Fauske test loops with strainer flow velocities that bound the maximum two-train flow and LPSI single failure with two-train flow conditions. This analysis calculated minimal head loss through the strainer cartridges, which was confirmed during the strainer tests prior to debris addition. The strainer tests involved individual strainer cartridge assemblies, or in the case of the Fauske test facility two strainer cartridges mounted side-by-side. The strainer cartridges used in the Fauske testing consisted of 20 pockets with two vertical columns of ten pockets each.

The testing did not replicate or address potential head loss in the composite strainer and plenum assembly mounted above the sump pit. The internal flow losses within the new strainer assemblies are incorporated into the ECCS pump NPSH calculation, which also includes the losses in the suction piping from the sump pit to the pumps. The flow distribution between the two strainer “arms” extending away from the plenum partially around the annulus region between the containment wall and SG cavity wall was analyzed using CFD methods. Calculations using standard hydraulic analysis methods were also performed of the strainer and plenum assembly internal resistance or head loss. These analyses were used to establish equivalent loss coefficients for the clean strainer and plenum assemblies in the NPSH calculation to provide a strainer non-debris related head loss that varied with flow through the system.

**B13. The testing conducted by the contractor utilized a debris addition sequence that was potentially non-prototypical and non-conservative. The addition of fibrous debris prior to particulates generally results in lower head losses. The contractor’s testing added fibrous debris first. During earlier interactions with the licensee, the NRC staff had commented on the debris addition sequence. It was stated that sensitivity testing had been completed on the debris addition sequence. Since ANO-2 has a low fibrous debris term (as stated in your letter dated February 26, 2008) it is possible that the addition of fibrous debris first would not result in non-conservative results. In addition, the staff noted that in some tests additional particulate was added to the test after stability for the first test condition was reached in order to test multiple conditions without starting a new test (Reference 2, page 17 of 50). Given the relatively low fiber condition, it doesn’t appear likely that this method of conducting multiple tests on the same basic debris bed found the worst-case thin-bed debris bed head loss. Please provide the information regarding the sensitivity testing or other analyses showing that the addition of fibrous debris prior to other types of debris is conservative or at least neutral to the test results.**

The test method developed by Entergy and employed at Fauske was intended to conservatively maximize strainer head loss response, regardless of whether this biased the test in a prototypic or non-prototypic condition. NEI 04-07, Volume 2, which consists of the NRC’s SE of the PWR Sump Performance Evaluation Methodology (Vol. 1), states the following in Appendix VIII addressing thin-bed strainer head loss:

*“When conducting thin-bed debris tests, it is advantageous to establish as uniform a fibrous debris bed as reasonably possible before significant head loss is achieved. This can be achieved more easily when the particulate is not involved with the fibrous bed formation. When the fibrous debris and particulate debris are introduced at the same time, the debris bed tends toward homogeneity for thicker debris but can lead to lesser head losses for thin-bed formations compared to establishing the fibrous debris bed first at flow velocities sufficient to compact the fiber before the arrival of the particulates. Establishing a fibrous debris bed first and then introducing the particulate can create a more stratified debris bed.” “Although a truly stratified bed is not the anticipated plant accident condition debris bed, it is useful for determining specific debris head-loss properties and generally leads to more severe head losses than the truly mixed debris beds.”*

The arrival of a significant portion of the fiber debris at the strainer during the initial sump inventory turnover is considered to be prototypic due to the readily transportable characteristics of fiber fines and small pieces. This is particularly true in the case of ANO-2 where latent fiber is a significant portion of the fiber debris for the credited limiting break. It is important to note that due to limited total available fiber, only fiber layers considerably less than the traditional 1/8” thin-bed conditions are possible for ANO-2, with tested fiber quantities capable of a layer <1/32” for the limiting break, if evenly distributed, ranging up to a fiber almost 1/8” for other tests. The ANO-2 limiting break test also was performed with an excess of fiber totaling 261% of the total fiber determined by the debris generation analysis and latent debris survey. This excess fiber was added to provide margin for variations in latent debris survey results and minor changes to installed or analyzed fiber insulation, as well as to assist in establishing a thin-bed condition to achieve conservatively bounding head loss test results.

Given the very limited available fiber quantity, added care was taken in the testing to avoid conditions such as agglomeration that might reduce fiber distribution on the test strainer. The fiber materials were intentionally segregated from the particulate debris materials to avoid potential weighting down of the fiber and biasing the fiber into the lower strainer cartridges. Clumped or agglomerated fibers, could significantly skew even distribution of the fiber, resulting in either open sections of strainer or sections with minimal fiber base. For plants having a significant excess of fiber, this issue would be of less concern for producing non-conservative results. For plants with less than 1/8” available fiber, the less evenly distributed the fiber material, the more likely that debris bed perforations would develop at lower head loss values and the resulting maximum strainer head loss would be reduced. Considerable care was taken to shred the fiber material into fines and very small pieces, and the material was maintained diluted in a significant number of different containers in order to allow maximum distribution of the fibers over the strainer.

The test flume was constructed of clear plastic, allowing observation of the fiber debris as it was poured into the test loop and transported to the strainer. The addition of numerous small batches of fiber (performed over a 15 to 20-minute time span) was performed to promote uniform distribution over strainer surfaces. These actions were in response to previous NRC comments regarding observations of strainer tests at other facilities. The February 2, 2007, report addressing the NRC observation of CCI strainer

testing notes on page 11 of Attachment 3 “the Staff considered the agglomeration-induced settling of highly concentrated debris as having significant potential to affect the test results in a non-conservative manner.” While this test involved settling, which was avoided in the Fauske testing, the concern with agglomeration was noted. An earlier trip report from August 29 – September 1, 2005, testing by General Electric Energy notes in Appendix 2, page 3, “The important issue with fibrous debris transport is to ensure the fraction of ZOI debris that is destroyed or eroded finely enough that it transports as suspended fiber is conservatively evaluated and represented in the head loss testing.” Later on page 4 of Appendix 2 it states, “Since much of the particulate could arrive after the fibrous debris bed is completely or nearly completely formed, a possibility of forming a stratified bed exists. If stratification is an issue, it would apply to the maximum fibrous debris bed rather than thin-beds.”

The insulation reduction efforts at ANO significantly reduced the remaining volume of calcium-silicate debris (approximately 1/7” layer if evenly distributed). Testing conducted prior to the final qualification tests had indicated that the debris bed head loss is significantly impacted by the combination of available fiber and calcium-silicate insulation. A deflection point or “knee” was observed in several tests, with head loss remaining near zero prior to reaching this point. Tests with progressively thinner fiber layers (ultrathin-bed) generally resulted in the need for larger quantities of calcium-silicate insulation to reach this deflection point. This occurrence is assumed to be associated with the capture of sufficient fiber binder fragments from the calcium-silicate insulation in the existing fiber bed until a sufficient filtering layer is formed to develop thin-bed filtration of particulates. Thus, while particulate and calcium-silicate debris could have been added first during the test sequence, without the presence of a thin-bed fiber layer, the material would simply pass through the strainer and continue to recirculate (with the assistance of stirring) until sufficient fiber accumulated on the strainer surface to begin to filter the particulate material. The addition of fiber into a test flume mixture having the particulate and calcium-silicate insulation being circulated and maintained in suspension was believed to be more likely to result in the potential agglomeration of fiber fines and a resulting non-conservative reduction in the uniformity of the fiber bed. Post-testing inspections of debris accumulation on the strainer following a series of earlier tests confirmed that the debris bed was well formed over all of the interior surfaces, which combined with the careful fiber preparation, segregation, slow addition to a flowing flume, and ability to establish particulate filtering debris beds with very thin fiber layers provided confidence that the fiber bed was evenly distributed and would provide conservative head loss results.

The fiber layer initially established in the strainer was thin (i.e., < 1/8”) and appeared to remain at least partially porous for some period of time based on the murky water condition and the strainer head loss building gradually. The initial debris addition for the LPSI pump condition was performed over the initial 1.5 hours of recirculation with repeated stirring of the test loop. After a peak head loss was reached, which was followed by a gradual decline, additional debris was added for margin for the two-train NPSH limiting (three-day condition) head loss test and flow was reduced from the two-train plus LPSI pump value to a two-train maximum flow value, with a maximum head loss reached at approximately 5.4 hours into the test. Additional calcium-silicate debris was added for the 30-day head loss test with repeated stirring performed to achieve debris transport prior to chemical addition which was started about 26 hours into the test.

The debris bed achieved peak head loss conditions after periods of sustained stirring, but would exhibit declining head loss afterwards. A flow adjustment to one-train and then back to two-train flow values was made to evaluate the debris beds responsiveness to flow adjustments. While the head loss tracked with the flow adjustments, the debris bed showed evidence of porosity based on the peaking and declining values associated with stirring, believed to be associated with the pass through of particulate through the debris bed, followed by settling if the flume was not continuously stirred, allowing the head loss to decline, but if settled materials were agitated such that the more porous or breached areas in the debris bed were refilled with material the head loss would increase to comparable peak values. The peak head loss values were not sustained or stable and their use as the credited head loss is considered bounding relative to what might be expected in actual field conditions with comparable debris loads. All of the non-chemical debris was added in approximately the initial 6 ¼ hours providing ample time with the frequent stirring to achieve the maximum achievable transport and distribution (the term "maximum achievable" is used due to bed porosity and/or jetting resulting in limited amounts of particulate debris continuing to recirculate within the test loop) prior to chemical addition, which was started after approximately 26 hours of testing.

The NRC Staff observations of ANO's strainer testing at the Fauske test facilities on August 13-14, 2007, included a demonstration of various aspects of the strainer testing and included the addition of debris at the end of the test that was not intended to replicate strainer qualification testing, but was done to create elevated differential pressures for the benefit of the NRC Staff, allowing those in attendance to witness bore hole or jetting phenomenon without having to wait for an additional test that created higher head loss using "normal" debris addition sequencing. The trip report noted "atypical" debris addition sequence of "Fiber, Particulate, Chemical Precipitate, Fiber, Particulate, Chemical Precipitate, Fiber", with a test observation noting, "the addition of calcium-silicate after the chemical precipitate could lead to non-prototypical sequencing effects." The addition of further insulation debris after the introduction of chemical precipitates, was not part of the standard test or the qualification test. This sequencing was performed specifically during the NRC witnessed test for expediency to generate a higher flume head loss in a short time period to allow the NRC Staff to observe additional test conditions such as bore holes and reduced head loss sensitivity to flow changes when bore holes are present.

In summary, the debris addition sequence used in the ANO strainer head loss testing was designed to maximize strainer head loss for the relatively small volumes of detrimental insulation materials remaining and was performed in accordance with the guidance provided in the NRC's SE of NEI 04-07 for producing the most limiting head loss condition from a thin-bed. While fiber agglomeration and even distribution concerns could potentially have been addressed via the same slow addition of multiple small batches of fiber to the flume after particulate and calcium-silicate insulation had been added, the resulting ultrathin-bed development and associated head loss would not be expected to be more limiting than those achieved with an initial fiber addition. Attention was given to NRC comments from strainer test report observations conducted for various vendors prior to ANO testing at Fauske, as well as comments provided during the NRC Staff observation of the ANO tests. Numerous lessons learned from the series of tests performed by ANO were also incorporated in an effort to obtain the most conservatively bounding strainer test results. Entergy concurs that many aspects of the strainer tests

are non-prototypical, although it remains the site's conclusion based on NRC guidance as well as performance and observation of over 20 tests that these non-prototypic deviations contribute to a significant conservative impact on the test results relative to actual expected response and that non-conservative biases in the testing do not exist.

**B14. The testing head loss values listed in Section 3.f.4 of your letter dated September 15, 2008, did not seem to correspond to the head loss values listed in the chemical effects section table of results. The values for the LPSI pump failure and the non-chemical results listed in the head loss section were lower than the corresponding values in the chemical effects test results. The value for chemical effects head loss seemed to be about the same in both sections. Your letter dated September 15, 2008, stated that no viscosity correction was made to the test results. It appears that some manipulation of the data for the first two cases occurred. Please provide information that explains why the values in the two sections are not equivalent.**

As discussed in Sections 3.f.4 and 3.f.7, and elsewhere in the final supplemental response dated September 15, 2008, there are three distinct conditions or periods evaluated for head loss:

- LPSI pump failure to trip with two-train HPSI and CSS pump flows, which includes partial debris loading and no chemical effects. Pump NPSH is the limiting head loss parameter for this case.
- Two-train HPSI and CSS pump flows with partial debris loading (conservatively applied as three days recirculation) and no chemical effects. Pump NPSH is the limiting parameter for this case.
- Two-train HPSI and CSS pump flows with full 30-day debris loading and chemical effects. Strainer structural analysis is the limiting head loss parameter for this case.

The results of these three test cases and the corresponding limits are presented in Section 3.f.4 of the final supplemental response dated September 15, 2008, in discussing head loss testing results. The associated source of the test results given in Section 3.f.4 from the test data summary in Table 3.o.2.17.i are provided below:

	Time (sec)	Head Loss
LPSI + 2-train flow	6040	0.283 psid (0.65 ft, Section 3.f.4 lists < 0.7ft)
2-train flow debris only	19538	0.377 psid (0.87 ft, Section 3.f.4 lists < 1.0 ft)
2-train flow chem. effects	268204	1.40 (3.23 measured with 3.4 ft credited, Section 3.f.4 lists <3.5 ft)

The most limiting head loss was determined by comparing the head loss and test loop flow and adjusting the test loop flow by the scaling factor of 85.97:1 to obtain the equivalent plant strainer flow. The table below provides a comparison of both the measured head loss versus allowable head loss and equivalent flow versus the maximum design flow.

	Measured Head Loss	Allowable Head Loss	Equivalent Flow	Maximum Design Flow
LPSI Flow	0.65 ft	0.984 ft	14,300 gpm	12,735 gpm
2-Train Flow w/o chemicals	0.87 ft	1.8 ft	7033 gpm	7035 gpm
2-Train Flow w/ chemical effects debris load	3.23 ft* 3.4 ft	5.9 ft	6924* 7035 gpm	7035 gpm

\* Measured flow below maximum design, credited head loss of 3.4 ft adjusted upward to bound 7035 gpm maximum design flow.

The tested debris loads for each debris type relative to the generated/erosion totals are summarized as follows:

Material	Debris Gen. Calc. Max. Qty	Debris Fines at Strainer 3-day/30-day	Strainer Test w/ LPSI flow	Strainer Test w/ 2-train flow 3-day	Strainer Test w/ 2-train flow 30-day
Cera-Fiber	1.01 ft <sup>3</sup>	1.01/1.01 ft <sup>3</sup>	1.077 ft <sup>3</sup>	2.15 ft <sup>3</sup>	2.15 ft <sup>3</sup>
Latent Fiber	7.05 lbs	7.05/7.05 lbs	22.37 lbs	22.37 lbs	22.37 lbs
Total Fiber	15.13 lbs	15.13/15.13 lbs	30.99 lbs	39.57 lbs	39.57 lbs
Calcium-Sil.	48.2 ft <sup>3</sup>	20/25.3 ft <sup>3</sup>	23.7 ft <sup>3</sup>	35.6 ft <sup>3</sup>	55.14 ft <sup>3</sup>
Coating Total	6.6 ft <sup>3</sup>	6.6/6.6 ft <sup>3</sup>	7.5 ft <sup>3</sup>	7.5 ft <sup>3</sup>	7.5 ft <sup>3</sup>
Latent Debris	47 lbs	47/47 lbs	150 lbs	150 lbs	150 lbs

The head loss testing for the condition of a single failure of a LPSI pump to stop or trip upon start of sump recirculation included greater than 100% of the debris generation calculated total material for fibers, coatings, latent debris, and over 49% of the calcium-silicate. These totals significantly exceed amounts that would credibly arrive at the strainer during initial sump recirculation until manual operator action secured the LPSI pump that failed to stop upon sump recirculation.

The strainer head loss is limited by pump NPSH only while the sump temperatures are at elevated temperatures (i.e., above 200°F), for which a conservatively bounding duration of the initial three days of accident response was used in order to maximize calcium-silicate debris erosion. While the test loop already contained bounding debris quantities at this point for the initial fines and three-day erosion total for calcium-silicate

as well as bounding quantities for all other debris types, additional fiber and calcium-silicate debris were added to provide margin for any future changes in plant configuration or analysis.

The strainer head loss is limited by the structural analysis limit for the strainer and plenum assembly during subsequent periods when sump temperatures are cooled and additional NPSH margin is available due to the sub-cooled water. This time period includes the period when chemical precipitates from aluminum compounds may develop and extends to the end of the 30-day mission time. To account for the continued erosion of calcium-silicate insulation pieces an additional quantity of calcium-silicate insulation was added to the test flume. The 30-day erosion totals for ANO-2 conservatively credit 30% of the total calcium-silicate insulation debris as becoming fines that 100% transport to the strainer during this period. To provide margin for future changes in installed or analyzed calcium-silicate debris loads an additional quantity of calcium-silicate debris above this amount was added. The tested debris loading was equivalent to 218% of the erosion credited calcium-silicate debris or 114% of the total calcium-silicate insulation affected (i.e., without credit for erosion reduction). The equivalent debris loads used in the strainer qualification test for other materials relative to the amounts determined by their associated debris generation calculations included the following: fiber = 261% of total debris generation quantity (including latent fiber); coatings = 114%; latent particulate = 319%; chemical precipitates = 393%; allowance for miscellaneous foreign material blockage = 760%.

As additional clarification to the September 15, 2008, final supplemental response, the strainer head loss values noted are the ambient temperature head losses, which are shown to be acceptable even before viscosity corrections are applied. Strainer testing included flow adjustment checks to verify that jetting or blow hole conditions would not inhibit the expected head loss reduction associated with reduced viscosity. Viscosity corrections may be applied in the future to the head loss results for determining NPSH margin or elevated temperature head losses, but the acceptability of the results prior to having applied this correction, as shown here, provides an indication of the significant margin available to address changes in system design or analysis. Head losses associated with chemical precipitates are not subject to viscosity correction, since these precipitates occur when sump water temperatures have cooled.

The above provides clarification regarding the debris loading, the three test head loss conditions of interest and the associated time periods from Table 3.o.2.17.i in the final supplemental response dated September 15, 2008. Thus, the values presented in Table 3.o.2.17.i and the head loss values listed in Section 3.f.4 are consistent for the first two head loss periods of interest and did not involve data manipulation or adjustment, but were lower than the chemical effects head loss results because these head losses were measured prior to the chemical precipitates being added. The chemical effects precipitates would not be present during the early time periods when NPSH limits the allowable strainer head loss due to the elevated temperatures present.

**Debris Source Term:**

**B15. Please reference and describe the specific procedures mentioned in the debris source term for control and maintenance of containment cleanliness.**

The general control of area cleanliness for the site is addressed in procedure 1000.018, *Housekeeping*. The containment buildings are designated as housekeeping Level II, with some exceptions associated with Level I requirements around the reactor vessel and fuel transfer areas when the reactor head is removed. The procedure describes Level II housekeeping areas as those where a high order of cleanliness is required and that the purpose is to prevent foreign material from adversely impacted safety-related systems. The containment buildings are noted specifically due to the potential for debris to impact operability of the containment sump. Specific instructions are provided to contain grinding and welding activities to avoid the introduction of grit; use of mats when dust, debris or particles are generated; periodic cleaning of the work area with loose items controlled and loose trash/debris disposed of properly; consumable items being removed from the work area immediately upon completion of the activity; and cleaning the work area upon completion of work such that surface or airborne abrasive dirt or grit is minimized. The procedure applies to all workers in the affected housekeeping level and also includes the assignment of specific plant areas to work groups for oversight and ownership as well as the use of job-site ownership signs for specific activities, both of which are intended to ensure a level of direct responsibility for maintaining cleanliness.

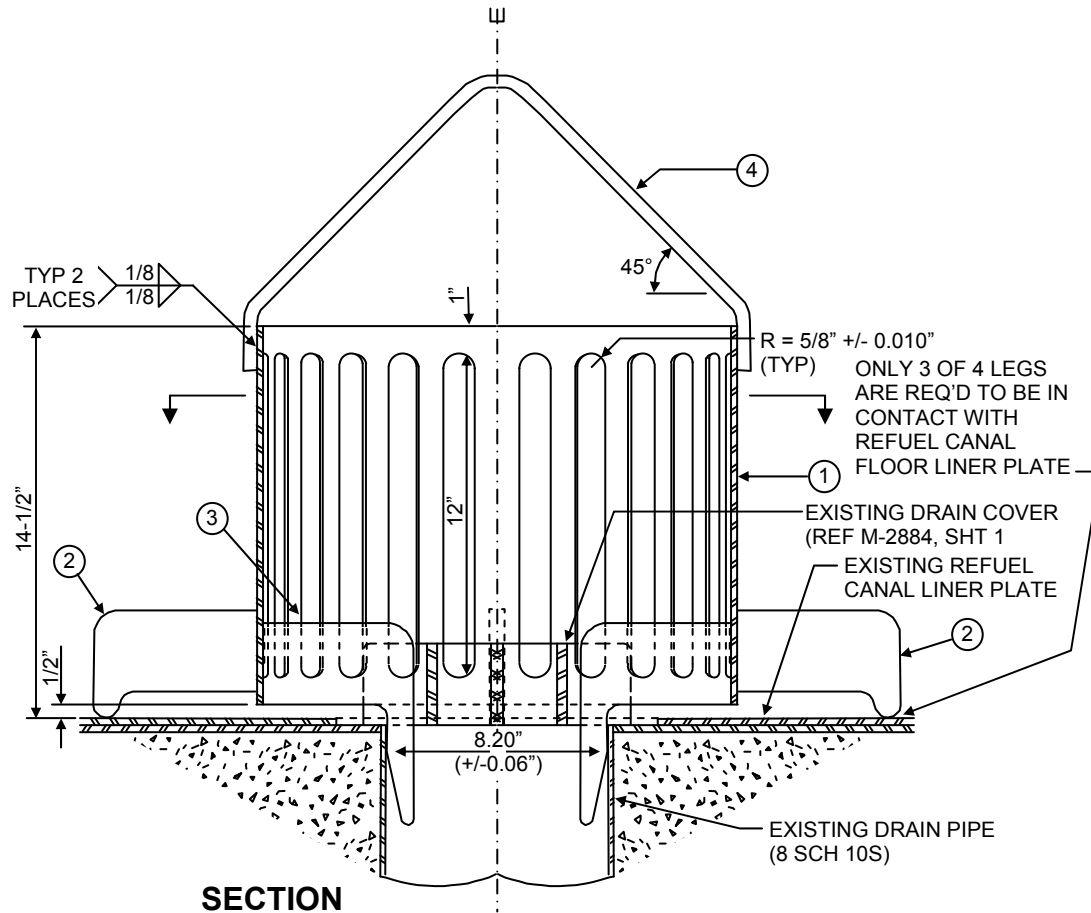
Procedure 1015.036, *Containment Building Closeout*, includes specific guidance regarding inspections of the sump screens and areas within containment prior to plant heatup and again prior to containment closeout (criticality). The inspections performed per 1015.036 involve multi-discipline teams that address detailed checklist inspections of the sump strainers as well as all accessible areas of the containment building. Instructions are provided to address a wide variety of potential sources of debris or foreign material as well as the storage of materials inside containment.

In addition to these controls, periodic performance of the latent debris surveys will be performed (as noted in Section 3.i.1 of the final supplemental response dated September 15, 2008) to ensure the latent debris quantities remain within tested and analyzed limits. The sump strainer head loss testing and downstream effects analysis included additional margin beyond the measured latent debris value to allow for variations in the periodically measured value without exceeding the tested or analyzed limits. Adjustments to cleanliness practices and/or latent debris sample frequency will be made as needed to ensure conditions remain within analyzed and tested limits.

**Upstream Effects:**

**B16. Your letter dated September 15, 2008, states that a larger drain cover will be placed over the refueling canal drain. Please describe the size of this cover, the size of the openings in the cover, and state whether it has a raised design or other features that would prevent debris blockage. Also, please discuss the types of debris that could be blown into the upper containment and potentially reach the refueling canal drains, including large pieces of insulation, smaller pieces of insulation, and other types of debris (e.g., miscellaneous debris). In addition, please discuss the potential for sheeting flow in the refueling canal and for temporary floatation and transport of debris over the drain due to refueling canal drain surface currents, absorption of water into the material, and subsequent sinking of the material to cover the drains. In light of the considerations above, please provide the basis for concluding that the refueling canal drain would not become blocked by post-LOCA debris.**

As noted in final supplemental response dated September 15, 2008, Section 3.1.4 the refueling canal drain strainers installed are made from 18" diameter pipe and are 14-1/2" in height. A diagram is provided below. The strainers include 24 slots measuring 1-1/4" wide by 12" long in the sides to allow water flow while avoiding the risk of blockage.



Debris blockage of the ANO-2 refueling canal deep-end drains is not considered credible following a primary system pipe break that requires sump recirculation. The vast majority of surface area of RCS piping that could result in such an event is located in the two SG cavities. A significant amount of debris could potentially be created by such a high energy pipe rupture; however, very little of this debris would be expected to exit the top of the SG cavities. The larger RCS pipes, hot leg and cold leg, are located in the lower elevations of the SG cavities, with the hot leg and two cold leg penetrations from the reactor cavity entering at approximately elevation 371' and the cold legs extending down to 364.7' elevation. The SG compartment includes grating platforms covering portions of the cavity above these elevations at 375', 387', 405' and 413', as well as having a grating cover on top of the SG cavity at elevation 426'. In addition to grating there are numerous other barriers such as the reactor coolant pumps, seismic restraints, and structural steel beams (and the pressurizer compartment in the south cavity).

These obstacles between the possible break locations and the exit point for the top of the SG cavity would likely provide significant screening for larger debris. This is a secondary effect versus a credited design function for this equipment. The grating on top of the SG cavities is "hinged" by design in order to avoid possible excessive pressure build-up in the cavities from such a break. The grating is restrained with chains on one side to allow it to lift up or open if sufficient pressure differential develops. While it would be expected to be a very limited amount, it is possible for some larger pieces of debris to exit the SG cavity.

The potential debris types associated with a postulated primary system pipe rupture in the SG cavity is of interest when considering the potential for refuel canal drain blockage. The principal insulation material on the primary system piping and components is RMI which is composed of heavier gauge outer metal jacketing with interior layers of thin film stainless steel foil. Insulation on non-RCS piping is primarily calcium-silicate with stainless steel outer lagging held in place with sheet metal screws or banding. There is a relatively small amount of Thermal-Wrap insulation, consisting of fiberglass insulation encapsulated within a woven fabric covering, which is installed on both the top and bottom heads of the pressurizer.

Testing conducted for ANO by Westinghouse at the Wyle Laboratories test facility has indicated that the Thermal-Wrap insulation is of sufficient distance from the hot and cold leg piping that it would not be destroyed by a break in those pipes, as discussed elsewhere in this document. A break in the 12" surge line below the pressurizer could destroy most of the Thermal-Wrap fiberglass insulation below the pressurizer. A break of one of the smaller pipes on top of the pressurizer would destroy a portion of the Thermal-Wrap insulation in the vicinity of the break. A break in the pressurizer spray piping would be a significantly smaller break size which would not be expected to result in sufficient pressure build-up in the SG cavity to cause the grating on top of the cavity to lift. Thus, only debris that can fit through the grating openings would be credible at the refueling canal from this break location. A break in the surge line below the pressurizer may produce both Thermal-Wrap outer covering blanket and fiberglass insulation debris along with calcium-silicate and RMI insulation debris, however, this break would likely have a downward trajectory due to the floor slab below the pressurizer, thereby reducing the amount of debris ejected upward.

While it is not likely that significant quantities of large pieces of debris would be ejected from the SG cavities, it is reasonable to conclude that this debris would consist primarily of RMI foils, stainless steel lagging, pieces of calcium-silicate, and small quantities of miscellaneous foreign material debris such as tape, stickers, tags, or labels. The grating on top of the SG cavities is chained such that it can lift to avoid excessive pressurization within the D-ring shaped compartments. The refueling canal is adjacent to and in between the two SG cavities and is a potential recipient of some portion of debris that is ejected from the SG cavity toward the side.

Debris that does land in the refueling canal would include some material that is not readily transportable. Material that is transported to the drain strainers is not expected to consist of materials that are effective at creating head loss through the relatively large openings of the drain strainers, due to the limited sources of fibrous materials. Metal foils and fragments, which constitute the majority of debris material from LBLOCAs, tend to have multiple angles and shapes, which do not create an effective seal or resistance to flow. Sump strainer head loss tests have not shown noticeable pressure drop with RMI foil material. Thus, the absence of any significant source of fibrous material makes establishment of a significant differential pressure causing blockage non-credible.

The eight-inch refueling canal drains include a grate cover fabricated from three-inch tall flat bar with three parallel bars crossed by two parallel bars with each set of bars on approximately three inch centers. Blockage of either the top or sides of the deep end drain covers individually would not prevent flow through the drains, although neither of these scenarios was considered realistic. However, in spite of the remote possibility of blockage, given the limited size of the drain covers and the potential consequence of significant water hold-up in the refueling canal, the decision was made to install a larger strainer cover around the floor drain openings during the 2R19 (spring 2008) refueling outage to ensure an adequate flow path remained available from the refueling canal deep ends.

The conclusion of the review of potential debris sources and types combined with the significantly increased surface area of the refueling canal deep end drain strainers is that the design is conservative with respect to potential blockage from potential LOCA generated debris. Complete blockage of the drains is not considered credible, and partial obstruction, while considered highly improbable is shown to be acceptable based on the analyzed hold-up inventory as discussed in response to RAI B17.

**B17. Please provide justification for the sources and hold-up volumes that are predicted to affect water inventory to the post-LOCA sump for the limiting cases. The minimum water level included inventory from the safety injection tanks (SITs). It is not clear that the SITs would be available for all breaks that require recirculation. In addition, it was noted that the refueling canal was credited as a hold-up volume only for some breaks because other breaks will not produce debris that can plug the refueling canal drain lines. Please provide a justification for the assumption that some breaks will not produce debris that can block drainage from the refueling canal. Additionally, please provide the total volume that could be held up in the refueling canal. Provide information that justifies that the reported minimum water level is applicable to all cases where strainer operation is required. If necessary provide an updated minimum water level and update the required calculations and the minimum submergence level for the strainer if it is necessary to revise the submergence calculation.**

The minimum water level analysis credits the SIT water inventory based on acknowledgement that breaks of such a small size that a controlled depressurization of the RCS would have a correspondingly small ZOI and would produce significantly less debris loading than the limiting debris load tested. SBLOCA analysis for ANO-2 confirms that breaks as small as 0.05 ft<sup>2</sup> result in SIT inventory release to the RCS. This break size is equivalent to a three-inch diameter pipe compared to the 30" diameter cold leg break (S6) evaluated as the limiting break for strainer head loss. The ANO-2 sump strainer screen surface area is approximately 4800 ft<sup>2</sup>. Strainer tests conducted for ANO show that the strainer head loss remains very low (i.e., the "knee" in head loss response is not reached) similar to a clean strainer for debris conditions that are appreciably below the limiting break, due to the limited amounts of fiber and calcium-silicate insulation materials remaining in containment. Thus, while the SIT inventory is approximately 10% of the total water inventory added to the basement, the absence of strainer head loss more than compensates for the potential reduction in inventory. The reduction in sump water level if the SIT inventory were excluded is to approximately the top of the strainer assemblies.

Another factor why a break that does not release SIT inventory is not limiting include the HPSI pump NPSH, which is limiting for LBLOCA conditions with maximum pump flows, but for SBLOCAs the flow is lower and the NPSH margin is considerably higher. The reduction in NPSH required value for the HPSI pump exceeds five feet at flow values associated with SBLOCA versus LBLOCA with reductions in hydraulic losses at the reduced flows providing additional NPSH margin. Thus, in addition to minimal strainer head loss, the NPSH margin is considerably higher for SBLOCA conditions. Therefore, the most limiting conditions associated with minimum containment water level relative to sump strainer head loss and pump NPSH include the SIT inventory released in LBLOCA conditions.

Refueling canal water hold-up was calculated at 6600 gallons or less than 2% of the water inventory released into containment. The refueling canal drain covers, as noted in Section 3.1.4 of the final supplemental response dated September 15, 2008, and RAI B16, were supplemented with a larger additional strainer type cover of 18" diameter and 14-1/2" height. While the potential for significant quantities of debris from a SG cavity break reaching the refueling cavity are relatively low and the potential for such debris to

transport in the refueling canal floor to the drain cover is also low, these augmented drain covers were installed to ensure the refueling canal drain path is conservatively addressed. Regarding break evaluations of interest with regard to the refueling canal water hold-up, the breaks with potential for strainer head loss being the hot legs or cold legs, which would result in the release of more water inventory from the RCS than the amount credited with hold-up in the refueling canals. Complete blockage of the refueling canal deep end drain strainers is not considered credible for any break scenario. Partial obstruction of the drain strainers is conservatively credited for breaks that produce larger quantities of debris. Thus, the credited minimum water level remains conservatively bounding for the limiting breaks of interest with regards to strainer head loss and NPSH requirements for the pumps taking suction from the sump.

**Screen Modification Package:**

**B18. In your letter dated September 15, 2008, you stated that a stainless steel divider plate with square openings of 0.132" is installed between the two halves of the sump. Please provide the technical basis for concluding that blockage will not occur at this plate. Note that if blockage could occur at this plate, then any credit for single-train operation could be with only roughly half the strainer area.**

The stainless steel divider plate inside the sump has square openings of 0.132", as noted in the RAI, with a screen opening area of 15 ft<sup>2</sup>. The strainer is fabricated with perforated plate having 1/16" holes, as noted in Section 3.j.1 of the final supplemental response dated September 15, 2008. Thus, the area of the openings in the internal divider plate is greater than five times larger than the strainer openings. The strainer head loss qualification is based on two-train flow conditions. While it is expected that actions would be taken to secure one of the operating trains after accident conditions have stabilized, this action is not procedurally required, nor credited in the sump analysis. The flow distribution for the two halves of the strainer and divider plate for two-train flow is approximately equal with 53% of the flow on one side versus 47% on the other, based on analysis of the strainer and plenum assembly. Single failure conditions such as failure of a LPSI pump to stop or failure of a CSS or HPSI pump would result in significantly larger flow across the internal divider plate, but would be of short duration in the case of the LPSI pump failure to stop, or associated with lower total flow through the strainer and an associated reduction in total head loss in the case of a failure of CSS or HPSI pumps.

The small surface area divider plate screen could potentially be vulnerable to the accumulation of a fiber bed due to the fiber bypass fraction assigned to the strainer, particularly when significant flow is passing through the divider plate screen such as following a postulated single failure of one train, due to part of the operating train flow passing through the screen. The scenario of greatest interest is the potential for a particulate filtering thin-bed fiber layer to develop on the internal screen from the bypassed fibers and this occurring before most of the debris has transported to the strainer. This scenario is theoretically possible due to the rather large surface area ratio between the strainer and the divider plate screen. A thin-bed fiber layer on the divider plate screen could result in limiting the flow and therefore the associated debris accumulation on the side of the strainer not having an active suction flow path. This could result in uneven debris distribution across the strainer, directing a disproportionate amount of debris to the portion of the strainer with a flow path not passing through the

internal screen. The uneven debris accumulation could subsequently result in the debris loads exceeded those addressed by strainer head loss testing. The potential for this occurrence is related to the total available fiber, fiber bypass for the main strainer, flow through the divider plate, fiber bypass for the internal divider plate screen, and the fiber bed thickness needed on the divider plate screen to create thin-bed type filtration conditions. These topics are discussed in additional detail below.

The equivalent total fiber volume used in the ANO-2 strainer head loss test for the high fiber break (surge line) was approximately 62 ft<sup>3</sup>. This quantity included additional fiber (approximately 11.5 ft<sup>3</sup>) beyond the fiber debris load conservatively determined by the debris generation calculation to allow for future changes in analysis or installed insulations. This high fiber debris load test did not produce the most limiting strainer head loss, but is discussed in this response, since it provides the bounding fiber analysis. The vast majority (>80%) of this fiber source is Transco Thermal-Wrap blankets having fiberglass insulation filler. The strainer head loss test conservatively credited all of this material as being ejected from the heavy fabric covering and transported to the strainer as fines and very small pieces. No credit was taken for size distribution, fiber erosion, or debris transport reductions.

A fiber bypass value of 5% was conservatively applied to the main strainer for downstream effects evaluations even though fiber bypass tests conducted for the CCI strainers found substantially lower fiber bypass values. The fiber bypass tests indicated an average fiber bypass of less than 1.25%.

Maximum flow across the internal divider plate screen would occur in conjunction with a LPSI pump failure to stop upon initiation of sump recirculation, but as noted in RAI B9a, this event is short-lived (30 minutes) and was therefore not considered a limiting case for potential fiber build-up on the sump divider plate screen. Therefore, the flow across the divider plate screen associated with a single train out of service is considered the bounding case. Hydraulic analysis has determined that the flow imbalance across the two halves of the screen on either side of the divider plate is approximately 53% and 47%. The limiting flow of interest across the divider plate screen would be 53% of a single train, such that 53% of the bypassed fibers from the main strainer would pass across the divider plate screen.

A high fiber bypass is expected for the interior divider plate screen. Fiber strands with properties more conducive to screen capture would be trapped on the exterior strainer perforated plate surface, while fibers passing through these holes would be primarily fragments and isolated strands. These fibers would be expected to have a considerably higher bypass percentage for a clean second screen, even if it had the same size openings. Given that the interior screen does not have the same size openings, but has an opening area greater than five times larger than the exterior screen, the subsequent fiber bypass percentage for the interior screen would be expected to be very high. Sources of test data were not found that evaluated the capture efficiency of very fine fibers (i.e., that would pass through a 1/16" hole) on a wire mesh screen having approximately 1/8" square openings (0.132" square). Most test reports credited that smaller debris could accumulate on screen openings of this size, but such accumulation generally credits a large amount of available fiber or build-up from repeated recirculation of the fiber, with the fiber bed filling in very slowly at first, but more rapidly as the fiber layer becomes established.

Due to the absence of applicable data for the fiber bypass rate for fiber fines that have passed through a small opening and subsequently collect on a much larger opening, a reasonable bounding nominal value of 66% bypass is assigned and is combined with a reduction of the strainer fiber bypass value to 1.25% for discussion of the blockage potential of the internal divider plate. The divider plate screen bypass value of 66% (or 34% accumulation) is supported by NUREG/CR-6885 fiber accumulation data for a 1/8" screen. Table 5-1 of NUREG/CR-6885 found that for blender processed Nukon fiberglass fiber collected on the screen amounted to less than 25% of the total, which even when conservatively increased to account for "missing" fiber at the end of the test the bypass values were still approximately 63%. Given that these tests were conducted without upstream filtration by a screen having a smaller opening, as is applicable to the ANO-2 divider plate configuration, the use of a 66% bypass value is considered appropriate. The main strainer bypass value is supported by specific test data and is further considered acceptable for this review considering its combination with a bypass value of 66% for the internal divider plate, which is considered significantly low given the 5:1 size ratio for the two screen openings.

A high capture percentage at the sump screen effectively results in only one pass opportunity for accumulation on the interior divider plate screen. For example, a 5% bypass value of transported fibers for their first pass would be reduced to only 0.25% of the fiber total passing through the strainer on its second pass, if capture on the internal divider plate and other surfaces is ignored and no settling in the system or basement occurs. Similarly, for a 1.25% bypass value on the first pass, the reduction would be to 0.0156% of the fiber total passing through the strainer on its second pass. This results in the potential for debris build-up on the interior divider plate screen being reduced to the initial pass of fiber material that bypasses the main strainer.

In order for a fiber bed on the divider plate screen to be capable of thin-bed particulate filtration and the associated build-up of differential pressure, it would be expected to be at least 1/8" in thickness. This is based on the size of the openings being bridged (0.132" square) and the fiber bed being composed of smaller fiber fragments with limited cross-linkage (i.e., that would pass through the 1/16" holes of the outer strainer).

Given the above analysis the resulting potential fiber accumulation on the internal divider plate screen is summarized as follows:

Initial Fiber	% Bypass Main Strainer	% Flow Crossing Divider Plate	% Accumulation on Divider Plate	Fiber on Divider Plate
62 ft <sup>3</sup>	1.25%	53%	34%	0.14 ft <sup>3</sup>

$$\text{Fiber thickness on divider plate screen} = (0.14 \text{ ft}^3 / 15 \text{ ft}^2) \times 12 \text{ inches/ft} = 0.112" < 0.125"$$

Therefore, insufficient fiber is available, even including the excess fiber in the strainer test, to develop a layer 1/8" thick given the credible fiber bypass values for the strainer and internal divider plate.

In summary, considerably less than the tested amount of fiber debris is expected to arrive at the strainer as fines and very small pieces due to portions of it remaining inside the heavy cloth Thermal-Wrap insulation covering and portions ejected as large pieces. However, even with the conservative treatment of fiber debris combined with the additional fiber debris used in the strainer head loss test, and the most limiting flow condition through the internal divider plate associated with any active failure, the build-up of a particulate filtering fiber bed on the strainer's internal divider plate is not a credible outcome.

It is important when considering uncertainties with the preceding analysis to also weigh the potentially beneficial protective function provided by the internal divider plate. The plate, while not providing the same level of filtration protection as the main strainer, does provide an added degree of safety with respect to avoiding a possible common mode failure mechanism associated with a single sump pit providing suction source for both safety-related trains of equipment. Such a condition would be beyond the plant's design bases given the seismic qualification and other analysis to avoid possible threats (i.e., Seismic III, HELB dynamic effects, etc.) and detailed cleanliness and closeout inspections that are established to prevent the risk of foreign material intrusion or maintenance activities from affecting the strainer function. The presence of the internal divider plate provides an added defense in depth safety factor by greatly diminishing the potential for any of those conditions to adversely affect both trains of safety-related equipment required to function during sump recirculation.

**Structural Analysis:**

**B19. The Revised Content Guide for GL 2004-02 Supplemental Responses, Section 3k, requests a summary of structural qualification design margins for the various components of the sump strainer structural assembly. This summary should include interaction ratios and/or design margins for structural members, welds, concrete anchorages, and connection bolts as applicable. Please provide this information.**

Additional details of the structural analysis for the sump strainer are provided below.

**Design Conditions:**

Minimum sump water temperature during recirculation	=	60°F
Maximum sump water temperature during recirculation	=	233°F
Maximum containment air temperature	Normal	= 120°F
	Accident	= 285°F
Ambient temperature during installation	=	80°F

The following table shows event combinations to be considered.

Load Combinations:

LC No.	Temp. °F	Load Combination	Applicable Stress Limits
1	285	D (pool dry)	Normal Allowables
2	120	D + E (pool dry)	Normal Allowables
3	285	D + E' (pool dry)	1.5 x Normal Allowables
4	233	D + E' (pool filled)	1.5 x Normal Allowables
5	233	D + L <sub>Debris</sub> + E' (pool filled) + ΔP	1.5 x Normal Allowables
6	70	D + L <sub>Shielding</sub>	Normal Allowables

Where:

- D = Dead load of strainers and supporting structures
- L<sub>Debris</sub> = Weight of Debris
- ΔP = Differential pressure across strainer (3.382 psi = 0.0233 Mpa)
- E = Operating basis earthquake
- E' = Safe shutdown earthquake
- L<sub>Shielding</sub> = Additional load during outage for lead shielding

Allowable Stresses:

Allowable stresses are in accordance with the AISC Manual of Steel Construction with consideration of the requirements of ASCE Standard 8-02 as appropriate. It should be noted that the strainers are constructed primarily from plate elements, for which neither the AISC Steel Manual nor the ASCE Standard 8-02 directly provide guidance on allowable stress. For these elements, allowable stresses are considered on a 3D stress state using Von Mises failure theory criterion, with normal operating conditions limited to 0.6F<sub>y</sub> and extreme environmental conditions (accident and design basis earthquake (DBE)) limited to 0.9F<sub>y</sub>.

A separate structural analysis for trash racks was not necessary, since this function is incorporated into the strainer design. The front face of the CCI strainer module design serves as a barrier for large debris pieces from reaching the strainer perforated plate surfaces which are recessed in pockets in each module. The vertical height of the strainers also serves to limit large debris from reaching the front of most of the modules since larger debris pieces, if transported, would be expected to remain on or near the floor.

The maximum east side brace loads for DBE conditions are provided in the following table.

<b>Maximum East Side Brace Loads for the DBE Condition</b>					
<b>Element</b>	<b>Point</b>	<b>BP</b>	<b>Force (lbs)<sup>(1)</sup></b>	<b>Stress (lb/in<sup>2</sup>)</b>	<b>Time of Occurrence</b>
1	1	7	-586.4	277.9	6.01 sec
2	1	8	736.1	348.8	6.015 sec
3	1	3	-1,921.8	910.8	6.015 sec
4	1	3	652.9	309.4	6.015 sec
5	1	3	4,205.1	1,993.0	6.015 sec
6	1	4	-4,044.8	1,917.0	6.015 sec
7	1	4	-746.3	353.7	6.015 sec
8	1	4	1,218.3	577.4	6.01 sec
9	1	5	-582.3	276.0	6.015 sec
10	1	6	656.6	311.2	6.02 sec

**Notes**

(1) A negative force puts the brace member in compression and a positive force is in tension. The brace members are analyzed as if in compression (for either indicated compression or tension force), the worst condition (lowest allowable stress) for brace members.

The following load combinations represent the worst case loading for each component.

The members are 3"x3"x3/8" angles with the worst case load is for base plate 3 of 4,205.1 lbs and a stress of 1,993.0 psi. Radius of Gyration, r, for a L3"x3"x3/8" member = 0.587" (for z-z axis).  $Kl/r = 36"/0.587" = 61.3$  (L1 is 36" and using K = 1, appropriate for pinned-pinned end conditions). Normal allowable stress = 17.30 ksi > 1.993 ksi.

The braces are connected with two 3/4" A325 bolts loaded in pure shear. The gross area of the 3/4" bolts is 0.4418 in<sup>2</sup>. The shear stress on the bolts is  $f_v = 4,205.1 \text{ lbs}/(2*0.4418 \text{ in}^2) = 4,759 \text{ psi} < 15.0 \text{ ksi}$  normal allowable for A325 bolts.

The bolts are connected at the top of the base plate to 1/4" plate that is SA-240 Type 304 stainless steel with  $F_y = 23.6 \text{ ksi}$  at 250°F. The bearing stress on one of the two provided 3/4" bolts on the 1/4" plate is  $f_p = [4,205.1 \text{ lbs}/(2*0.25"*0.75")] = 11,213.6 \text{ psi}$ . The normal allowable bearing stress is  $F_p = 1.35*23.6 \text{ ksi} = 31.86 \text{ ksi} > 11.214 \text{ ksi}$ ; therefore, the bearing stress is within normal allowable stress limits for the DBE load.

The braces for base plate 7, base plate 8, base plate 5, and base plate 6 are connected to the gusset angle with two 1/2" A325 bolts. The largest load on these braces is 1218.3 lbs controlled by base plate 8. The gross area of the 1/2" bolts is 0.1963 in<sup>2</sup>. The shear stress on the bolts is  $f_v = 1218.3 \text{ lbs}/(2*0.1963 \text{ in}^2) = 3,103 \text{ psi} < 15.0 \text{ ksi}$  normal

allowable (DBE loads meet criteria for operating basis earthquake (OBE)). Check of bearing stress of bolt on connected part (for the 1/2" bolts) is  
 $f_p = [1218.3 \text{ lbs}/(2 \times 0.25" \times 0.50")] = 4,873 \text{ psi} < 31.86 \text{ ksi}$  (normal allowable).

The maximum potentially governing global loads at the wall plates are shown in the table below.

<b>Maximum East Side Brace Wall Plate Loads for the DBE Condition<sup>(1)</sup></b>				
<b>BP</b>	<b>Node</b>	<b>Force X-X<sup>(2)</sup> (lbs)</b>	<b>Force Y-Y<sup>(2)</sup> (lbs)</b>	<b>Time of Occurrence</b>
7	2401	284.5	-815.9	4.665 sec
8	2402	472.0	-663.1	4.955 sec
3	2403	-4,645.2	-533.2	6.015 sec
4	2404	1,485.0	-610.8	4.980 sec
4	2404	-1,323.7	872.2	6.240 sec
5	2405	1,055.0	-684.8	4.980 sec
6	2406	-943.8	459.7	7.345 sec

Notes:

- (1) Force in the Z-Z and all moments are equal to zero for all plate reactions.
- (2) The forces are in global coordinate reaction forces at the wall plates and are equal and opposite the force resultant from the braces.

Converting the forces in table above to local coordinates results in the following local loads as shown in the table below.

<b>East Braces Wall Plate Loads for the DBE Condition in Local Coordinates<sup>(1)</sup></b>				
<b>BP</b>	<b>Node</b>	<b>Force Z-Z<sup>(2)</sup> (lbs)</b>	<b>Force X-X<sup>(3)</sup> (lbs)</b>	<b>Time of Occurrence</b>
7	2401	-815.9	-284.5	4.665 sec
8	2402	-802.6	-135.1	4.955 sec
3	2403	2,907.7	-3,661.7	6.015 sec
4	2404	-1,482.0	618.2	4.980 sec
4	2404	1,552.7	-319.3	6.240 sec
5	2405	-1,055.0	684.8	4.980 sec
6	2406	943.8	-459.7	7.345 sec

Notes:

- (1) Force in the Local Y-Y and all moments are equal to zero for all plate reactions.
- (2) The forces in the -Z direction are in compression, however, are taken as an upper bound for tension on the wall plates.
- (3) The shear whether negative or positive is evaluated as positive shear on the wall plates.

Envelope loads on the four-bolt configuration is FZ = 2,907.7 lbs., FX = 3,661.7 lbs as shown below. The plate and anchorage is evaluated using a spreadsheet developed for this specific purpose. It is noted that the 13.5" distance between the bolts is less than the minimum spacing for 3/4" Maxi-Bolts in 5,000 psi strength concrete. However, per the actual pour data, the minimum concrete strength for the concrete in this area of the wall is  $f_c' = 7,750$  psi.

**Plate Number BP3 & BP4**

FX =	3661.7	lb	I1 =	13.500	in
FY =	0.00	lb	I2 =	13.500	in
FZ =	2907.7	lb	S1 =	6.750	in
MX =	0.00	in-lb			
MY =	0.00	in-lb	X =	6.250	in
MZ =	0.00	in-lb	Y =	6.250	in
SY =	36000.00	psi	d =	8.839	in
Plate (W)	16.000	in	Plate (H)	16.000	in
Prying Factor	1.000				
t (plate) =	0.750	in			
T (Allow) =	10850.00	lb	V (Allow) =	6270.00	lb

**Max Tension & Shear on Bolts**

T (max) =	726.9	lb/bolt	<	8999.05
V (max) =	915.4	lb/bolt	<	6270.00

**Wall Plate Stress**

FB (Allow)	27000			
fb (Plate)	6542.3		<	27000

The gusset plate is welded to the wall plate with a 1/4" fillet all the way around. The gusset plate is 13" per length; therefore, the weld loading is conservatively calculated as follows by adding the tension and shear load on the weld by absolute sum:  $f_w = (2,907.7 \text{ lbs.} + 3,661.7 \text{ lbs.})/26" \text{ (of weld)} = 252.7 \text{ lb/in.}$

Normal allowable weld load criteria:

$F_w = 0.30 \cdot 70 \text{ ksi} \cdot 0.707 \cdot 0.25" = 3.71 \text{ kips/in} > 0.253 \text{ kips/in}$

The allowable bolt tension and shear for the 1/2" bolts are shown below for both wall plates. For the 5"x10"x1/2" plate, the results are shown below:

**Plate Number BP5**

FX =	684.8	lb	I1 =	8.000	in
FY =	0.00	lb			
FZ =	1055.0	lb	S1 =	4.000	in
MX =	0.00	in-lb			
MZ =	0.00	in-lb			
SY =	36000.00	psi			
Plate (W)	5.000	in			
Prying Factor	1.000				
t (plate) =	0.500	in			
T (Allow) =	4600.00	lb	V (Allow) =	2660.00	lb

**Max Tension & Shear on Bolts**

T (max) =	527.5	lb/bolt	<	4600.00
V (max) =	342.4	lb/bolt	<	2660.00

**Wall Plate Stress**

FB (Allow)	27000			
fb (Plate)	10128.0		<	27000

For the 6"x15"x3/4" plate, the results are shown below:

**Plate Number BP5**

FX =	684.8	lb	I1 =	12.500	in
FY =	0.00	lb			
FZ =	1055.0	lb	S1 =	6.250	in
MX =	0.00	in-lb			
MZ =	0.00	in-lb			
SY =	36000.00	psi			
Plate (W)	6.000	in			
Prying Factor	1.000				
t (plate) =	0.750	in			
T (Allow) =	4600.00	lb	V (Allow) =	2660.00	lb

**Max Tension & Shear on Bolts**

T (max) =	527.5	lb/bolt	<	4600.00
V (max) =	342.4	lb/bolt	<	2660.00

**Wall Plate Stress**

FB (Allow)	27000			
fb (Plate)	5861.1		<	27000

The gusset is a 3"x3"x3/8" angle welded to the wall plate with a 3/16" fillet all the way around. The gusset angle has a total length of weld of 11.25"; therefore, the weld loading is conservatively calculated as follows by adding the tension and shear load on the weld be absolute sum:  $f_w = (1,055.0 \text{ lbs.} + 684.8 \text{ lbs.})/11.25" \text{ (of weld)} = 154.65 \text{ lb/in.}$

Normal allowable weld load criteria:

$F_w = 0.30 \cdot 70 \text{ ksi} \cdot 0.707 \cdot 0.1875" = 2.78 \text{ kips/in} > 0.155 \text{ kips/in}$

By inspection the prying potential for the two bolt configurations is less than the potential for the prying for the four bolt configuration that was determined to have no prying; therefore, the prying factor of 1.0 used in this calculation is justified.

East side braces conclusion:

The structural components for the east side braces meet the OBE acceptance criteria for DBE loads; therefore, these components are adequate for OBE loads.

West side wall brace evaluations:

The maximum forces on the braces in the local coordinates of the brace are as follows:

Maximum East Side Brace Loads for the DBE Condition					
Element	Point	BP	Force (lbs) <sup>(1)</sup>	Stress (lb/in <sup>2</sup> )	Time of Occurrence
1	1	10	-60.9	28.9	4.935 sec
2	1	9	-1,442.7	683.8	7.355 sec
3	1	2	969.5	459.5	7.35 sec
4	1	2	776.7	368.1	7.355 sec
5	1	2	-2,839.6	1,345.8	7.355 sec
6	1	1	2,311.3	1,095.4	7.35 sec
7	1	1	-139.6	66.1	7.355 sec
8	1	1	908.0	430.3	7.35 sec

Note:

- (1) A negative force puts the brace member in compression, and a positive force is in tension. The brace members are analyzed as if in compression the worst condition (lowest allowable stress) for the brace members

The members are 3"x3"x3/8" angles. The worst case load is for base plate 5 of 2839.6 lbs with a stress of 1,345.8 psi. It is noted that the angular braces for base plate 1 and base plate 2 have the highest loads and require larger bolting.

Normal AISC Allowable Stress calculation:

Radius of Gyration  $r$ , for a L3"x3"x3/8" member = 0.587 (for z-z axis (worst case for buckling), the buckling length  $L_1$  is 36".  $Kl/r = 36"/0.587" = 61.3$  (taking  $K = 1$ , appropriate for pinned-pinned end conditions). Normal allowable stress = 17.30 ksi > 1.35 ksi.

Other brace members have much higher margins by inspection due to the relatively low loads on the brace members. The braces are connected with two 3/4" A325 bolts loaded in pure shear. The gross area of the 3/4" bolts are 0.4418 in<sup>2</sup>. The shear stress on the bolts are  $f_v = 2,839.6 \text{ lbs}/(2*0.4418 \text{ in}^2) = 3,213.7 \text{ psi} < 15.0 \text{ ksi}$  normal allowable for A325 bolts.

For bearing type connections with threads included in the shear plane (worst case configuration), a check of bearing stress of bolt on connected part is: The bolts are connected at the top of the base plate to 1/4" plate that is SA-240 Type 304 stainless steel with  $F_y = 23.6 \text{ ksi}$  at 250°F. The bearing stress on one of the two provided 3/4" bolts on the 1/4" plate is:  $f_p = [2,839.6 \text{ lbs}/(2*0.25"*0.75")] = 7,572.3 \text{ psi}$ . The normal allowable bearing stress is  $F_p = 1.35*23.6 \text{ ksi} = 31.86 \text{ ksi} > 7.57 \text{ ksi}$ , (DBE loads acceptable for normal allowable stress).

The braces for base plate 9 and base plate 10 and the two braces perpendicular to base plate 1 and base plate 2 are connected to the gusset with two 1/2" A325 bolts. The largest load on these braces is 1442.7 lbs controlled by base plate 9. The gross area of the 1/2" bolts are 0.1963 in<sup>2</sup>, the shear stress on the bolts are:  $f_v = 1,442.7 \text{ lbs}/(2*0.1963 \text{ in}^2) = 3,674.7 \text{ psi} < 15.0 \text{ ksi}$  normal allowable (DBE loads meet criteria for OBE).

Check of bearing stress of bolt on connected part (for the 1/2" bolts) is:  $f_p = [1,442.7 \text{ lbs}/(2*0.25"*0.50")] = 5,770.8 \text{ psi} < 31.86 \text{ ksi}$  (normal allowable).

The maximum potentially governing global loads at the wall plates are shown in the table below.

<b>Maximum Brace West Side Wall Plate Loads for the DBE Condition<sup>(1)</sup></b>				
<b>BP</b>	<b>Node</b>	<b>Force X-X<sup>(2)</sup> (lbs)</b>	<b>Force Y-Y<sup>(2)</sup> (lbs)</b>	<b>Time of Occurrence</b>
1	2405	-1,699.5	-585.9	6.000 sec
1	2405	1,229.3	1,392.4	5.380 sec
2	2404	-3,434.1	170.7	7.355 sec
9	2403	-796.8	-1,202.7	7.355 sec
10	2402	-290.3	-1,209.9	6.005 sec

Notes:

- (1) Force in the Z-Z and all moments are equal to zero for all plate reactions.
- (2) The forces are in global coordinate reaction forces at the wall plates and are equal and opposite the force resultant from the braces.

Converting the forces in the above table to local coordinates results in the following local loads as shown in the table below.

<b>West Brace Wall Plate Loads for the DBE Condition in Local Coordinates<sup>(1)</sup></b>				
<b>BP</b>	<b>Node</b>	<b>Force Z-Z<sup>(2)</sup> (lbs)</b>	<b>Force X-X<sup>(3)</sup> (lbs)</b>	<b>Time of Occurrence</b>
1	2405	-1,616.0	787.4	6.000 sec
1	2405	1,853.8	115.3	5.380 sec
2	2404	-2,307.6	2,549.0	7.355 sec
9	2403	-1,413.9	-287.0	7.355 sec
10	2401	-1,209.9	290.3	6.005 sec

Notes:

- (1) Force in the Local Y-Y and all moments are equal to zero for all plate reactions.
- (2) The shear whether negative or positive is evaluated as positive shear on the wall plates.
- (3) Force Z-Z is evaluated as tension regardless of sign.

Envelope loads on the four bolt configuration is FZ = 2,307.6 lbs and FX = 2,549.0 lbs as shown below. The plate and anchorage evaluation results are shown below:

**Plate Number BP1 & BP2**

FX =	2549.0	lb	l1 =	13.500	in
FY =	0.00	lb	l2 =	13.500	in
FZ =	2307.6	lb	S1 =	6.750	in
MX =	0.00	in-lb			
MY =	0.00	in-lb	X =	6.250	in
MZ =	0.00	in-lb	Y =	6.250	in
SY =	36000.00	psi	d =	8.839	in
Plate (W)	16.000	in	Plate (H)	16.000	in
Prying Factor	1.000				
t (plate) =	0.750	in			
T (Allow) =	7320.00	lb	V (Allow) =	4230.00	lb

**Max Tension & Shear on Bolts**

T (max) =	576.9	lb/bolt	<	6473.04
V (max) =	637.25	lb/bolt	<	4230.00

**Wall Plate Stress**

FB (Allow)	27000		
fb (Plate)	5192.1	<	27000

Note that the plate bending meets normal allowable stress criteria for DBE loads, and therefore, the OBE is acceptable by comparison. The gusset plate is welded to the wall plate with a 1/4" fillet all the way around. The gusset plate is 13" per length; therefore, the weld loading is conservatively calculated as follows by adding the tension and shear load on the weld be absolute sum:  $f_w = (2549 \text{ lbs.} + 2307.6 \text{ lbs.})/26" \text{ (of weld)} = 186.8 \text{ lb/in.}$

Normal allowable weld load:

$F_w = 0.30 * 70 \text{ ksi} * 0.707 * 0.25" = 3.71 \text{ kips/in} > 0.187 \text{ kips/in.}$  Therefore, the components of the four-bolt plate configurations are acceptable by meeting the OBE criteria.

As shown in the table above, the two potentially limiting two bolt configurations are for the wall plates in base plate 9 and base plate 10. The enveloping loads on the two bolt configuration for these are  $F_Z = 1,413.9 \text{ lbs}$  and  $F_X = 290.3 \text{ lbs}$ . The plates are 5"x10"x3/4". The plate and anchorage evaluation results are shown below:

**Plate Number BP9 & BP10**

FX =	290.3	lb	I1 =	8.000	in
FY =	0.00	lb			
FZ =	1413.9	lb	S1 =	4.000	in
MX =	0.00	in-lb			
MZ =	0.00	in-lb			
SY =	36000.00	psi			
Plate (W)	5.000	in			
Prying Factor	1.000				
t (plate) =	0.750	in			
T (Allow) =	4600.00	lb	V (Allow) =	2660.00	lb

**Max Tension & Shear on Bolts**

T (max) =	706.95	lb/bolt	<	4600.00
V (max) =	145.15	lb/bolt	<	2660.00

**Wall Plate Stress**

FB (Allow)	27000		
fb (Plate)	6,032.6	<	27000

The components of the two-bolt configurations meet the normal allowable stress criteria for DBE loads, and therefore, the OBE is also acceptable.

The gusset is a 3"x3"x3/8" angle welded to the wall plate with a 3/16" fillet all the way around. The gusset angle has a total length of weld of 11.25"; therefore, the weld loading is conservatively calculated as follows by adding the tension and shear load on the weld be absolute sum:  $f_w = (1,413.9 \text{ lbs.} + 290.3 \text{ lbs.})/11.25" \text{ (of weld)} = 151.5 \text{ lb/in.}$

Normal allowable weld load:

$$F_w = 0.30 * 70 \text{ ksi} * 0.707 * 0.1875" = 2.78 \text{ kips/in} > 0.15 \text{ kips/in}$$

West side braces conclusion:

The structural components for the west side braces meet the acceptance criteria for DBE loads; therefore, the west side brace components are acceptable for OBE loads by comparison.

Strainer Anchor Bolt Analysis:

The anchorage to the floor for the strainers consists of 5/8" diameter A193 Gr. B8M Class 1 Maxi-bolts (VA = 3.58 k, TA = 6.10 k). These anchor bolts are analyzed for the dead weight + DBE loading including the debris loading plus hydrodynamic mass as follows:

**Eastside Strainer Summary of Forces on Anchor Bolts to Floor  
 Maximum for any Bolt at time – 6.015 seconds**

Location	Node	Shear X (lb)	Shear Y (lb)	Tension (-) Compression (+) (lb)	Shear Ratio	Tension Allowable (lb)	Tension Ratio
1	39	-194.71	-299.42	-59.02	0.101	6100.000	0.010
	40	-233.36	-0.35	-284.01	0.066	6100.000	0.047
2	239	-193.22	-375.06	-103.95	0.120	6100.000	0.017
	240	-272.34	-38.67	-185.76	0.078	6100.000	0.030
3	291	-139.18	-292.79	-206.53	0.092	6100.000	0.034
	292	-249.43	-55.69	-263.28	0.072	6100.000	0.043
4	343	-118.72	-288.62	-240.94	0.088	6100.000	0.039
	344	-265.78	-65.69	-249.19	0.078	6100.000	0.041
5	395	-117.75	-269.61	-326.23	0.083	6100.000	0.053
	396	-288.57	-63.08	-198.05	0.084	6100.000	0.032
6	447	-104.55	-288.77	-319.24	0.087	6100.000	0.052
	448	-317.26	-63.58	-194.51	0.092	6100.000	0.032
7	499	-93.09	-338.04	-237.73	0.099	6100.000	0.039
	500	-337.12	-87.08	-246.68	0.099	6100.000	0.040
8	551	-98.96	-333.18	-273.34	0.098	6100.000	0.045
	552	-346.97	-90.78	-253.42	0.102	6100.000	0.042
9	603	-74.33	-358.58	-189.37	0.104	6100.000	0.031
	604	-321.70	-122.85	-380.09	0.098	6100.000	0.062
10	655	-52.89	-383.60	-136.72	0.110	6100.000	0.022
	656	-301.25	-154.67	-463.31	0.096	6100.000	0.076
11	707	-34.91	-401.85	-156.62	0.114	6100.000	0.026
	708	-361.82	-147.48	-358.72	0.111	6100.000	0.059
12	759	-79.93	-390.38	-412.91	0.113	6100.000	0.068
	760	-440.20	-172.10	-392.00	0.134	6100.000	0.064
13	811	-92.64	-397.51	-530.11	0.116	6100.000	0.087
	812	-486.95	-211.98	-416.78	0.150	6100.000	0.068
14	863	-44.61	-484.58	-607.80	0.138	6100.000	0.100
	864	-577.93	-260.84	-488.98	0.180	6100.000	0.080
15	915	-146.40	201.14	-484.41	0.070	6100.000	0.079
	916	103.85	44.26	-334.56	0.032	6100.000	0.055
End Braces	2000	-189.20	-417.73	544.45	0.130	6100.000	0.089
	2001	-190.35	-396.07	531.46	0.124	6100.000	0.087
Maximum Interactions for Individual Bolts					0.180		0.100
Envelopes	Max	103.85	201.14	544.45	0.064	6100.00	0.089
	Min	-577.93	-484.58	-607.80	0.214	6100.00	0.100

**Westside Strainer Summary of Forces on Anchor Bolts to Floor  
 Maximum for Any Bolt at Time – 7.35 seconds**

Location	Node	Shear X (lb)	Shear Y (lb)	Tension (-) Compression (+) (lb)	Shear Ratio	Tension Allowable (lb)	Tension Ratio
1	39	-204.54	-26.58	-232.09	0.058	6100.000	0.038
	40	-209.12	112.30	-190.43	0.067	6100.000	0.031
2	239	-301.88	-97.36	-206.21	0.090	6100.000	0.034
	240	-226.23	224.69	-209.05	0.090	6100.000	0.034
3	291	-318.28	-71.25	-202.68	0.092	6100.000	0.033
	292	-189.41	209.20	-237.36	0.080	6100.000	0.039
4	343	-372.28	-38.88	-163.57	0.106	6100.000	0.027
	344	-183.49	192.96	-250.83	0.075	6100.000	0.041
5	395	-491.46	-74.67	35.56	0.141	6100.000	0.006
	396	-193.37	189.18	-251.38	0.077	6100.000	0.041
6	447	-486.22	-44.92	-5.11	0.138	6100.000	0.001
	448	-171.32	211.25	-151.70	0.077	6100.000	0.025
7	499	-482.18	-40.59	19.09	0.137	6100.000	0.003
	500	-156.19	202.85	-111.60	0.073	6100.000	0.018
8	551	-474.14	-43.91	56.26	0.135	6100.000	0.009
	552	-144.01	216.11	-25.27	0.074	6100.000	0.004
9	603	-305.22	-46.66	63.72	0.087	6100.000	0.010
	604	-28.31	211.18	182.98	0.060	6100.000	0.030
Braces	2000	-227.00	272.11	-261.13	0.100	6100.000	0.043
	2001	-240.41	274.92	-320.14	0.103	6100.000	0.052
Maximum Interactions for Individual Bolts					0.141		0.041
Envelope s	Max	-28.31	274.92	182.98	0.078	6100.00	0.030
	Min	-491.46	-97.36	-320.14	0.142	6100.00	0.052

For the anchor bolts considered with consistent loads on any one bolt, the maximum interaction is due to shear with a value of 0.180. For an envelope of maximum shear and tension forces on any bolt, the maximum interaction is due to shear with a value of 0.214. Hence, the anchor bolts are adequate for the design loadings.

End Braces:

The anchor bolts for the end braces were analyzed above for the floor anchorage of the strainer sections. For the braces themselves, the maximum forces and stresses are given in the table below.

<b>Forces and Stresses on End Braces For D + DBE</b>				
<b>Model</b>	<b>Force (lb)</b>	<b>Stress (psi)</b>	<b>Allowable Stress (psi)</b>	<b>Stress Ratio</b>
East Side	-621.7 (C)	-489.5	15000	0.03
West Side	-394.7 (C)	-310.8	15000	0.02

Interface Loads on Plenum:

Interface loads to the plenum are given at the top and bottom connection bolts for the duct extension between the first retaining structure for the east and west strainers as shown in the table below.

**Maximum Forces on the Plenum**

Loads Applied to the Plenum from the East Side Strainer

<b>Loading</b>	<b>Location</b>	<b>F<sub>x</sub> (lb)</b>	<b>F<sub>y</sub> (lb)</b>	<b>F<sub>z</sub> (lb)</b>
DW + OBE	Top	4.98	3.09	0.79
	Bottom	0.41	3.03	100.6
DW + DBE	Top	65.9	6.6	2.6
	Bottom	9.7	5.7	324.5

Loads Applied to the Plenum from the West Side Strainer

<b>Loading</b>	<b>Location</b>	<b>F<sub>x</sub> (lb)</b>	<b>F<sub>y</sub> (lb)</b>	<b>F<sub>z</sub> (lb)</b>
DW + OBE	Top	4.6	2.9	0.69
	Bottom	0.62	2.9	88.8
DW + DBE	Top	76.2	6.2	2.0
	Bottom	7.6	5.3	256.4

Notes:

- (1) Forces are given at top and bottom bolts of duct to plenum - consider as + or -.
- (2) +X = East, +Y = North, +Z = Vertical
- (3) Seismic loads have deadweight combined, but should still be taken as acting plus or minus for the given directions.

#### Global Displacements Due to Seismic Loadings:

The maximum resultant displacement for the east side strainer was 0.0122", and the maximum resultant displacement for the west side strainer was 0.008". For both strainer sides, the maximum global displacement for dynamic loadings is less than 1/16" (0.0625").

The maximum displacement from any case was applied to the single module model of the strainer support to determine stress levels. The maximum stress in the plates is 2144 psi occurring at the junction of the vertical retainer plates at the weld location to the upper base plate.

For the plate stress,  $2144 \text{ psi} < 0.9F_y = 0.9(20608 \text{ psi}) = 18547 \text{ psi}$  at 233°F.

#### Seismic Sloshing Analysis:

From the sloshing analysis, the force in the brace is 902.6 lbs on the east strainer. From the inertial DBE analysis for this brace, the maximum force is 582.3 lbs and was applied on the wall brace modeled as element 9. Combining these forces by square root of the sum of the squares (SRSS) gives a resultant force of  $(902.6^2 + 582.3^2)^{1/2} = 1074.1 \text{ lbs}$ .

For the highest loaded brace from the seismic inertia loading applied on the brace, the sloshing load is 11.0 lbs, and the inertial load is 4205.1 lbs. Combining these forces by SRSS gives a resultant force of  $(11.0^2 + 4205.1^2)^{1/2} = 4205.1 \text{ lbs}$ . For this brace, this is effectively a zero increase over the seismic inertial load alone. It is concluded that sloshing effects have minimal impact on the strainer supports and anchorage when combined with the greater magnitude seismic inertial loads.

#### Thermal Expansion Analysis:

The bolt which attaches to the anchor bolt is 30 mm (1.181") in diameter. This bolt runs through a 36 mm (1.417") diameter hole in the upper adjustable disc and a 35 mm (1.378 in) diameter hole in the lower adjustable disk. The lower adjustable disc also has an additional 0.5 mm (0.02") clearance within the lower base plate. This gives a nominal clearance of 0.217" to 0.236" at the anchor bolts. Maximum potential length of the base plate between the anchor bolts is 780 mm (30.709"). For a maximum temperature differential of  $(285^\circ\text{F} - 70^\circ\text{F}) = 215^\circ\text{F}$ , and a coefficient of thermal expansion  $9.17 \times 10^{-6} \text{ in/in}^\circ\text{F}$ , the change in length due to thermal expansion is  $215(9.17 \times 10^{-6})(30.709) = 0.061"$ .

There is more than sufficient clearance at the anchor bolts such that thermal expansion does not induce loads from expansion of the base plate. Maximum length of any duct section is approximately 39.7". For this length, the thermal movement would be  $215(9.17 \times 10^{-6})(39.7) = 0.078"$ . Additionally, the load path from the ducts to the anchor bolts is not direct, and additional flexibility of the support components would also accommodate the thermal displacements.

To determine the thermal expansion effect on the strainer support structure, the single module model was run for the case of 233°F corresponding to the highest seismic loading case. The maximum stress in the bottom plate of the duct (localized at the bolt connection point) is 22908 psi. This is less than the yield stress at temperature of 24580 psi, and only slightly higher than  $0.9(24580) = 22122$  psi. The 39375 psi stress is in the base plate between the anchor bolts. For this analysis, the clearances discussed above were not considered; hence, this stress would be relieved if this were considered.

#### Other Vertical Loads on Strainers:

##### Cartridges:

Models for the 400 mm and 200 mm cartridges were developed. The maximum differential pressure due to debris and head loss would be associated with the case of 60°F water; hence, the material properties used were those at 60°F. Allowable stress is then  $0.9F_y/2.24 = 0.9(30,000 \text{ psi})/2.24 = 12054$  psi. The 400 mm cartridge model (which was found to control over the 200 mm cartridge model) was run with varying differential pressures until the limiting allowable stress of 12054 psi was obtained. From these runs, the maximum differential pressure was determined to be 3.66 psi. The indicated maximum deflection is 0.023".

##### Seal Plates:

As for the cartridges, the material properties were modified (same as for the perforated plates for the cartridges), and the differential pressure was varied until the equivalent allowable stress of 12,054 psi was obtained. A limiting pressure for the seal plates was determined to be 4.26 psi.

These high stress points are due to the discontinuity at these points. These points were taken as the controlling stresses. The calculated displacement of 0.074" is slightly greater than 0.0625"; however, the seal plates would bear on the retaining structures at these locations, and no gaps would occur.

##### Lists:

As a conservative estimate of loads on the screws, the upper list is considered as a simple beam supported between the screws and loaded by the maximum global displacement of 0.0121" (lateral displacement of the modules is from the analysis models is less).

For a concentrated load, the maximum tensile force on each screw would be:

$$T = \frac{\Delta_{\max}(48)(E)(I)}{2l^3} = \frac{0.0121 \text{ in}(48)(28,300,000 \text{ psi})(0.0006 \text{ in}^4)}{2(26.5 \text{ in})^3} = 0.27 \text{ lb}$$

For shear, consider the list as a cable using the same displacement, and the shear load taken as the “cable” force:

$$V = \frac{\pi^2 EA}{4l^2} \quad Y_{\max}^2 = \frac{\pi^2(28.3E6 \text{ psi})(0.186 \text{ in}^2)}{4(26.5 \text{ in})^2} \quad (0.0121 \text{ in})^2 = 2.7 \text{ lb}$$

Tensile and shear demand on the screws is small. The vendor indicated minimum tensile strength was 70,000 psi. This would give normal allowable stress values of about 23 ksi for tension and 15 ksi for shear. Indicated stress levels are on the order of 6 psi tension and 62 psi shear (area for M6 screws is about 0.044 in<sup>2</sup>).

Based on this review, it is concluded that the M6x20 Type 316 bolts with nuts and serrated locking washers performs the intended design function.

**B20. The Revised Content Guide for GL 2004-02 requests a summary of the evaluations performed for dynamic effects such as pipe whip and jet impingement associated with HELBs. The submittal dated September 15, 2008, merely states, “...the identified HELB concerns have been evaluated and found acceptable.” Please provide a summary of the evaluation which was performed to justify this conclusion.**

The evaluation of potential dynamic effects such as pipe whip and jet impingement associated with High Energy Line Breaks (HELBs) was performed using standard criteria for such reviews. The evaluation includes both drawing reviews and field walkdown inspections. Some of the key inputs, assumptions, and analysis points are noted below:

Inputs:

When evaluating HELB impacts on pipe and conduit, break locations greater than ten pipe diameters from the target pipe or conduit are excluded from consideration for jet impingement damage. This exclusion is based on the common industry practice of considering jet impingement effects insignificant at a distance of ten pipe diameters from the source. The industry practice is based on NUREG/CR-2913 which demonstrates that the pressure on a target asymptotically approaches zero at a distance of ten pipe diameters from the break. As a strainer and plenum may be somewhat less robust than pipe or conduit, an additional distance margin (80%) was (L/D > 18). (L) is the vertical distance from the break to the maximum water level, and (D) is the nominal pipe diameter. The actual L/D was determined and where applicable, shows to be greater than 18 pipe diameters.

ANO-2 Safety Analysis Report (SAR) Section 3.6.2.1.A postulated breaks in the RCS main loop were eliminated from the ANO-2 RCS dynamic effects design basis by application of leak-before-break (LBB) methodology. However, in accordance with NUREG-1061 Volume 3, the non-mechanistic RCS main loop pipe rupture design basis is maintained for containment design, ECCS performance analysis, and electrical and mechanical environmental qualification.

Method of Analysis:

The existing calculations addressing HELBs were reviewed along with associated piping isometric and piping layout drawings to identify the locations of HELBs within containment. Calculations addressing mainsteam, feedwater or SG blowdown piping were not considered, as breaks in these lines do not require the plant to enter recirculation mode and thus do not require operation of the containment sump strainer. For the remaining calculations, the elevation of identified break locations was compared with the elevation of the maximum post-LOCA contamination flood level, which is used as it bounds the elevation of the strainer modules and plenum. The vertical distance (L) from the break to the maximum water level is divided by the nominal pipe diameter (D). This resultant L/D is used to evaluate the potential for damage due to jet impact and pipe whip. An L/D greater than 18 is established by engineering judgment to be sufficient to preclude damage to the strainer/plenum. Based on this conservative, one-dimensional, vertical distance L/D value, many HELB locations are demonstrated not to require further consideration.

The maximum containment flood elevation level is higher than the top of the new strainer and plenum. The maximum flood level was compared with each HELB elevation to determine whether the break has the potential to impact the strainer or the piping penetrating the sump seal plate. Using this conservative technique the majority of HELB locations are eliminated from further consideration.

The remaining break locations were then reviewed on a case-by-case basis. The HELB locations may be eliminated as potential impacts for any of the following reasons:

- The HELB locations are sufficiently distant (in three dimensions) from the strainer, strainer plenum, or piping entering the sump.
- The strainer, strainer plenum, or sump piping is shielded from the HELB by a wall floor or other structure.
- The HELB does not result in the plant entering recirculation mode, and thus the strainer is not called upon to safely shut down the plant.

In summary, the above inspection and analysis criteria was applied with the location of the ANO-2 sump strainer assemblies to conclude that there are no potential HELB sources that create pipe whip, jet impact, or missile hazards for the containment sump strainers. The HELB lines evaluated were addressed as not posing a threat due to distance from the strainers, a break not requiring sump recirculation, shielding, or similar criteria as described above.

**Downstream Effects/In-Vessel:**

**B21. The NRC staff does not consider in-vessel downstream effects to be fully addressed at ANO-2 as well as at other PWRs. ANO-2’s submittal refers to draft WCAP-16793-NP, “Evaluation of Long-Term Cooling Considering Particulate, Fibrous, and Chemical Debris in the Recirculating Fluid.” The NRC staff has not issued a final SE for WCAP-16793-NP. The licensee may demonstrate that in-vessel downstream effects issues are resolved for ANO-2 by showing that the licensee's plant conditions are bounded by the final WCAP-16793-NP and the corresponding final NRC staff SE, and by addressing the conditions and limitations in the final SE. The licensee may also resolve this item by demonstrating without reference to WCAP-16793 or the NRC staff SE that in-vessel downstream effects have been addressed at ANO-2. In any event, the licensee should report how it has addressed the in-vessel downstream effects issue within 90 days of issuance of the final NRC staff SE on WCAP-16793. The NRC staff is developing a Regulatory Issue Summary to inform the industry of the NRC staff’s expectations and plans regarding resolution of this remaining aspect of GSI-191.**

The following preliminary review relative to the WCAP-16793, Revision 1 acceptance criteria is provided for comparison purposes only, since this document is not yet approved by the NRC, and additional changes to the acceptance criteria may be forthcoming.

The following table provides an ANO-2 comparison to the fuel analysis report associated with Westinghouse fuel designs and CE Guardian grid fuel designs.

Debris Type	Debris Load per fuel assembly (lb)	Maximum Debris Load per qualification testing (lb)	% of allowable
Fiber	≤ 0.44	0.05	14
Particulate	≤ 29	7.8	27
Chemical	≤ 13	3.2	25
Calcium-silicate	≤ 6	4.5	75
Microporous Insulation	≤ 3.2	0	0

As can be seen from the above comparisons, the ANO-2 maximum debris load per analysis and testing remains well below the allowable values in the preliminary revision to WCAP-16793. While the final SE approved acceptance criteria for fuel blockage may change, given the margins to the current acceptance criteria the ANO-2 fuel analysis is anticipated to remain satisfactory. Formal response to this issue will be provided pending issuance of the final approved acceptance criteria for fuel blockage.

**Attachment 3 to**

**0CAN090901**

**Generic RAIs Applicable to both ANO-1 and ANO-2 Concerns with  
Westinghouse Debris Generation Testing**

Generic RAIs Applicable to both ANO-1 and ANO-2 Concerns with  
Westinghouse Debris Generation Testing

**B22. The issues listed below are a generic set of requests for additional information (RAIs) that should be asked of licensees that credit ZOI reductions based on Westinghouse testing conducted at Wyle. The Pressurized Water Reactor (PWR) Owners Group (PWROG) has committed to consider resolving some of these issues generically. The issues to be resolved by the PWROG have not been identified as of this time. The licensee should coordinate with the PWROG, as appropriate, to resolve the issues being treated generically. Note that the concerns discussed below are based on the review of WCAP-16710-P, "Jet Impingement Testing to Determine the zone-of-influence (ZOI) of Min-K and NUKON® Insulation for Wolf Creek and Callaway Nuclear Operating Plants," and WCAP-16851-P, "Florida Power and Light (FPL) Jet Impingement Testing of calcium-silicate Insulation." However, the NRC staff believes that the issues identified below likely apply to all Westinghouse debris generation testing conducted at Wyle Labs.**

See RAI responses B23 through B50 and the Westinghouse ZOI testing at Wyle Labs discussion provided in Attachment 4 for additional detail.

**B23. Although the American National Standards Institute/American Nuclear Society (ANSI/ANS) standard predicts higher jet centerline stagnation pressures associated with higher levels of subcooling, it is not intuitive that this would necessarily correspond to a generally conservative debris generation result. Please justify the initial debris generation test temperature and pressure with respect to the plant-specific reactor coolant system (RCS) conditions, specifically the plant hot and cold leg operating conditions. If ZOI reductions are also being applied to lines connecting to the pressurizer, then please also discuss the temperature and pressure conditions in these lines. Were any tests conducted at alternate temperatures and pressures to assess the variance in the destructiveness of the test jet to the initial test condition specifications? If so, please provide that assessment.**

Reference Westinghouse ZOI testing at Wyle Labs discussion in Attachment 4 for a general discussion of the testing performed.

**B24. Please describe the jacketing/insulation systems used in the plant for which the testing was conducted and compare those systems to the jacketing/insulation systems tested. Demonstrate that the tested jacketing/insulation system adequately represented the plant jacketing/insulation system. The description should include differences in the jacketing and banding systems used for piping and other components for which the test results are applied, potentially including SGs, pressurizers, reactor coolant pumps, etc. At a minimum, the following areas should be addressed:**

See responses to RAIs B25 and B26.

**B25. Please describe how the characteristic failure dimensions of the tested jacketing/insulation compare with the effective diameter of the jet at the axial placement of the target. The characteristic failure dimensions are based on the primary failure mechanisms of the jacketing system (e.g., for a stainless steel jacket held in place by three latches where all three latches must fail for the jacket to fail, then all three latches must be effectively impacted by the pressure for which the ZOI is calculated). Applying test results to a ZOI based on a centerline pressure for relatively low target length-to-diameter ratio nozzle to target spacing would be non-conservative with respect to impacting the entire target with the calculated pressure.**

The WCAP-16836-P jet impingement tests conducted for Arkansas Nuclear One (ANO) were performed on two separate insulating materials: calcium-silicate insulation on piping with stainless steel lagging fastened with sheet metal screws, and Transco Thermal-Wrap blankets or pads. The responses discuss these two insulation tests separately below.

The calcium-silicate insulation test was performed at an equivalent ZOI of 25D with the test article placed 33.8 ft away from the jet nozzle. The test specimen consisted of a pipe section with approximately four-foot length of calcium-silicate insulation covered with stainless steel lagging having an overlap of approximately two inches and secured with sheet metal screws on approximately eight-inch intervals along the seam. The seam was oriented at an angle of approximately 45° to allow the high energy jet the greatest potential to open the seam and peel the lagging away from the underlying calcium-silicate. Inspection of the test specimen following the test provided evidence that the full length of the seam was impacted by the test jet based on the “wavy” lip along the length of the seam edge, a sheet metal screw near the center of the specimen that was still in the overlap of the lagging but had pulled out of the underlap, visible screw threads in the gap between the overlap and underlap on other screws, and a screw torn free from the overlap on the right edge of the specimen. The test article showed signs of deformation but there was no significant damage to either the lagging material or the underlying calcium-silicate insulation. None of the calcium-silicate insulation was exposed and there were no breaches of the jacketing material.

Thus, the test provides a conservatively bounding ZOI for this material configuration. Additional conservatism exists based on the test configuration having the overlap seam oriented at an optimum angle for the jet to open the seam. While this configuration could occur at random sections in the plant, the specified installation practice is to stagger the seams and have the lap joints oriented downward for horizontal pipe. Since approximately half of the affected calcium-silicate insulation is located in horizontal pipes below the limiting break, much of the pipe insulation would have a lower susceptibility to failure based on less favorable seam orientation relative to the break than that tested.

The Transco Thermal-Wrap blanket tests were intended to evaluate the potential for failure of the covering fabric and/or seams, since this material is installed at ANO-2 without metal covering or encapsulation. There are no buckles or latches involved with this test or the associated failure mode. The test was intended to determine if the destructive pressure of the high energy jet at the tested equivalent ZOIs was sufficient to result in breaches of the tightly woven fabric or seams which would allow the interior fiberglass insulation batting to be released. Since the test involved direct impingement

on the test specimen and there was not an associated failure dependency on the need for multiple spaced sub-components to also fail, the test is not considered susceptible to the potential biases being addressed by this RAI.

**B26. Please describe if the insulation and jacketing system used in the testing of the same general manufacturer and manufacturing process as the insulation used in the plant. If not, what steps were taken to ensure that the general strength of the insulation system tested was conservative with respect to the plant insulation? For example, it is known that there were generally two very different processes used to manufacture calcium-silicate whereby one type readily dissolved in water but the other type dissolves much more slowly. Such manufacturing differences could also become apparent in debris generation testing as well.**

As noted in the response to RAI B25, the WCAP-16836-P jet impingement tests conducted for ANO were performed on two separate insulating materials: calcium-silicate insulation on piping with stainless steel lagging fastened with sheet metal screws, and Transco Thermal-Wrap blankets or pads. The calcium-silicate insulation over pipe test specimen was prepared at ANO using materials (i.e., calcium-silicate, stainless steel lagging and sheet metal screws) and fabrication methods consistent with those specified and installed at the plant. The Transco Thermal-Wrap insulation blankets were obtained from Transco and fabricated using the same materials and processes as those supplied to ANO and used as insulation on the ANO-2 pressurizer top head, bottom head, and skirt regions. Thus, the materials used in the jet impingement tests were consistent with those installed and did not introduce a potential source for additional uncertainty with the test results.

**B27. The information provided should also include an evaluation of scaling the strength of the jacketing or encapsulation systems to the tests. For example, a latching system on a 30-inch pipe within a ZOI could be stressed much more than a latching system on a ten-inch pipe in a scaled ZOI test. If the latches used in the testing and the plants are the same, the latches in the testing could be significantly under-stressed. If a prototypically sized target were impacted by an undersized jet it would similarly be under-stressed. Evaluations of banding, jacketing, rivets, screws, etc., should be made. For example, scaling the strength of the jacketing was discussed in the Ontario Power Generation report on calcium-silicate debris generation testing.**

This issue is not believed to be applicable to the WCAP-16836-P ZOI tests as applied at ANO. As noted in the above responses the tests included two different insulating systems: calcium-silicate insulation on piping with stainless steel lagging fastened with sheet metal screws, and Transco Thermal-Wrap blankets or pads. The calcium-silicate insulation system was being tested due to the use of sheet metal screws to secure the lagging seam at ANO instead of banding, which was used in the tests which formed the basis for the ZOI in NEI 04-07. The pullout strength of the sheet metal screw from the stainless steel lagging should not be affected by the size of the pipe covered since neither the lagging thickness nor sheet metal screw size changes. Further, the test specimen pipe size was consistent with most of the installed calcium-silicate insulation using sheet metal screws, which is smaller bore piping, with the only larger pipe size included in the limiting break as debris due to the relatively large ZOI associated with a 30" pipe break (ZOI distance of 62.5 ft).

The Transco Thermal-Wrap blanket tests are also not believed to be affected by scaling of the blanket size between the test specimens and the installed Thermal-Wrap pads. Since the blankets are not covered by any type of metal lagging or encapsulation and do not include buckles or latches, there is no associated reliance upon a specific fastener size or combination relative to failure of the blanket material. The tests were performed to determine if the blanket fabric would be torn or shredded or if the blanket seams would fail when exposed to a high energy jet. The size of the test blanket versus those installed on the ANO-2 pressurizer is not considered to have any effect on the robustness of the fabric covering and blanket seams relative to failure.

- B28. There are relatively large uncertainties associated with calculating jet stagnation pressures and ZOIs for both the test and the plant conditions based on the models used in the WCAP reports. Please explain the steps taken to ensure that the calculations resulted in conservative estimates of these values. Please provide the inputs for these calculations and the sources of the inputs.**

Reference Westinghouse ZOI testing at Wyle Labs discussion in Attachment 4 for a general discussion of the testing performed.

- B29. Please describe the procedure and assumptions for using the ANSI/ANS-58-2-1988 standard to calculate the test jet stagnation pressures at specific locations downrange from the test nozzle.**

Reference Westinghouse ZOI testing at Wyle Labs discussion in Attachment 4 for a general discussion of the testing performed.

- B30. Please explain if the analysis based on initial conditions (temperature) that matched the initial test temperature. If not, please provide an evaluation of the effects of any differences in the assumptions.**

Reference Westinghouse ZOI testing at Wyle Labs discussion in Attachment 4 for a general discussion of the testing performed.

- B31. Please explain if the water subcooling used in the analysis that of the initial tank temperature or was it the temperature of the water in the pipe next to the rupture disk? Test data indicated that the water in the piping had cooled below that of the test tank.**

Reference Westinghouse ZOI testing at Wyle Labs discussion in Attachment 4 for a general discussion of the testing performed.

- B32. The break mass flow rate is a key input to the ANSI/ANS-58-2-1988 standard. Please describe how the associated debris generation test mass flow rate was determined. If the experimental volumetric flow was used, then please explain how the mass flow was calculated from the volumetric flow given the considerations of potential two-phase flow and temperature-dependent water and vapor densities. If the mass flow was analytically determined, then please describe the analytical method used to calculate the mass flow rate.**

Reference Westinghouse ZOI testing at Wyle Labs discussion in Attachment 4 for a general discussion of the testing performed.

**B33. Noting the extremely rapid decrease in nozzle pressure and flow rate illustrated in the test plots in the first few tenths of a second, please explain how the transient behavior was considered in the application of the ANSI/ANS-58-2-1988 standard? Specifically, please explain if the inputs to the standard represent the initial conditions or the conditions after the first extremely rapid transient, e.g., say at one tenth of a second.**

Reference Westinghouse ZOI testing at Wyle Labs discussion in Attachment 4 for a general discussion of the testing performed.

**B34. Given the extreme initial transient behavior of the jet, please justify the use of the steady-state ANSI/ANS-58-2-1988 standard jet expansion model to determine the jet centerline stagnation pressures rather than experimentally measuring the pressures.**

Reference Westinghouse ZOI testing at Wyle Labs discussion in Attachment 4 for a general discussion of the testing performed.

**B35. Please describe the procedure used to calculate the isobar volumes used in determining the equivalent spherical ZOI radii using the ANSI/ANS-58-2-1988 standard.**

Reference Westinghouse ZOI testing at Wyle Labs discussion in Attachment 4 for a general discussion of the testing performed.

**B36. Please provide the assumed plant-specific RCS temperatures and pressures and break sizes used in the calculation. Note that the isobar volumes would be different for a hot leg break than for a cold leg break since the degrees of subcooling is a direct input to the ANSI/ANS-58-2-1988 standard and which affects the diameter of the jet. Note that an under-calculated isobar volume would result in an under-calculated ZOI radius.**

Reference Westinghouse ZOI testing at Wyle Labs discussion in Attachment 4 for a general discussion of the testing performed.

**B37. Please explain the calculational method used to estimate the plant-specific and break-specific mass flow rate for the postulated plant loss-of-coolant accident (LOCA), which was used as input to the standard for calculating isobar volumes.**

Reference Westinghouse ZOI testing at Wyle Labs discussion in Attachment 4 for a general discussion of the testing performed.

**B38. Given that the degree of subcooling is an input parameter to the ANSI/ANS-58-2-1988 standard and that this parameter affects the pressure isobar volumes, please state the steps taken to ensure that the isobar volumes conservatively match the plant-specific postulated LOCA degree of subcooling for the plant debris generation break selections and if multiple break conditions were calculated to ensure a conservative specification of the ZOI radii.**

Reference Westinghouse ZOI testing at Wyle Labs discussion in Attachment 4 for a general discussion of the testing performed.

**B39. Please provide a detailed description of the test apparatus specifically including the piping from the pressurized test tank to the exit nozzle including the rupture disk system.**

Reference Westinghouse ZOI testing at Wyle Labs discussion in Attachment 4 for a general discussion of the testing performed.

**B40. Based on the temperature traces in the test reports, it is apparent that the fluid near the nozzle was colder than the bulk test temperature. Please describe how the fact that the fluid near the nozzle was colder than the bulk fluid was accounted for in the evaluations.**

Reference Westinghouse ZOI testing at Wyle Labs discussion in Attachment 4 for a general discussion of the testing performed.

**B41. How was the hydraulic resistance of the test piping which affected the test flow characteristics evaluated with respect to a postulated plant-specific LOCA break flow where such piping flow resistance would not be present?**

Reference Westinghouse ZOI testing at Wyle Labs discussion in Attachment 4 for a general discussion of the testing performed.

**B42. Please discuss the specified rupture differential pressure of the rupture disks.**

Reference Westinghouse ZOI testing at Wyle Labs discussion in Attachment 4 for a general discussion of the testing performed.

**B43. Regarding a potential shock wave resulting from the instantaneous rupture of piping, please respond to the following questions:**

See responses to RAIs B44 through B47.

**B44. Was any analysis or parametric testing conducted to get an idea of the sensitivity of the potential to form a shock wave at different thermal-hydraulic conditions? Were temperatures and pressures prototypical of PWR hot legs considered?**

Reference Westinghouse ZOI testing at Wyle Labs discussion in Attachment 4 for a general discussion of the testing performed.

**B45. Was the initial lower temperature of the fluid near the test nozzle taken into consideration in the evaluation? Specifically, was the damage potential assessed as a function of the degree of subcooling in the test initial conditions?**

Reference Westinghouse ZOI testing at Wyle Labs discussion in Attachment 4 for a general discussion of the testing performed.

**B46. What is the basis for scaling a shock wave from the reduced-scale nozzle opening area tested to the break opening area for a limiting rupture in the actual plant piping?**

Reference Westinghouse ZOI testing at Wyle Labs discussion in Attachment 4 for a general discussion of the testing performed.

**B47. How is the effect of a shock wave scaled with distance for both the test nozzle and plant condition?**

Reference Westinghouse ZOI testing at Wyle Labs discussion in Attachment 4 for a general discussion of the testing performed.

**B48. In cases where the application of the reduced ZOI is applied to components other than piping, please respond to this question. Please provide the basis for concluding that a jet impact on piping insulation with a 45° seam orientation is a limiting condition for the destruction of insulation installed on steam generators (SGs), pressurizers, reactor coolant pumps, and other non-piping components in the containment. For instance, considering a break near the SG nozzle, once insulation panels on the SG directly adjacent to the break are destroyed, the LOCA jet could impact additional insulation panels on the SG from an exposed end, potentially causing damage at significantly larger distances than for the insulation configuration on piping that was tested. Furthermore, it is not clear that the banding and latching mechanisms of the insulation panels on a SG or other RCS components provide the same measure of protection against a LOCA jet as those of the piping insulation that was tested. One WCAP reviewed asserts that a jet cannot directly impact the SG, but will flow parallel to it. It seems that some damage to the SG insulation could occur near the break, with the parallel flow then jetting under the surviving insulation, perhaps to a much greater extent than predicted by the testing. Similar damage could occur to other component insulation. Please provide a technical basis to demonstrate that the test results for piping insulation are prototypical or conservative of the degree of damage that would occur to insulation on SGs and other non-piping components in the containment.**

The testing conducted for ANO and documented in WCAP-16836 involved two different insulation types: Calcium-silicate installed on piping covered with stainless steel lagging that was secured with sheet metal screws rather than banding; and Transco Thermal-Wrap blanket pads. The calcium-silicate test results were only applicable to piping insulation; therefore, this RAI is not applicable to those test results. The ZOI testing for Transco Thermal-Wrap blankets is discussed in responses to RAIs B1, B3a, and B3c.

In summary of the information previously provided in those responses, the Transco Thermal blanket insulation is installed on the ANO-2 pressurizer top and bottom heads and inside the base support or skirt below the lower head. The Thermal-Wrap blankets are not enclosed in metal cartridges or covered with metal lagging. Tests were conducted with the Thermal-Wrap blankets captured in a test stand oriented to determine if the high energy jet would cause failure of the tightly woven fabric covers and/or seams.

Thus, the insulation system tested does not rely upon latches or buckles and there are not protective panels or jacketing barriers that are credited with avoiding release of the internal fiberglass batting.

Since the Thermal-Wrap pads are constructed with a series of adjacent but discrete pads, failure of one does not affect the failure of nearby pads, since they do not rely upon a common barrier or cover. However, the extent of credited insulation destruction was considered to encompass all of the material at the affected location, consistent with the intent of this line of questioning. Since the application of this material is limited to the top and bottom of the pressurizer, the propagation of failure to further equivalent ZOI distances is not applicable beyond the immediate vicinity of the top head or the bottom head insulation.

The pressurizer surge line break which potentially affects the Thermal-Wrap insulation on the bottom head and skirt of the pressurizer was credited with 100% destruction of all of the Thermal-Wrap pads in this location with full release of all insulation content and subsequent destruction of the fiber batting into fines and very small pieces such that full transport to the sump strainer was assumed. Thus, the break did not credit partial destruction of the insulation pads and stop at an adjacent pad at the ZOI limit, but included all of the related insulation material in the vicinity.

**B49. Some piping oriented axially with respect to the break location (including the ruptured pipe itself) could have insulation stripped off near the break. Once this insulation is stripped away, succeeding segments of insulation will have one open end exposed directly to the LOCA jet, which appears to be a more vulnerable configuration than the configuration tested by Westinghouse. As a result, damage would seemingly be capable of propagating along an axially oriented pipe significantly beyond the distances calculated by Westinghouse. Please provide a technical basis to demonstrate that the reduced ZOIs calculated for the piping configuration tested are prototypical or conservative of the degree of damage that would occur to insulation on piping lines oriented axially with respect to the break location.**

The only piping insulation addressed by the WCAP-16836-NP was tested at an equivalent ZOI of 25D, thus this RAI is not considered applicable. The testing of Thermal-Wrap blankets performed by this WCAP is likewise not applicable. The ANO-2 Thermal-Wrap blankets are installed on the top and bottom heads of the pressurizer and are at a discrete distance from the potential break sources such that the described propagation of failure in the RAI is not applicable.

**B50. At least one WCAP noted damage to the cloth blankets that cover the fiberglass insulation in some cases resulting in the release of fiberglass. The tears in the cloth covering were attributed to the steel jacket or the test fixture and not the steam jet. It seems that any damage that occurs to the target during the test would be likely to occur in the plant. Please explain if the potential for damage to plant insulation from similar conditions was considered. For example, the test fixture could represent a piping component or support, or other nearby structural member. The insulation jacketing is obviously representative of itself. Please explain what provides the basis that damage similar to that which occurred to the end pieces is not expected to occur in the plant. It is likely that a break in the plant will result in a much more chaotic condition than that which occurred in testing. Therefore, it would be more likely for the insulation to be damaged by either the jacketing or other objects nearby.**

See the responses to RAIs B1, B3a, and B3c.

**Attachment 5 to**

**OCAN090901**

**List of Regulatory Commitments**

List of Regulatory Commitments

The following table identifies those actions committed to by Entergy in this document. Any other statements in this submittal are provided for information purposes and are not considered to be regulatory commitments.

<b>COMMITMENT</b>	<b>TYPE</b> (Check One)		<b>SCHEDULED COMPLETION DATE</b> (If Required)
	<b>ONE-TIME ACTION</b>	<b>CONTINUING COMPLIANCE</b>	
A formal response to RAIs A15 and B21 will be provided pending issuance of the NRC's SE.	X		Within 90 days of issuance of the final NRC Staff SE on WCAP-16793

**Attachment 6 to**

**0CAN090901**

**Westinghouse Affidavit**



Westinghouse Electric  
Company  
Nuclear Services  
Waltz Mill Service Center  
P.O. Box 158  
Madison, Pennsylvania 15663  
USA

Ms. Natalie Moser  
Entergy Operations, Inc.  
Arkansas Nuclear One  
1448 SR 333  
Russellville, AR 72802

Direct tel: 724-722-5692  
Direct fax: 724-722-5166  
e-mail: marklele@westinghouse.com

Our ref: CARK2-09-006  
August 3, 2009

Entergy Operations, Inc.  
Arkansas Nuclear One Unit 2  
**Westinghouse Authorization to Entergy for Providing Information  
from WCAP-16836-P, Rev.0 to the NRC in responding to RAIs**

Reference: WCAP-16836-P, Revision 0, "Arkansas Nuclear One - Jet Impingement Testing of Insulating Materials," dated October 2007

Dear Ms. Moser:

This letter officially transmits CAW-09-2622 which includes authorization to Entergy to provide information from WCAP-16836-P, Revision 0, "Arkansas Nuclear One - Jet Impingement Testing of Insulating Materials," dated October 2007, in your response to the NRC requests for additional information.

The following attachments to this letter are provided for Entergy's use:

1. Information to include in Entergy's Transmittal to the NRC
2. Westinghouse letter CAW-09-2622 "Application for Withholding Proprietary Information from Public Disclosure" with attachments to include:
  - Affidavit
  - Proprietary Information Notice to be attached to your NRC transmittal letter.
  - Copyright Notice to be attached to your NRC transmittal letter.

If you have any questions, please do not hesitate to call me at 724-722-5692.

Very truly yours,

A handwritten signature in black ink that reads "Larry E. Markle".

Larry E. Markle  
Customer Project Manager

/slb

Attachments

1. Information to include in Entergy's Transmittal to the NRC
2. CAW-09-2622

cc: J. A. Gresham (W)  
R. Bastien (W)  
C. Brinkman (W)  
A. Mrazik (W)  
T. Andreycheck (W)  
RCPL Administrative Aide (W)

ATTACHMENT 1

Information to include in Entergy's Transmittal to the NRC

The following information should be included in your letter to the NRC:

Reference documents:

1. WCAP-16836-P, Rev. 0, "Arkansas Nuclear One - Jet Impingement Testing of Insulating Materials" (proprietary)
2. Westinghouse authorization letter CAW-09-2622, accompanying Affidavit, Proprietary Information Notice, and Copyright Notice.

As WCAP-16836-P, Rev. 0 (Reference 1) contains information proprietary to Westinghouse Electric Company, LLC, it is supported by an Affidavit signed by Westinghouse, the owner of the information. The Affidavit sets forth the basis on which the information may be withheld from public disclosure by the Commission and addresses with specificity the considerations listed in paragraph (b) (4) of Section 2.390 of the Commission's regulations.

Accordingly, it is respectfully requested that the information which is proprietary to Westinghouse be withheld from public disclosure in accordance with 10 CFR Section 2.390 of the Commission's regulations.

Correspondence with respect to the copyright or proprietary aspects of the items listed above or the supporting Westinghouse Affidavit should reference CAW-09-2622 (Reference 2) and should be addressed to J. A. Gresham, Manager, Regulatory Compliance and Plant Licensing, Westinghouse Electric Company LLC, P.O. Box 355, Pittsburgh, Pennsylvania 15230-0355.

ATTACHMENT 2

Westinghouse Letter CAW-09-2622  
“Application for Withholding Proprietary Information from Public Disclosure”



Westinghouse Electric Company  
Nuclear Services  
P.O. Box 355  
Pittsburgh, Pennsylvania 15230-0355  
USA

U.S. Nuclear Regulatory Commission  
Document Control Desk  
Washington, DC 20555-0001

Direct tel: (412) 374-4643  
Direct fax: (412) 374-3846  
e-mail: greshaja@westinghouse.com

Our ref: CAW-09-2622

August 3, 2009

APPLICATION FOR WITHHOLDING PROPRIETARY  
INFORMATION FROM PUBLIC DISCLOSURE

Subject: WCAP-16836-P, Rev. 0, "Arkansas Nuclear One – Jet Impingement Testing of Insulating Materials" (proprietary)

The proprietary information for which withholding is being requested in the above-referenced report is further identified in Affidavit CAW-09-2622 signed by the owner of the proprietary information, Westinghouse Electric Company LLC. The Affidavit, which accompanies this letter, sets forth the basis on which the information may be withheld from public disclosure by the Commission and addresses with specificity the considerations listed in paragraph (b)(4) of 10 CFR Section 2.390 of the Commission's regulations.

The proprietary material for which withholding is being requested is to be considered proprietary in its entirety. As such, a non-proprietary version will not be issued. In conformance with 10 CFR Section 2.390, Affidavit CAW-09-2622 accompanies this Application for Withholding, setting forth the basis on which the proprietary information may be withheld from public disclosure.

Accordingly, this letter authorizes the utilization of the accompanying Affidavit by Entergy Operations, Inc. (Entergy).

Correspondence with respect to the proprietary aspects of the Application for Withholding Proprietary Information from Public Disclosure or the Westinghouse Affidavit should reference this letter, CAW-09-2622, and should be addressed to J. A. Gresham, Manager, Regulatory Compliance and Plant Licensing, Westinghouse Electric Company LLC, P.O. Box 355, Pittsburgh, Pennsylvania 15230-0355.

Very truly yours,

A handwritten signature in black ink, appearing to read "J. A. Gresham".

J. A. Gresham, Manager  
Regulatory Compliance and Plant Licensing

Enclosure

cc: George Bacuta (NRC OWFN 12E-1)

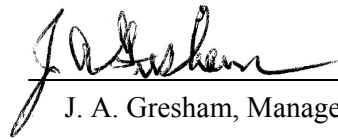
AFFIDAVIT

COMMONWEALTH OF PENNSYLVANIA:

SS

COUNTY OF ALLEGHENY:

Before me, the undersigned authority, personally appeared J. A. Gresham, who, being by me duly sworn according to law, deposes and says that he is authorized to execute this Affidavit on behalf of Westinghouse Electric Company LLC (Westinghouse), and that the averments of fact set forth in this Affidavit are true and correct to the best of his knowledge, information, and belief:



J. A. Gresham, Manager

Regulatory Compliance and Plant Licensing

Sworn to and subscribed before me  
this 3<sup>rd</sup> day of August, 2009



Notary Public

COMMONWEALTH OF PENNSYLVANIA

Notarial Seal  
Sharon L. Markle, Notary Public  
Monroeville Bore, Allegheny County  
My Commission Expires Jan. 29, 2011

Member, Pennsylvania Association 01 Notaries

- (1) I am Manager, Regulatory Compliance and Plant Licensing, in Nuclear Services, Westinghouse Electric Company LLC (Westinghouse), and as such, I have been specifically delegated the function of reviewing the proprietary information sought to be withheld from public disclosure in connection with nuclear power plant licensing and rule making proceedings, and am authorized to apply for its withholding on behalf of Westinghouse.
- (2) I am making this Affidavit in conformance with the provisions of 10 CFR Section 2.390 of the Commission's regulations and in conjunction with the Westinghouse "Application for Withholding" accompanying this Affidavit.
- (3) I have personal knowledge of the criteria and procedures utilized by Westinghouse in designating information as a trade secret, privileged or as confidential commercial or financial information.
- (4) Pursuant to the provisions of paragraph (b)(4) of Section 2.390 of the Commission's regulations, the following is furnished for consideration by the Commission in determining whether the information sought to be withheld from public disclosure should be withheld.
  - (i) The information sought to be withheld from public disclosure is owned and has been held in confidence by Westinghouse.
  - (ii) The information is of a type customarily held in confidence by Westinghouse and not customarily disclosed to the public. Westinghouse has a rational basis for determining the types of information customarily held in confidence by it and, in that connection, utilizes a system to determine when and whether to hold certain types of information in confidence. The application of that system and the substance of that system constitutes Westinghouse policy and provides the rational basis required.

Under that system, information is held in confidence if it falls in one or more of several types, the release of which might result in the loss of an existing or potential competitive advantage, as follows:

    - (a) The information reveals the distinguishing aspects of a process (or component, structure, tool, method, etc.) where prevention of its use by any of

Westinghouse's competitors without license from Westinghouse constitutes a competitive economic advantage over other companies.

- (b) It consists of supporting data, including test data, relative to a process (or component, structure, tool, method, etc.), the application of which data secures a competitive economic advantage, e.g., by optimization or improved marketability.
- (c) Its use by a competitor would reduce his expenditure of resources or improve his competitive position in the design, manufacture, shipment, installation, assurance of quality, or licensing a similar product.
- (d) It reveals cost or price information, production capacities, budget levels, or commercial strategies of Westinghouse, its customers or suppliers.
- (e) It reveals aspects of past, present, or future Westinghouse or customer funded development plans and programs of potential commercial value to Westinghouse.
- (f) It contains patentable ideas, for which patent protection may be desirable.

There are sound policy reasons behind the Westinghouse system which include the following:

- (a) The use of such information by Westinghouse gives Westinghouse a competitive advantage over its competitors. It is, therefore, withheld from disclosure to protect the Westinghouse competitive position.
- (b) It is information that is marketable in many ways. The extent to which such information is available to competitors diminishes the Westinghouse ability to sell products and services involving the use of the information.
- (c) Use by our competitor would put Westinghouse at a competitive disadvantage by reducing his expenditure of resources at our expense.

- (d) Each component of proprietary information pertinent to a particular competitive advantage is potentially as valuable as the total competitive advantage. If competitors acquire components of proprietary information, anyone component may be the key to the entire puzzle, thereby depriving Westinghouse of a competitive advantage.
  - (e) Unrestricted disclosure would jeopardize the position of prominence of Westinghouse in the world market, and thereby give a market advantage to the competition of those countries.
  - (f) The Westinghouse capacity to invest corporate assets in research and development depends upon the success in obtaining and maintaining a competitive advantage.
- (iii) The information is being transmitted to the Commission in confidence and, under the provisions of 10 CFR Section 2.390, it is to be received in confidence by the Commission.
- (iv) The information sought to be protected is not available in public sources or available information has not been previously employed in the same original manner or method to the best of our knowledge and belief.
- (v) The proprietary information sought to be withheld in this submittal is that which is appropriately marked in WCAP-16836-P, Rev. 0, "Arkansas Nuclear One - Jet Impingement Testing of Insulating Materials" (proprietary) dated October 2007, for Arkansas Nuclear One Unit 2 (ANO2), being transmitted by the Entergy letter and Application for Withholding Proprietary Information from Public Disclosure, to the Document Control Desk. The proprietary information as submitted by Westinghouse for ANO2 is expected to be potentially applicable for other licensee submittals in response to NRC requests for additional information regarding Generic Letter (GL) 2004-02, Potential Impact of Debris Blockage on Emergency Recirculation During Design Basis Accidents at Pressurized-Water Reactors (PWRs)," dated September 13, 2004 (0CNA090401).

This information is part of that which will enable Westinghouse to:

- (a) Support Entergy's response to the request for additional information from the NRC regarding significant and bounding conservatisms in the overall holistic approach taken for resolution of GL 2004-02 issues which provide reasonable assurance that sufficient margin exists for the ANO units.

Further this information has substantial commercial value as follows:

- (a) Westinghouse plans to sell the use of similar information to its customers for purposes of justification of calculations related to the jet impingement of materials during a potential high-energy line break in an operating Pressurized Water Reactor (PWR).
- (b) Westinghouse can sell support and defense of justification of reduced Zone of Influence (ZOI) about the postulated pipe break that will result in various insulation materials being treated as debris.
- (c) The information requested to be withheld reveals the distinguishing aspects of a methodology which was developed by Westinghouse.

Public disclosure of this proprietary information is likely to cause substantial harm to the competitive position of Westinghouse because it would enhance the ability of competitors to provide similar calculations and licensing defense services for commercial power reactors without commensurate expenses. Also, public disclosure of the information would enable others to use the information to meet NRC requirements for licensing documentation without purchasing the right to use the information.

The development of the technology described in part by the information is the result of applying the results of many years of experience in an intensive Westinghouse effort and the expenditure of a considerable sum of money.

In order for competitors of Westinghouse to duplicate this information, similar technical programs would have to be performed and a significant manpower effort, having the requisite talent and experience, would have to be expended.

Further the deponent sayeth not.

### **PROPRIETARY INFORMATION NOTICE**

The proprietary material for which withholding is being requested is to be considered proprietary in its entirety. As such, a non-proprietary version will not be issued. In conformance with 10 CFR Section 2.390(b)(1), the Affidavit that accompanies this transmittal sets forth the basis on which the proprietary information may be withheld from public disclosure as identified in Sections (4)(ii)(a) through (4)(ii)(f).

### **COPYRIGHT NOTICE**

The reports transmitted herewith each bear a Westinghouse copyright notice. The NRC is permitted to make the number of copies of the information contained in these reports which are necessary for its internal use in connection with generic and plant-specific reviews and approvals as well as the issuance, denial, amendment, transfer, renewal, modification, suspension, revocation, or violation of a license, permit, order, or regulation subject to the requirements of 10 CFR 2.390 regarding restrictions on public disclosure to the extent such information has been identified as proprietary by Westinghouse, copyright protection notwithstanding. With respect to the non-proprietary versions of these reports, the NRC is permitted to make the number of copies beyond those necessary for its internal use which are necessary in order to have one copy available for public viewing in the appropriate docket files in the public document room in Washington, DC and in local public document rooms as may be required by NRC regulations if the number of copies submitted is insufficient for this purpose. Copies made by the NRC must include the copyright notice in all instances and the proprietary notice if the original was identified as proprietary.